

Supporting Information

Intense fluorescence of air-stable sodium diarylformamidinate: effective control with a novel electron-withdrawing 4-cyano-3,5-bis(trifluoromethyl)phenyl group

**Kenichi Michigami,*^a Daiki Kawakami,^a Ichiro Ueda,^b Shunya Ito,^a Takuya Ogaki,^{c,d}
Hiroshi Ikeda,^{c,d} and Masato Ohashi*^a**

^a *Department of Chemistry, Graduate School of Science, Osaka Metropolitan University
Sugimoto-cho, Sumiyoshi-ku, Osaka-shi, Osaka 558-8585, Japan*

^b *Department of Chemistry, Graduate School of Science, Osaka Prefecture University
Gakuen-cho, Naka-ku, Sakai-shi, Osaka 599-8531, Japan*

^c *Department of Applied Chemistry, Graduate School of Engineering, Osaka Metropolitan University
Gakuen-cho, Naka-ku, Sakai-shi, Osaka 599-8531, Japan*

^d *The Research Institute for Molecular Electronic Devices (RIMED), Osaka Metropolitan University
Gakuen-cho, Naka-ku, Sakai-shi, Osaka 599-8531, Japan*

E-mail: kn1michigmai@omu.ac.jp, ohashi@omu.ac.jp

Table of Contents

(A)	General	S2
(B)	Materials & Methods	S3
(C)	Cyclic Voltammetry (CV)	S10
(D)	Absorption & Emission Properties	S11
(E)	Cation Effects on the Absorption & Emission Spectra	S19
(F)	Solid-State Emission Properties	S22
(G)	Solvent Effects on the Absorption & Emission	S23
(H)	Emission Lifetimes	S24
(I)	Temperature Dependence of Photoluminescence	S25
(J)	Computational Details	S26
(K)	Copies of NMR Spectra	S50
(L)	References	S70

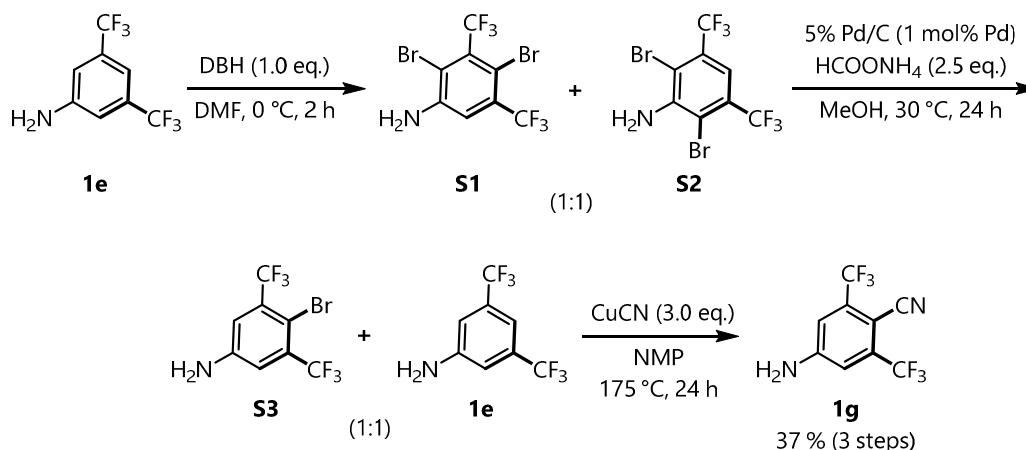
(A) General

All manipulations were carried out under an atmosphere of N₂ or inside N₂-filled glove box unless otherwise noted. Column chromatography was performed with Cica silica gel 60N (40–100 μm, spherical, neutral). NMR spectra were recorded on a JEOL ECS-400 spectrometer or a Varian 400-MR FT-NMR spectrometer, operating at 400 MHz (¹H), or 101 MHz (¹³C), or 376 MHz (¹⁹F). Chemical shifts in the internal reference solvents were reported in the following scales: for ¹H NMR, CDCl₃, CD₃CN, and DMSO-*d*₆ were relative to CHD₂CN (1.94 ppm), and CHD₂SOCD₃ (2.50 ppm), respectively, and for ¹³C NMR, CD₃CN (1.32 ppm), and (CD₃)₂SO (39.52 ppm) were reported, respectively. Chemical shifts in each solvent for ¹⁹F NMR were reported in the scale relative to PhCF₃ (-65.64 ppm) as an external reference. NMR data are reported as follows: chemical shifts, multiplicity (s: singlet, d: doublet, t: triplet, q: quartet, m: multiplet, br: broad signal), coupling constant (Hz), and integration. Infrared (IR) spectroscopy was performed using a Jasco FT/IR-4100 spectrometer. High-resolution mass spectra (HRMS) were measured on a Bruker micrOTOFII time-of-flight mass spectrometer fitted with an ESI. Melting points (Mp.) were measured on a Yanaco Mp-JS apparatus equipped with a thermometer (30–300 °C). X-ray diffraction data were collected on either a HyPix-6000HE detector equipped in Rigaku XtaLAB Synergy attached with multi-layer mirror monochromate and PhotonJet-S (Cu-K, λ = 1.54187 Å) or a Rigaku R-AXIS RAPID diffractometer using multi-layer mirror monochromated Mo-K_α radiation (λ = 0.71075 Å). The hydrogen atoms were refined using the riding model. All the calculations and refinement were performed by using SHELXL Version 2022/1. UV-Vis absorption spectra were recorded on a JASCO V-670 spectrometer. Emission spectra were recorded on a JASCO FP-8500 spectrometer and a JASCO FP-6200 spectrofluorometer with a UNISOKU CoolSpeK cryostat. Emission lifetimes were determined using a HORIBA Jobin Yvon FluoroCube lifetime spectrofluorometer equipped with HORIBA NanoLED-455 (excitation wavelength = 455 nm) as an excitation light source and analyzed by a DAS6 FL decay analysis software. Solvents and reagents were obtained from commercial suppliers and used as received. The solvents marked as “SPS” (THF, Et₂O, toluene, and hexane) were purified by the solvent purification system GlassContour 4S. The solvents marked as “distilled” were stored in the glove box after purification by distillation using the following drying agents: Na/benzophenone for THF, Et₂O, toluene, and hexane; CaH₂ for MeCN, CD₃CN, and CH₂Cl₂. Distilled water was purchased from Nacalai Tesque Inc. and used as received.

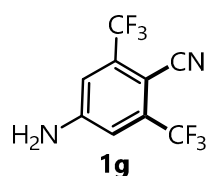
(B) Materials & Methods

Methyl 4-aminobenzoate (**1a**), 4-aminophenyl methyl sulfone (**1b**), 4-cyanoaniline (**1c**), 4-nitroaniline (**1d**), 3,5-bis(trifluoromethyl)aniline (**1e**), and 4-cyano-3-(trifluoromethyl)aniline (**1f**) were purchased from commercial sources and used as received.

(B-1) Synthesis of **1g**



4-Amino-2,6-bis(trifluoromethyl)benzonitrile (**1g**)^{S1}



1g was prepared basically according to the known procedures, but modified to increase the selectivity of bromination at 4-position: Under air, 1,3-dibromo-5,5-dimethyl-hydantoin (DBH) (28.6 g, 100 mmol, 1.0 equiv) was added in one portion to the stirred solution of 3,5-bis(trifluoromethyl)aniline (**1e**) (22.9 g, 100 mmol, 1.0 equiv) in DMF (100 mL) and stirred at 0 °C for 4 h. After monitoring the reaction progress by TLC, the mixture was diluted with water (300 mL) and extracted with EtOAc (30 mL, 3 times). The combined organic layer was washed with water (100 mL, 5 times) and brine (30 mL, twice), and dried over MgSO₄. After the solids were filtered off, the solvent was removed under reduced pressure and the residue was dried under vacuum. The contents other than **1e**-derived materials including 2,4-dibromo-3,5-bis(trifluoromethyl)aniline (**S1**) 2,6-dibromo-3,5-bis(trifluoromethyl)aniline (**S2**)^{S2} in the residue were roughly removed by silica-gel column chromatography (eluent: hexane/EtOAc, 100:0 to 10:1) to afford a mixture containing **S1** and **S2** (*ca.* 1:1) as major products. The obtained red oil was used to the next step without further purification.

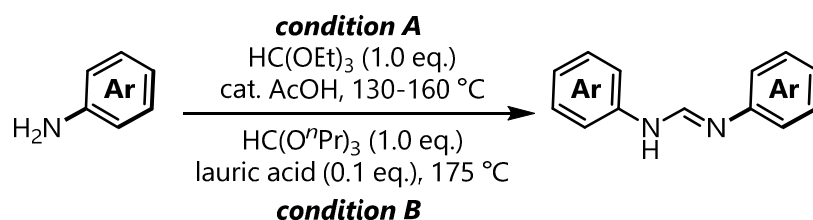
A 500 mL recovery flask was charged with 5 wt% Pd/C (2.13 g, 20.0 mmol, 1 mol% Pd) and dried by heating for 5 min using a heat gun under vacuum. After cooling to ambient temperature, the flask was evacuated and backfilled with nitrogen (three times). A solution of **S1** and **S2** in MeOH (200 mL) was injected to the flask and HCO₂NH₄ (15.6 g, 250 mmol, 2.5 equiv) were added subsequently under a gentle stream of nitrogen, and the resulting mixture was stirred at 30 °C for 24 h. After cooling to room temperature, the reaction progress was monitored by TLC. The mixture was filtered through Celite[®] and all volatiles of the filtrate were removed under reduced pressure. The residual solids were dissolved in water (100 mL) and extracted with EtOAc (100 mL, 3 times). The combined organic layer was washed with water (100 mL, 3 times) and brine (30 mL, twice), and dried over MgSO₄. After the solids were filtered off, the solvent was removed under reduced pressure and the residue was dried under vacuum to afford a mixture of 3,5-bis(trifluoromethyl)-4-bromoaniline (**S3**)^{S2aNa} and **1e** (*ca.* 1:1), which was used without further purification.

Under air, to a 200 mL recovery flask containing the above mixture (*ca.* 50 mmol of **S3**) was added CuCN (11.2 g, 125 mmol, 2.5 equiv) and the solids were suspended in NMP (100 mL). The resulting mixture was stirred at 175 °C for 24 h before cooling to room temperature. After monitoring the reaction progress by TLC, the mixture was diluted with EtOAc and water. The precipitates were removed by filtration through Celite[®] and the filtrate was extracted with EtOAc (5 times).

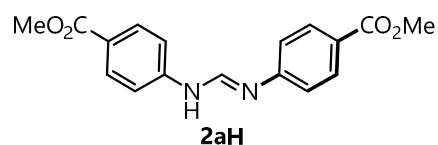
The combined organic layer was washed with water (200 mL, 10 times) and brine (30 mL, 4 times), and dried over MgSO₄. The solids were filtered off and the solvent was removed under reduced pressure and the residue was passed through a pad of silica gel (dry charge, eluent: hexane/EtOAc = 1:5), giving a mixture of 4-amino-2,6-bis(trifluoromethyl)benzotrile (**1g**) and **1e**. After concentration of the filtrate, the residual solids were washed with hexane to afford **1g** (9.40 g, 37 mmol, 37% in 3 steps) as brown solids. If necessary, **1g** can be further purified by silica-gel column chromatography or vacuum sublimation (*ca.* 20 Torr, *ca.* 130 °C), providing pale-yellow solids.

¹H NMR (400 MHz, CD₃CN): δ 5.67 (br s, 2H), 7.20 (s, 2H) ppm. The spectral data were consistent with the literature.^{S1}

(B-2) Preparation of 1,3-Diarylfornamidines



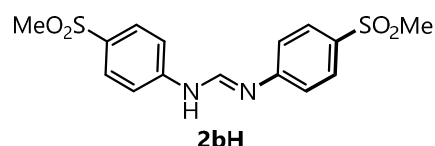
1,3-Di(4-methoxycarbonylphenyl)formamidine (**2aH**)^{S4}



Condition A: Under air, to a 50 mL recovery flask were added Methyl 4-aminobenzoate (750 mg, 5.00 mmol, 2.0 equiv), triethyl orthoformate (371 mg, 2.50 mmol, 1.0 equiv), and AcOH (15.0 mg, 0.500 mmol, 0.1 equiv). The resulting mixture was stirred at 130 °C for 24 h before cooling to room temperature. The mixture was washed with toluene (3 mL, 3 times) and the solids were dried under vacuum to afford **2aH** (704.5 mg, 2.25 mmol, 90%) as pale-yellow solids.

¹H NMR (400 MHz, DMSO-*d*₆): δ 3.82 (s, 6H), 7.33 (s, 4H), 7.90 (d, *J* = 8.3 Hz, 4H), 8.45 (s, 1H), 10.4 (s, 1H) ppm. The spectral data were consistent with the literature.

1,3-Di(4-methanesulfonylphenyl)formamidine (**2bH**)^{S5}

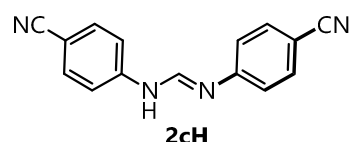


Condition A: Under air, to a 50 mL recovery flask were added 4-(methanesulfonyl)aniline (856 mg, 5.00 mmol, 2.0 equiv), triethyl orthoformate (371 mg, 2.50 mmol, 1.0 equiv), and AcOH (15.0 mg, 0.250 mmol, 0.1 equiv). The

resulting mixture was suspended in *p*-xylene (4 mL) was stirred at 130 °C for 24 h before cooling to room temperature. The mixture was washed with toluene (3 mL, 3 times) and the solids was dried under vacuum to afford **2bH** (858 mg, 2.43 mmol, 98%) as white solids.

¹H NMR (400 MHz, DMSO-*d*₆): δ 3.17 (s, 6H), 7.36-7.61 (br s, 4H), 7.83 (d, *J* = 8.3 Hz, 4H), 8.48 (br s, 1H), 10.5 (br s, 1H) ppm; **¹³C NMR** (101 MHz, DMSO-*d*₆): δ 44.0, 119.3, 128.4, 134.3, 149.6 ppm; **IR** (KBr): ν 3492, 3343, 3013, 2921, 1685, 1585, 1499, 1304, 1145 cm⁻¹; **HRMS** (ESI, negative, MeCN): *m/z* calcd. for C₁₅H₁₅N₂O₄S₂⁻ [M-H]⁻: 351.0478, found: 351.0463; **Mp.**: 272.2–274.4 °C.

1,3-Di(4-cyanophenyl)formamidine (**2cH**)^{S6}



Condition A: Under air, to a 50 mL recovery flask were added 4-aminobenzotrile (1.18 g, 10.0 mmol, 2.0 equiv), triethyl orthoformate (741 mg, 5.00 mmol, 1.0 equiv), and AcOH (30.1 mg, 0.500 mmol, 0.1 equiv). The resulting mixture was stirred at 130 °C for 24 h

before cooling to room temperature. The mixture was washed with hexane (3 mL, 3 times) and the solids were dried under vacuum to afford **2cH** (1.21 g, 4.91 mmol, 98%) as yellow solids.

¹H NMR (400 MHz, DMSO-*d*₆): δ 7.41 (br s, 2H), 7.74 (d, *J* = 8.4 Hz, 4H), 8.45 (br s, 2H), 10.49 (br s, 1H) ppm; **¹³C NMR** (101 MHz, DMSO-*d*₆): δ 104.5, 113.5, 119.4, 119.6, 133.4, 149.5 ppm; **IR** (KBr): ν 3477, 3326, 3074, 2224, 1667, 1580, 1498, 1314, 1209, 1179 cm⁻¹; **HRMS** (ESI, negative, MeCN): *m/z* calcd. for C₁₅H₉N₄⁻ [M-H]⁻: 245.0832, found: 245.0793.

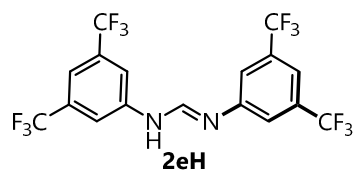
1,3-Di(4-nitrophenyl)formamidine (2dH)^{S4}



Condition A: Under air, to a 50 mL recovery flask were added 4-nitroaniline (1.38 g, 10.0 mmol, 2.0 equiv), triethyl orthoformate (741 mg, 5.00 mmol, 1.0 equiv), and AcOH (30.1 mg, 0.5 mmol, 0.1 equiv). The resulting mixture was suspended in *p*-xylene (4 mL) was stirred at 130 °C for 24 h before cooling to room temperature. The mixture was washed with toluene (3 mL, 3 times) and the solids was dried under vacuum to afford **2dH** (1.29 g, 4.53 mmol, 91 %) as white solids.

¹H NMR (400 MHz, DMSO-*d*₆): δ 7.49 (s, 4H), 8.21 (d, *J* = 8.3 Hz, 4H), 8.60 (s, 1H), 10.8 (s, 1H) ppm; **¹³C NMR** (100 MHz, DMSO-*d*₆): δ 119.3 (br) , 125.1, 142.4, 159.8 ppm; **HRMS** (ESI, negative, MeCN): *m/z* calcd. for C₁₃H₉N₄O₄⁻ [M-H]⁻ : 285.0629, found: 285.0614. The spectral data were consistent with the literature.

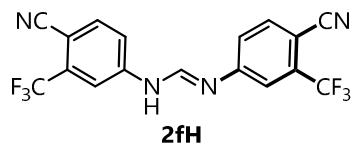
1,3-Di{3,5-bis(trifluoromethyl)phenyl}formamidine (2eH)^{S7}



Condition A: Under air, to a 100 mL recovery flask were added 3,5-bis(trifluoromethyl)aniline (1.270 g, 5.0 mmol, 2.0 equiv), triethyl orthoformate (371 mg, 2.50 mmol, 1.0 equiv), and AcOH (15 mg, 0.25 mmol, 0.1 equiv). The resulting mixture was stirred at 130 °C for 24 h before cooling to room temperature. The mixture was washed with hexane (3 mL, 3 times) and the solids were dried under vacuum to afford **2eH** (901 mg, 1.92 mmol, 77%) as white solids.

¹H NMR (400 MHz, Acetone-*d*₆): δ 7.69 (br s, 4H), 8.01 (br s, 1H), 8.67 (br, s, 1H), 9.66 (br s, 1H) ppm; **HRMS** (ESI, negative, MeCN): *m/z* calcd. for C₁₇H₇F₁₂N₂⁻ [M-H]⁻: 467.0423, found: 467.0425. The spectral data were consistent with the literature.

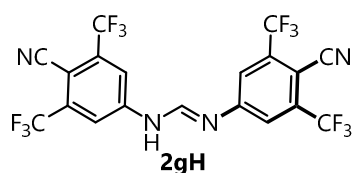
1,3-Di{4-cyano-3-(trifluoromethyl)phenyl}formamidine (2fH)



Condition B: Under air, to a 100 mL recovery flask were added 4-amino-2-(trifluoromethyl)benzonitrile (3.70 g, 19.9 mmol, 2.0 equiv), tri-*n*-propyl orthoformate (2.02 g, 10.0 mmol, 1.0 equiv), and lauric acid (200 mg, 1.00 mmol, 0.1 equiv). The resulting mixture was stirred at 170 °C for 24 h before cooling to room temperature. The mixture was washed with toluene and hexane (3 mL, 3 times for each) and the solids were dried under vacuum to afford **2fH** (3.29 g, 8.62 mmol, 86%) as pale-beige solids.

¹H NMR (400 MHz, CD₃CN): δ 7.62 (br s, 2H), 7.80 (br s, 2H), 7.89 (d, *J* = 8.8 Hz, 2H), 8.26 (br s, 1H) ppm; **¹³C NMR** (101 MHz, DMSO-*d*₆): δ 101.3, 116.1, 117.4, 122.6 (q, ¹*J*_{CF} = 274 Hz), 122.9, 132.1 (1, ²*J*_{CF} = 31.8 Hz), 136.5, 150.5, 151.3 ppm; **¹⁹F NMR** (376 MHz, CD₃CN): δ -62.70 (s, 6F) ppm; **IR** (KBr): ν 3427, 3307, 3076, 2989, 2226, 1665, 1604, 1576, 1435, 1341, 1293, 1185, 1134 cm⁻¹; **HRMS** (ESI, negative, MeCN): *m/z* calcd. for C₁₇H₇F₆N₄⁻ [M-H]⁻: 381.0580, found: 381.0583. **Mp.**: 268.2–270.0 °C.

1,3-Di{4-cyano-3,5-bis(trifluoromethyl)phenyl}formamidine (2gH)



Condition B: Under air, to a 100 mL recovery flask were added 4-amino-2,6-bis(trifluoromethyl)benzonitrile (3.57 g, 14.0 mmol, 2.0 equiv), tri-*n*-propyl orthoformate (1.33 g, 7.00 mmol, 1.0 equiv), and lauric acid (140.2 mg, 0.700 mmol, 0.1 equiv). The resulting mixture was stirred at 170 °C for 24 h before cooling to room temperature. The

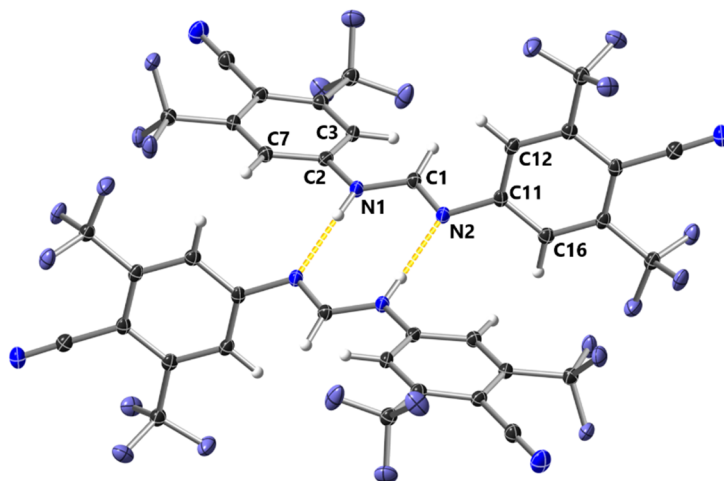
mixture was carefully washed with EtOAc (3 mL, 3 times) and the solids were dried under vacuum to afford **2gH** (2.35 g, 4.58 mmol, 65%) as beige solids.

¹H NMR (400 MHz, CD₃CN): δ 8.02 (br s, 4H), 8.37 (br s, 1H) ppm; **¹³C NMR** (101 MHz, DMSO-*d*₆): δ 98.6, 112.6, 121.9 (q, ¹J_{CF} = 275 Hz), 134.6 (q, ²J_{CF} = 31.8 Hz), 150.3, 152.9 ppm; **¹⁹F NMR** (376 MHz, CD₃CN): δ -62.74 (s, 12F) ppm;

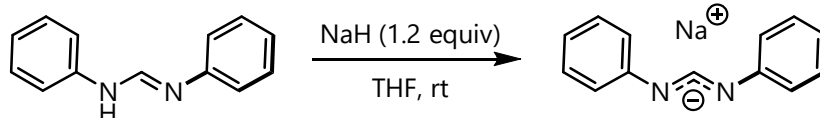
IR (KBr): ν 3432, 3323, 3088, 2239, 1674, 1605, 1524, 1478, 1372, 1294, 1215, 1188, 1166, 1139 cm⁻¹;

HRMS (ESI, negative, MeCN): *m/z* calcd. for C₁₉H₅F₁₂N₄⁻ [M-H]: 517.0328, found: 517.0320; **Mp.**: 244.1–247.4 °C;

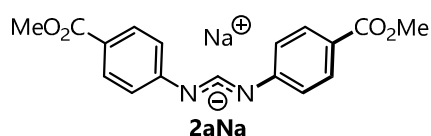
X-ray data: M = 518.28, block, colorless, triclinic, *P* $\bar{1}$ (#2), *a* = 8.2148(2) Å, *b* = 10.0468(3) Å, *c* = 11.6137(3) Å, α = 90.297(2)°, β = 102.341(2)°, γ = 93.315(2)°, *V* = 934.64(4) Å³, *Z* = 2, *D*_{calcd} = 1.842 g/cm³, *T* = 100.01(10) K, *R*₁ (*wR*₂) = 0.0306 (0.0822).



(B-3) Deprotonation of Amidinates



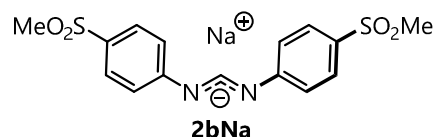
Sodium 1,3-Di(4-methoxycarbonylphenyl)formamidinate (2aNa)



A 20 mL recovery flask containing **2aH** (312 mg, 1.00 mmol, 1.0 equiv) was taken into the N₂-filled glove box and oil-free NaH (pre-washed with hexane, 28.8 mg, 1.20 mmol, 1.2 equiv) was added. The solids were suspended in THF (5 mL) and stirred at room temperature for 24 h. The mixture was filtered through Celite® and the cake was washed with THF. The filtrate was concentrated and dried under reduced pressure to furnish 0.4 THF adduct of **2aNa** (310 mg, 0.854 mmol, 85%) as moisture-sensitive yellow solids.

¹H NMR (400 MHz, CD₃CN): δ 1.75–1.85 (m, 2H), 3.59–3.68 (m, 2H), 3.79 (s, 6H), 6.99 (d, *J* = 8.8 Hz, 4H), 7.76 (d, *J* = 8.8 Hz, 4H), 8.93 (s, 1H) ppm; **¹³C NMR** (101 MHz, DMSO-*d*₆): δ 25.2, 51.2, 67.1, 118.4, 119.3, 130.3, 159.5, 159.8, 166.7 ppm; **HRMS** (ESI, negative, MeCN): *m/z* calcd. for C₁₇H₁₅N₂O₄⁻ [M]: 311.1037, found: 311.1030.

Sodium 1,3-Di(4-methanesulfonylphenyl)formamidinate (2bNa)



A 20 mL recovery flask containing **2bH** (352 mg, 1.00 mmol, 1.0 equiv) was taken into the N₂-filled glove box and oil-free NaH (pre-washed with hexane, 28.8 mg, 1.20 mmol, 1.2 equiv) was added. The solids were suspended in THF (5 mL)

and stirred at room temperature for 24 h. The mixture was filtered through Celite® and the cake was washed with THF. The filtrate was concentrated and dried under reduced pressure to afford 0.6 THF adduct of **2bNa** (350 mg, 0.838 mmol, 84%) as moisture-sensitive yellow solids.

¹H NMR (400 MHz, DMSO-*d*₆): δ 1.75–1.85 (m, 2H), 2.98 (s, 6H), 3.59–3.68 (m, 2H), 7.12 (d, *J* = 8.7 Hz, 4H), 7.63 (d, *J* = 8.7 Hz, 4H), 8.91 (s, 1H) ppm; **¹³C NMR** (101 MHz, DMSO-*d*₆): δ 25.1, 44.4, 67.0, 119.6, 127.9, 128.5, 159.5, 159.7 ppm; **HRMS** (ESI, negative, MeCN): *m/z* calcd. for C₁₅H₁₅N₂O₄S₂⁻ [M]⁻: 351.0478, found: 351.0481.

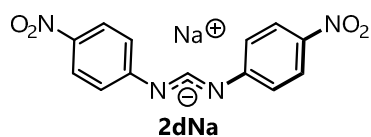
Sodium 1,3-Di(4-cyanophenyl)formamidinate (**2cNa**)



A 20 mL recovery flask containing **2cH** (98.5 mg, 0.400 mmol, 1.0 equiv) was taken into the N₂-filled glove box and oil-free NaH (pre-washed with hexane, 11.5 mg, 0.480 mmol, 1.2 equiv) was added. The solids were suspended in THF (5 mL) and stirred at room temperature for 24 h. The mixture was filtered through Celite® and the cake was washed with THF. The filtrate was concentrated and dried under reduced pressure to afford 0.25 THF adduct of **2cNa** (74.0 mg, 0.258 mmol, 65%) as moisture-sensitive yellow-orange solids.

¹H NMR (400 MHz, DMSO-*d*₆): δ 1.75–1.80 (m, 1H), 3.58–3.63 (m, 1H), 6.98 (d, *J* = 8.4 Hz, 4H), 7.41 (d, *J* = 8.6 Hz, 4H), 8.45 (s, 1H) ppm; **¹³C NMR** (101 MHz, DMSO-*d*₆): δ 25.1, 67.0, 98.5, 120.3, 120.9, 132.6, 158.4, 158.9 ppm; **HRMS** (ESI, negative, MeCN): *m/z* calcd. for C₁₅H₉N₄⁻ [M]⁻: 245.0832, found: 245.0789.

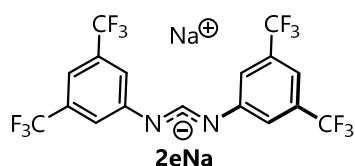
Sodium 1,3-Di(4-nitrophenyl)formamidinate (**2dNa**)



A 20 mL recovery flask containing **2dH** (286 mg, 1.00 mmol, 1.0 equiv) was taken into the N₂-filled glove box and oil-free NaH (pre-washed with hexane, 28.8 mg, 1.20 mmol, 1.2 equiv) was added. The solids were suspended in THF (5 mL) and stirred at room temperature for 24 h. The mixture was filtered through Celite® and the cake was washed with THF. The filtrate was concentrated and dried under reduced pressure to give 0.25 THF adduct of **2dNa** (281 mg, 0.861 mmol, 86%) as purple solids.

¹H NMR (400 MHz, DMSO-*d*₆): δ 1.70–1.80 (m, 1H), 3.57–3.61 (m, 1H), 7.10 (d, *J* = 9.0 Hz, 4H), 8.00 (d, *J* = 9.0 Hz, 4H), 8.69 (s, 1H) ppm; **¹³C NMR** (101 MHz, DMSO-*d*₆): δ 25.1, 67.0, 119.7, 125.1, 138.9, 158.4, 160.3 ppm; **IR** (KBr): ν 3544, 3179, 3103, 1660, 1579, 1523, 1300, 1108 cm⁻¹; **HRMS** (ESI, negative, MeCN): *m/z* calcd. for C₁₃H₉N₄O₄⁻ [M]⁻: 285.0629, found: 285.0621. **Mp.**: 258.1–259.6 °C.

Sodium 1,3-Di{3,5-bis(trifluoromethyl)phenyl}formamidinate (**2eNa**)



A 20 mL recovery flask containing **2eH** (187.2 mg, 0.400 mmol, 1.0 equiv) was taken into the N₂-filled glove box and oil-free NaH (pre-washed with hexane, 11.5 mg, 0.480 mmol, 1.2 equiv) was added. The solids were suspended in THF (5 mL) and stirred at room temperature for 24 h. The mixture was filtered through Celite® and the cake was washed with THF. The filtrate was concentrated and dried under reduced pressure to give 1.0 THF adduct of **2eNa** (172 mg, 0.306 mmol, 76%) as moisture-sensitive off-white solids.

¹H NMR (400 MHz, DMSO-*d*₆): δ 1.70–1.81 (m, 4H), 3.57–3.67 (m, 4H), 7.14 (s, 2H), 7.51 (s, 4H), 8.34 (s, 1H) ppm; **¹³C NMR** (101 MHz, DMSO-*d*₆): δ 25.1, 67.0, 109.5, 119.9, 124.0 (q, ¹J_{CF} = 273 Hz), 130.3 (q, ²J_{CF} = 31.8 Hz), 156.4, 159.1 ppm; **¹⁹F NMR** (376 MHz, DMSO-*d*₆): δ -61.32 (s, 12F) ppm; **HRMS** (ESI, negative, MeCN): *m/z* calcd. for C₁₇H₇F₁₂N₂⁻ [M]⁻: 467.0423, found: 467.0418.

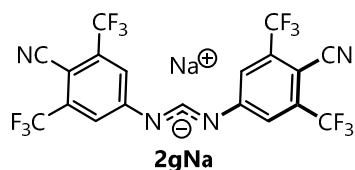
Sodium 1,3-Di{4-cyano-3-(trifluoromethyl)phenyl}formamidinate (2fNa)



A 20 mL recovery flask containing **2fH** (765 mg, 2.00 mmol, 1.0 equiv) was taken into the N₂-filled glove box and oil-free NaH (pre-washed with hexane, 57.6 mg, 2.40 mmol, 1.2 equiv) was added. The solids were suspended in THF (5 mL) and stirred at room temperature for 24 h. The mixture was filtered through Celite[®] and the cake was washed with THF. The filtrate was concentrated and dried under reduced pressure to give 0.25 THF adduct of **2fNa** (858 mg, 2.03 mmol, quant.) as moisture-sensitive brown solids.

¹H NMR (400 MHz, DMSO-*d*₆): δ 1.76–1.85 (m, 1H), 3.60–3.67 (m, 1H), 7.29 (d, *J* = 8.4 Hz, 2H), 7.33 (s, 2H), 7.69 (d, *J* = 8.4 Hz, 2H), 8.54 (s, 1H) ppm; **¹³C NMR** (101 MHz, DMSO-*d*₆): δ 25.1, 67.0, 94.6, 117.6, 119.1, 123.1 (q, ¹*J*_{CF} = 274 Hz), 122.3, 131.3 (q, ²*J*_{CF} = 24.7 Hz), 135.5, 159.2, 159.9 ppm; **¹⁹F NMR** (376 MHz, DMSO-*d*₆): δ -60.95 (s, 6F) ppm; **HRMS** (ESI, negative, MeCN): *m/z* calcd. for C₁₇H₇F₆N₄⁻ [M]⁻: 381.0580, found: 381.0577.

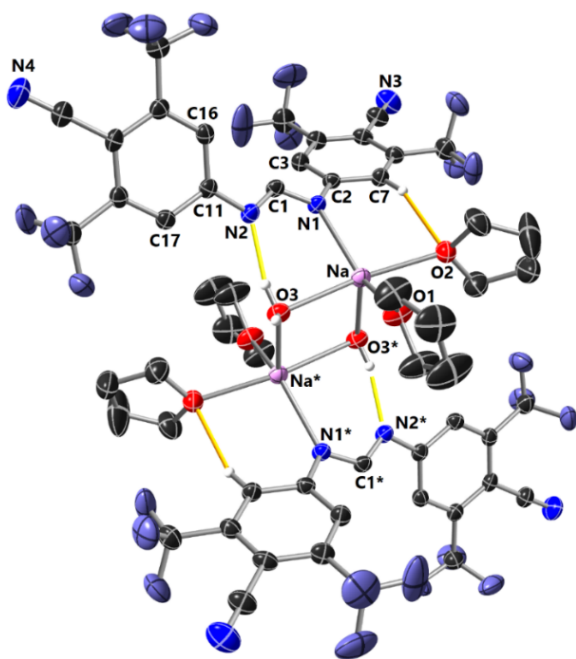
Sodium 1,3-Di{4-cyano-3,5-bis(trifluoromethyl)phenyl}formamidinate (2gNa)



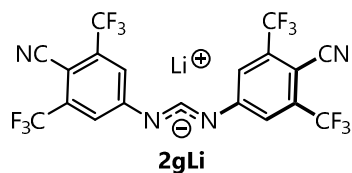
A 20 mL recovery flask containing **2gH** (1.04 g, 2.00 mmol, 1.0 equiv) was taken into the N₂-filled glove box and oil-free NaH (pre-washed with hexane, 57.6 mg, 2.40 mmol, 1.2 equiv) was added. The solids were suspended in THF (5 mL) and stirred at room temperature for 24 h. The mixture was filtered through Celite[®] and the cake was washed

with THF. The filtrate was concentrated and dried under reduced pressure to give **2gNa** (1.08 g, 1.99 mmol, 99%) as yellow solids. Single crystals suitable for X-ray crystallography were prepared by slow diffusion of hexane into a THF solution under air.

¹H NMR (400 MHz, CD₃CN): δ 7.84 (s, 4H), 8.55 (s, 1H) ppm; **¹³C NMR** (101 MHz, DMSO-*d*₆): δ 91.4, 114.0, 121.1 (app. q, ³*J*_{CF} = 1.5 Hz), 122.5 (q, ¹*J*_{CF} = 275 Hz), 134.0 (q, ²*J*_{CF} = 31.2 Hz), 159.1, 160.7 ppm; **¹⁹F NMR** (376 MHz, CD₃CN): δ -62.76 (s, 12F) ppm; **IR** (KBr): ν 3484, 3372, 3247, 2240, 2230, 1676, 1611, 1513, 14004, 1324, 1289, 1215, 1190, 1131 cm⁻¹; **HRMS** (ESI, negative, CH₃CN): *m/z* calcd. for C₁₉H₅F₁₂N₄⁻ [M]⁻: 517.0328, found: 517.0304; **Mp.**: >290 °C; **X-ray data**: *M* = 1404.97, block, yellow, triclinic, *P* $\bar{1}$ (#2), *a* = 10.1787(12) Å, *b* = 11.7677(17) Å, *c* = 14.651(2) Å, α = 73.314(5)°, β = 73.689(5)°, γ = 72.357(5)°, *V* = 1565.4(4) Å³, *Z* = 1, *D* = 1.490 g/cm³, *T* = 293(2) K, *R*₁ (*wR*₂) = 0.0587 (0.1570).



Lithium 1,3-Di{4-cyano-3,5-bis(trifluoromethyl)phenyl}formamidinate (**2gLi**)

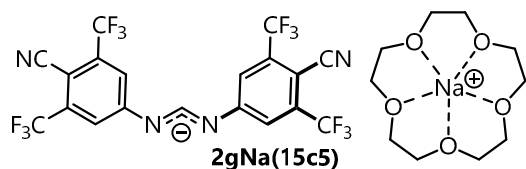


A 20 mL recovery flask containing **2gH** (155 mg, 0.300 mmol, 1.0 equiv) was taken into the N₂-filled glove box and LiH (2.86 mg, 0.360 mmol, 1.2 equiv) was added. The solids were then suspended in THF (3 mL) and stirred at room temperature for 24 h. The mixture was filtered through Celite® and the cake was washed with THF. The filtrate was

concentrated and dried under reduced pressure to give 1.0 THF adduct of **2gLi** (164 mg, 0.275 mmol, 92%) as yellow solids. **¹H NMR** (400 MHz, DMSO-*d*₆): δ 1.72–1.80 (m, 4H), 3.57–3.62 (m, 4H), 7.66 (s, 4H), 8.65 (s, 1H) ppm; **¹³C NMR** (101 MHz, DMSO-*d*₆): δ 25.1, 67.0, 91.2, 114.0, 121.0, 122.5 (q, ¹J_{CF} = 275 Hz), 133.9 (q, ²J_{CF} = 30.9 Hz), 159.2, 160.5 ppm; **¹⁹F NMR** (376 MHz, CD₃CN): δ -62.73 (s, 12F) ppm; **IR** (KBr): ν 3483, 3372, 3247, 2248, 2229, 1675, 1610, 1511, 1403, 1327, 1287, 1215, 1188, 1132 cm⁻¹; **HRMS** (ESI, negative, MeCN): *m/z* calcd. for C₁₉H₅F₁₂N₄⁻ [M]: 517.0328, found: 517.0317; **Mp.**: 244.2–246.3 °C.

(1,4,7,10,13-Pentaoxacyclopentadecane)sodium (**2gNa(15c5)**)

1,3-Di{4-cyano-3,5-bis(trifluoromethyl)phenyl}formamidinate

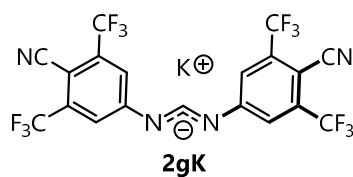


A 20 mL recovery flask containing **2gNa** (540.2 mg, 1.00 mmol, 1.0 equiv) was taken into the N₂-filled glove box and 15-crown-5 (220 mg, 1.00 mmol, 1.00 equiv) was added. The solids were then suspended in THF (4 mL) and stirred at room temperature for 24 h. The mixture was

concentrated and dried under reduced pressure to afford **2gNa(15c5)** (757 mg, 0.99 mmol, 99%) as yellow solids.

¹H NMR (400 MHz, CD₃CN): δ 3.61 (s, 24H), 7.70 (s, 4H), 8.63 (s, 1H) ppm; **¹³C NMR** (101 MHz, DMSO-*d*₆): δ 69.2, 91.6, 113.9, 120.9, 122.5 (q, ¹J_{CF} = 275 Hz), 133.9 (q, ²J_{CF} = 30.8 Hz), 158.7, 160.5 ppm; **¹⁹F NMR** (376 MHz, CD₃CN): δ -61.14 (s, 12F) ppm; **IR** (KBr): ν 3440, 3246, 2909, 2222, 1659, 1498, 1355, 1299, 1181, 1136 cm⁻¹; **HRMS** (ESI, positive, MeCN): *m/z* calcd. for C₁₀H₂₀O₅Na⁺ [M]⁺: 243.1203, found: 243.1199; (ESI, negative, MeCN): *m/z* calcd. for C₁₉H₅F₁₂N₄⁻ [M]: 517.0328, found: 517.0300; **Mp.**: 128.2–130.4 °C.

Potassium 1,3-Di{4-cyano-3,5-bis(trifluoromethyl)phenyl}formamidinate (**2gK**)

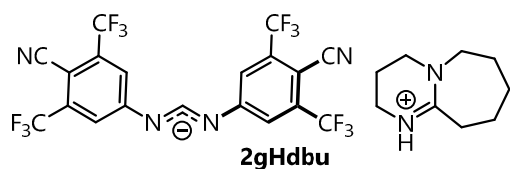


A 20 mL recovery flask containing **2gH** (77.7 mg, 0.150 mmol, 1.0 equiv) was taken into the N₂-filled glove box and KH (7.21 mg, 0.180 mmol, 1.2 equiv) was added. The solids were then suspended in THF (1 mL) and stirred at room temperature for 24 h. The mixture was filtered through Celite® and the cake was washed with THF. The filtrate was

concentrated and dried under reduced pressure to give adduct of **2gK** (82.1 mg, 0.148 mmol, 98%) as yellow solids.

¹H NMR (400 MHz, DMSO-*d*₆): δ 7.68 (s, 4H), 8.67 (s, 1H) ppm; **¹³C NMR** (101 MHz, DMSO-*d*₆): δ 91.8, 113.9, 121.0, 122.5 (q, ¹J_{CF} = 275 Hz), 134.0 (q, ²J_{CF} = 31.8 Hz), 158.5, 160.1 ppm; **¹⁹F NMR** (376 MHz, CD₃CN): δ -62.70 (s, 12F) ppm; **IR** (KBr): ν 3483, 3372, 2227, 1674, 1605, 1509, 1323, 1297, 1216, 1185, 1133 cm⁻¹; **HRMS** (ESI, negative, CH₃CN): *m/z* calcd. for C₁₉H₅F₁₂N₄⁻ [M]: 517.0328, found: 517.0310. **Mp.**: >275 °C (decomp.).

1,8-Diazabicyclo[5.4.0]undec-7-en-8-ium 1,3-Di{4-cyano-3,5-bis(trifluoromethyl)phenyl}formamidinate (**2gHdbu**)



A 20 mL recovery flask containing **2gH** (518 mg, 1.00 mmol, 1.0 equiv) was taken into the N₂-filled glove box and anhydrous DBU (152 mg, 1.00 mmol, 1.0 equiv) was added. The solids were suspended in THF (5 mL) and stirred at room temperature for 24 h. The mixture was concentrated and

dried under reduced pressure to give 0.2 THF adduct of **2gHdbu** (565 mg, 0.844 mmol, 84%) as yellow solids.

¹H NMR (400 MHz, DMSO-*d*₆): δ 1.57–1.70 (m, 6H), 1.73–1.78 (m, 0.8H), 1.86–1.91 (m, 2H), 2.57–2.60 (m, 2H), 3.23 (t, *J* = 5.7 Hz, 2H), 3.44 (t, *J* = 5.7 Hz, 2H), 3.49–3.51 (m, 2H), 3.57–3.61 (m, 0.8H), 7.66 (s, 4H), 8.65 (s, 1H) ppm; **¹³C NMR** (100 MHz, DMSO-*d*₆): δ 19.1, 23.5, 25.1, 26.1, 28.3, 32.1, 38.1, 47.9, 53.3, 67.0, 91.3, 114.0, 121.0, 122.5 (q, ¹*J*_{CF} = 272 Hz), 133.9 (q, ²*J*_{CF} = 30.6 Hz), 159.1, 160.5, 164.9 ppm; **¹⁹F NMR** (376 MHz, CD₃CN): δ -62.67 (s, 12F) ppm; **IR** (KBr): ν 3410, 3204, 2942, 2223, 1648, 1516, 1356, 1323, 1283, 1204, 1179, 1130 cm⁻¹; **HRMS** (ESI, negative, MeCN): *m/z* calcd. for C₁₉H₅F₁₂N₄⁻ [M]: 517.0328, found: 517.0294; **Mp.**: 118.2–122.5 °C.

(C) Cyclic Voltammetry (CV)

2gNa exhibited irreversible oxidation upon measurements. The voltammograms suggested decomposition of **2gNa**.

Conditions for the CV measurements using **2gNa**:

Reference: Ag/Ag⁺ (AgNO₃)

Electrodes: Pt/C

Solvent: MeCN

Electrolyte: TBAPF₆ (0.1 M)

Concentration: 1.0 × 10⁻³ M

Range: -1.5~+2.0 V (vs. SCE)

Result:

Resting potential: -0.94 V (vs. SCE)

*E*_{ox} = +0.23 (1st cycle), +0.14 V (2nd and 3rd cycles), +1.15 (1st cycle), +1.10 V (2nd and 3rd cycles) (vs. SCE)

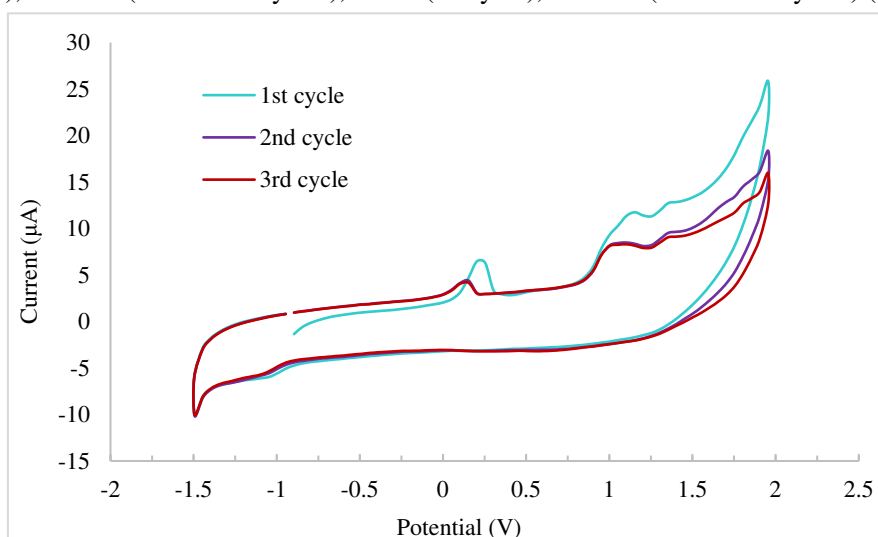


Figure S1. Cyclic voltammogram of **2gNa**.

(D) Absorption & Emission Properties

For **2aH** and **2aNa**:

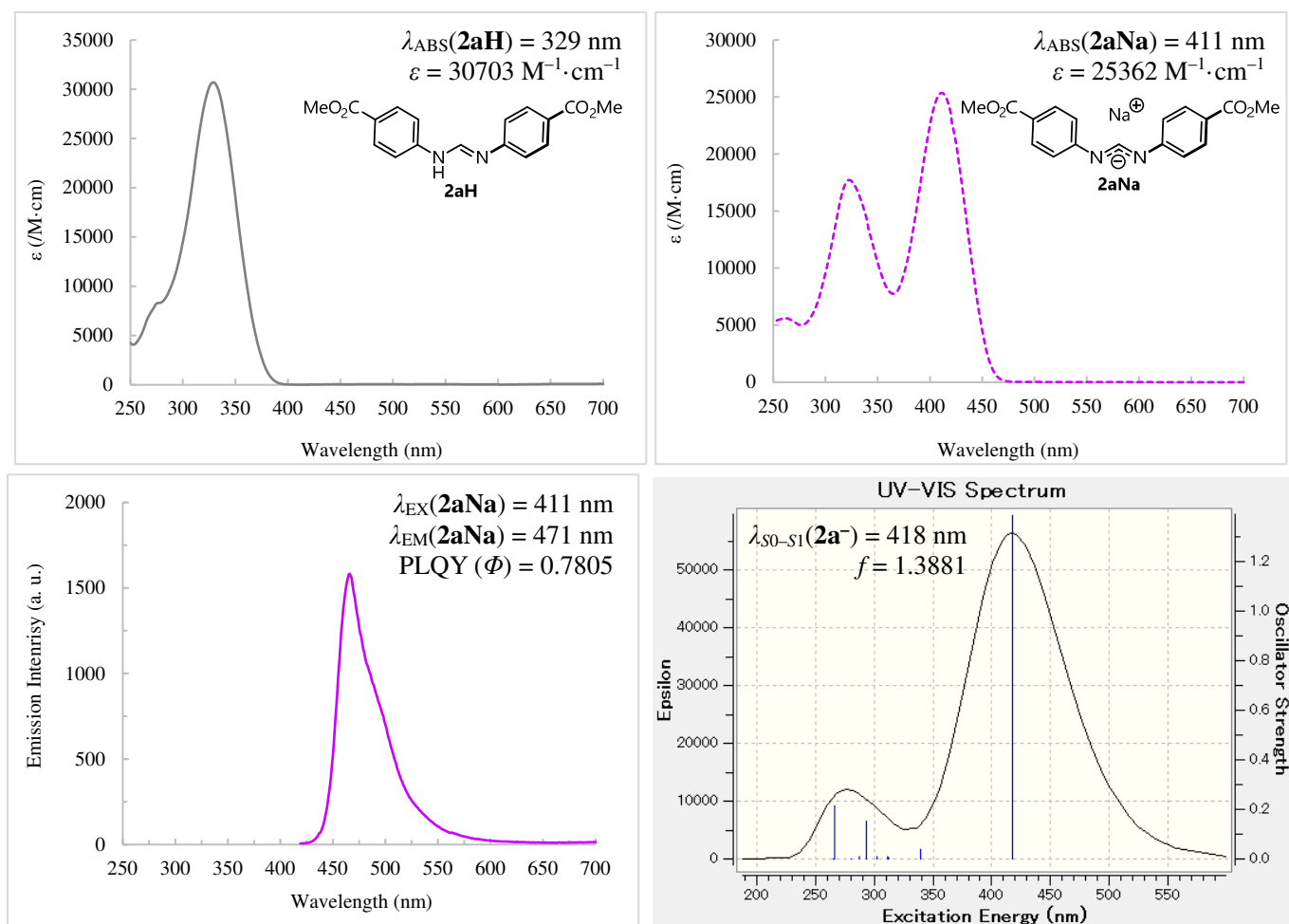


Figure S2. (Top, left) UV-Vis absorption spectrum of **2aH** in THF ($1.0 \times 10^{-5} \text{ M}$). (Top, right) UV-Vis absorption spectra of **2aNa** in THF ($1.0 \times 10^{-4} \text{ M}$). (Bottom, left) emission spectra of **2aNa** in THF ($1.0 \times 10^{-4} \text{ M}$). (Bottom, right) DFT-based simulation of UV-Vis spectrum, the excitation energies, and the oscillator strengths for the optimized geometry of **2a-**.

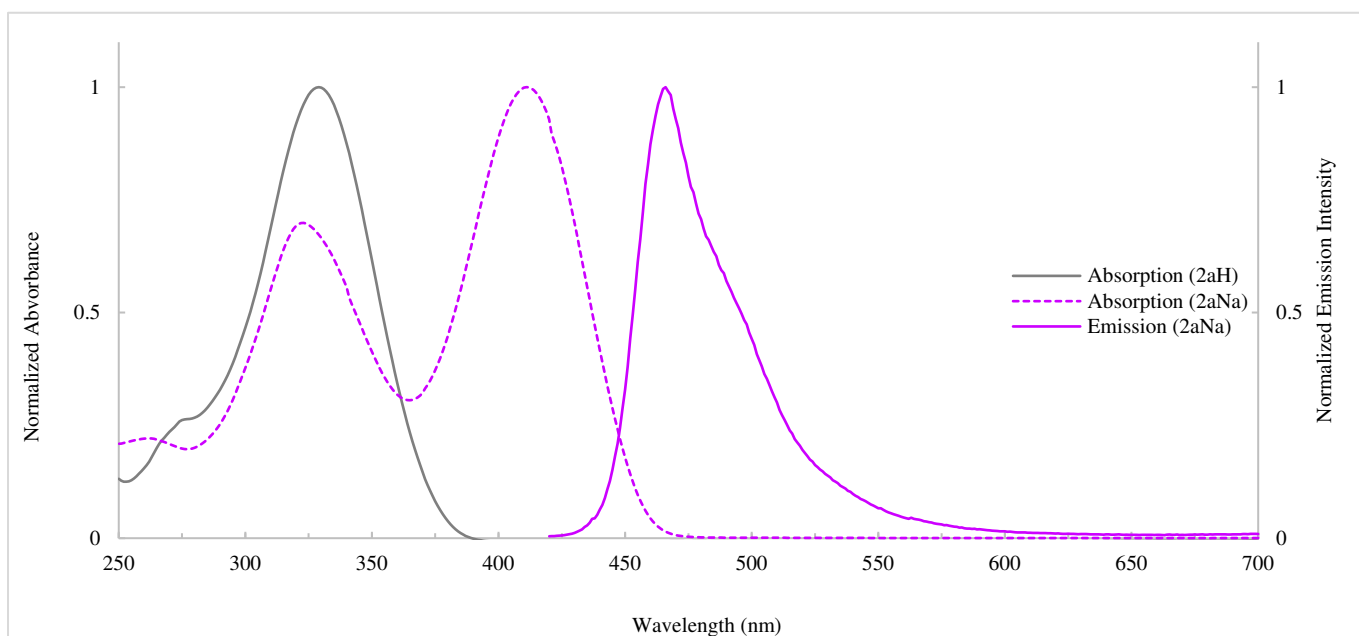


Figure S3. Normalized absorption and emission spectra of **2aH** and **2aNa** in THF.

For **2bH** and **2bNa**:

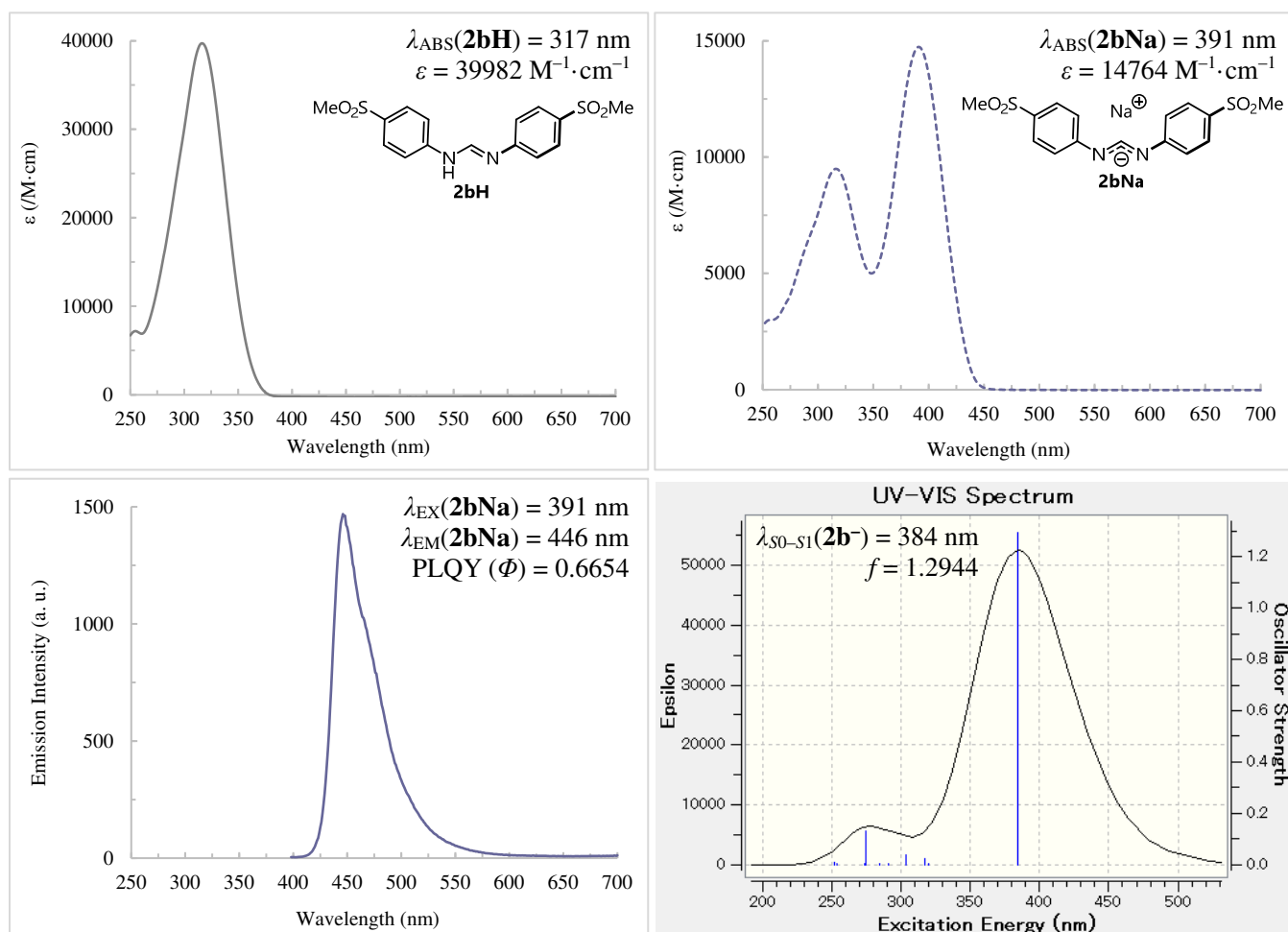


Figure S4. (Top, left) UV-Vis absorption spectrum of **2bH** in THF ($1.0 \times 10^{-5} \text{ M}$). (Top, right) UV-Vis absorption spectra of **2bNa** in THF ($1.0 \times 10^{-4} \text{ M}$). (Bottom, left) emission spectra of **2bNa** in THF ($1.0 \times 10^{-4} \text{ M}$). (Bottom, right) DFT-based simulation of UV-Vis spectrum, the excitation energies, and the oscillator strengths for the optimized geometry of **2b-**.

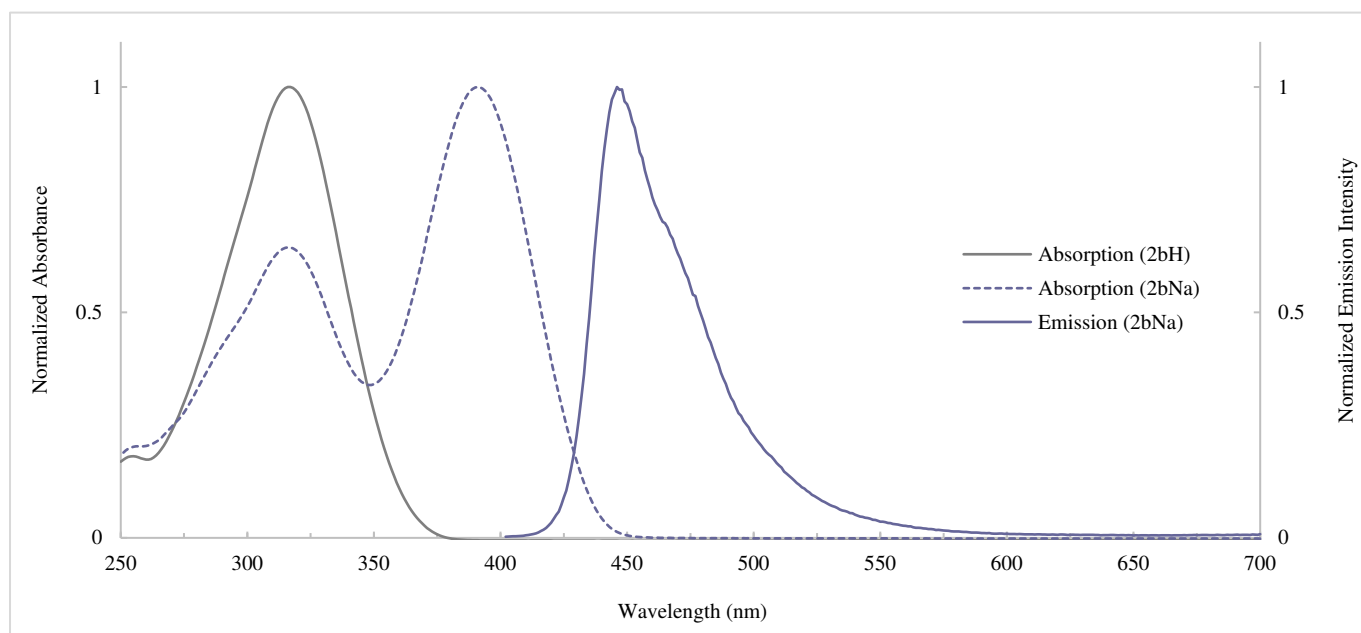


Figure S5. Normalized absorption and emission spectra of **2bH** and **2bNa** in THF.

For **2cH** and **2cNa**:

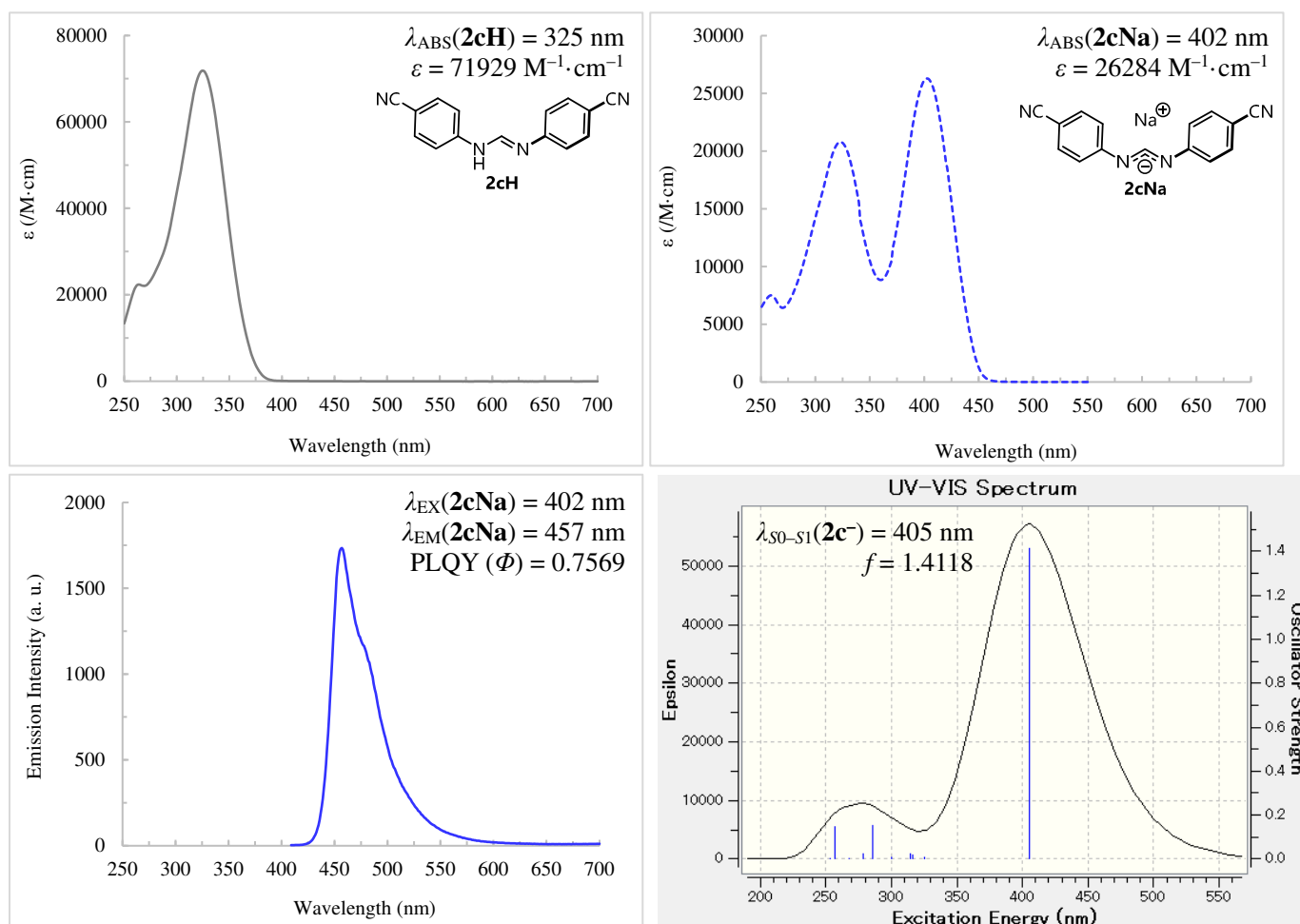


Figure S6. (Top, left) UV-Vis absorption spectrum of **2cH** in THF ($1.0 \times 10^{-5} \text{ M}$). (Top, right) UV-Vis absorption spectra of **2cNa** in THF ($1.0 \times 10^{-4} \text{ M}$). (Bottom, left) emission spectra of **2cNa** in THF ($1.0 \times 10^{-4} \text{ M}$). (Bottom, right) DFT-based simulation of UV-Vis spectrum, the excitation energies, and the oscillator strengths for the optimized geometry of **2c⁻**.

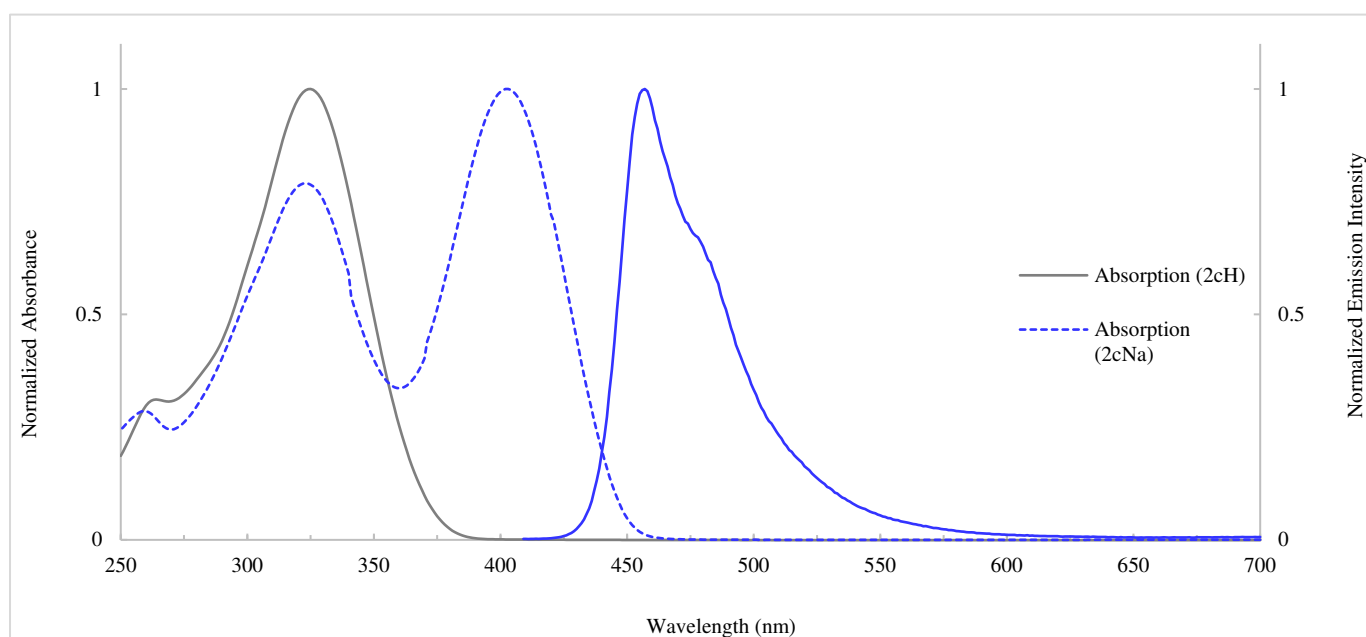


Figure S7. Normalized absorption and emission spectra of **2cH** and **2cNa** in THF.

For **2dH** and **2dNa**:

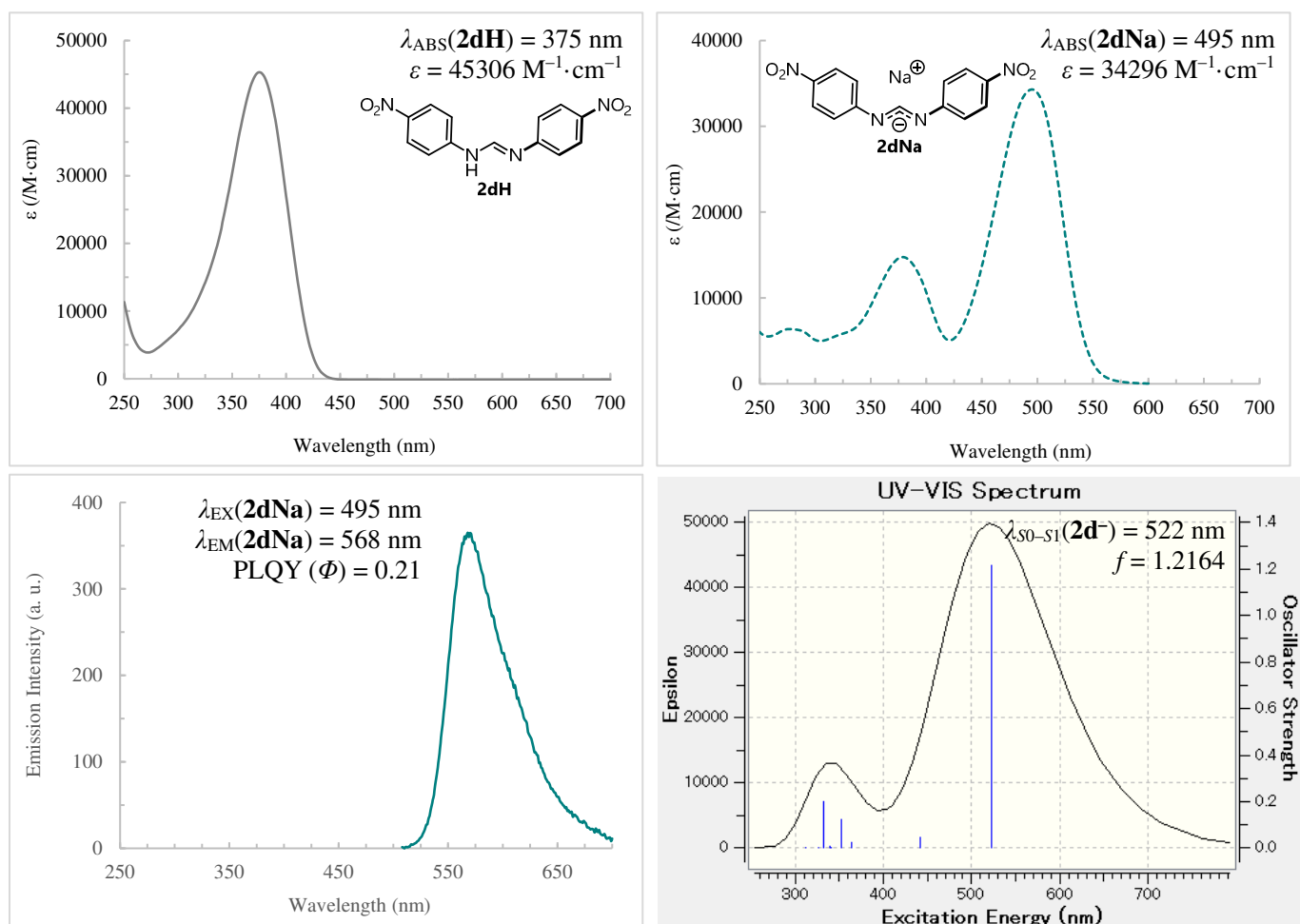


Figure S8. (Top, left) UV-Vis absorption spectrum of **2dH** in THF (1.0 × 10⁻⁵ M). (Top, right) UV-Vis absorption spectra of **2dNa** in THF (1.0 × 10⁻⁴ M). (Bottom, left) emission spectra of **2dNa** in THF (1.0 × 10⁻⁴ M). (Bottom, right) DFT-based simulation of UV-Vis spectrum, the excitation energies, and the oscillator strengths for the optimized geometry of **2d⁻**.

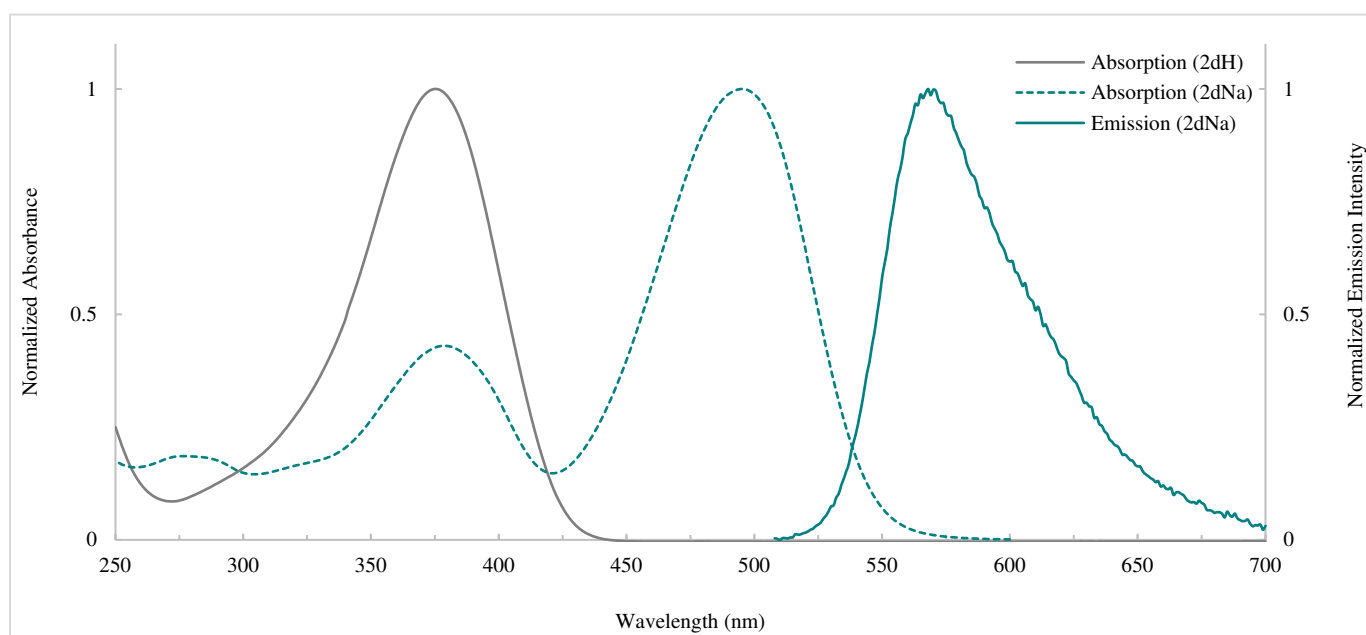


Figure S9. Normalized absorption and emission spectra of **2dH** and **2dNa** in THF.

For **2eH** and **2eNa**:

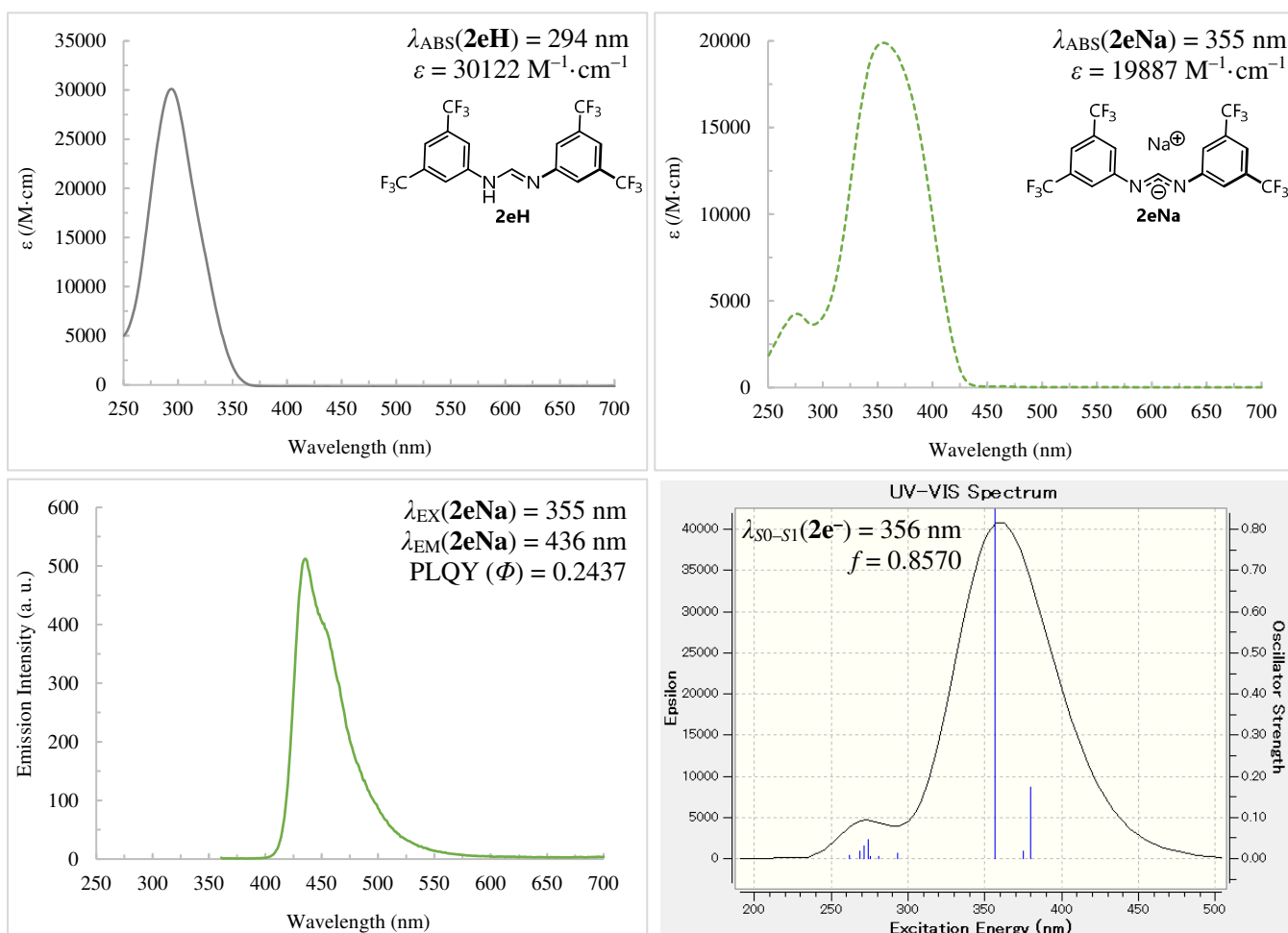


Figure S10. (Top, left) UV-Vis absorption spectrum of **2eH** in THF (1.0×10^{-5} M). (Top, right) UV-Vis absorption spectra of **2eNa** in THF (1.0×10^{-4} M). (Bottom, left) emission spectra of **2eNa** in THF (1.0×10^{-4} M). (Bottom, right) DFT-based simulation of UV-Vis spectrum, the excitation energies, and the oscillator strengths for the optimized geometry of **2e⁻**.

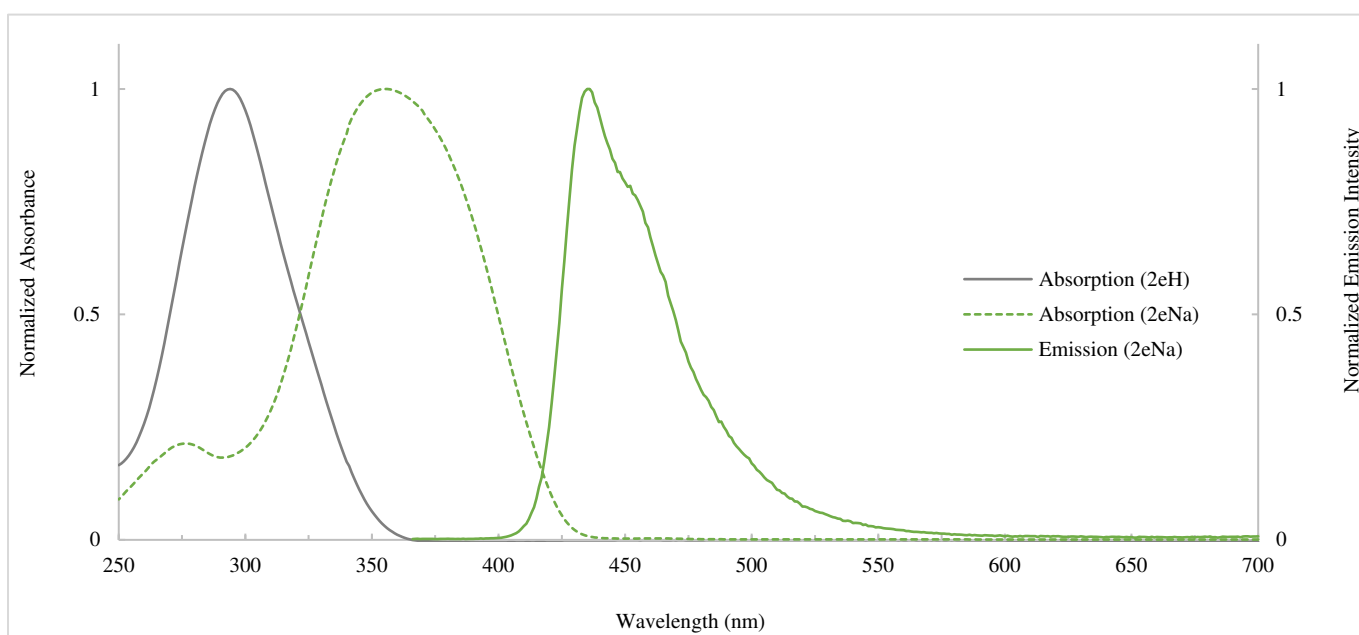


Figure S11. Normalized absorption and emission spectra of **2eH** and **2eNa** in THF.

For **2fH** and **2fNa**:

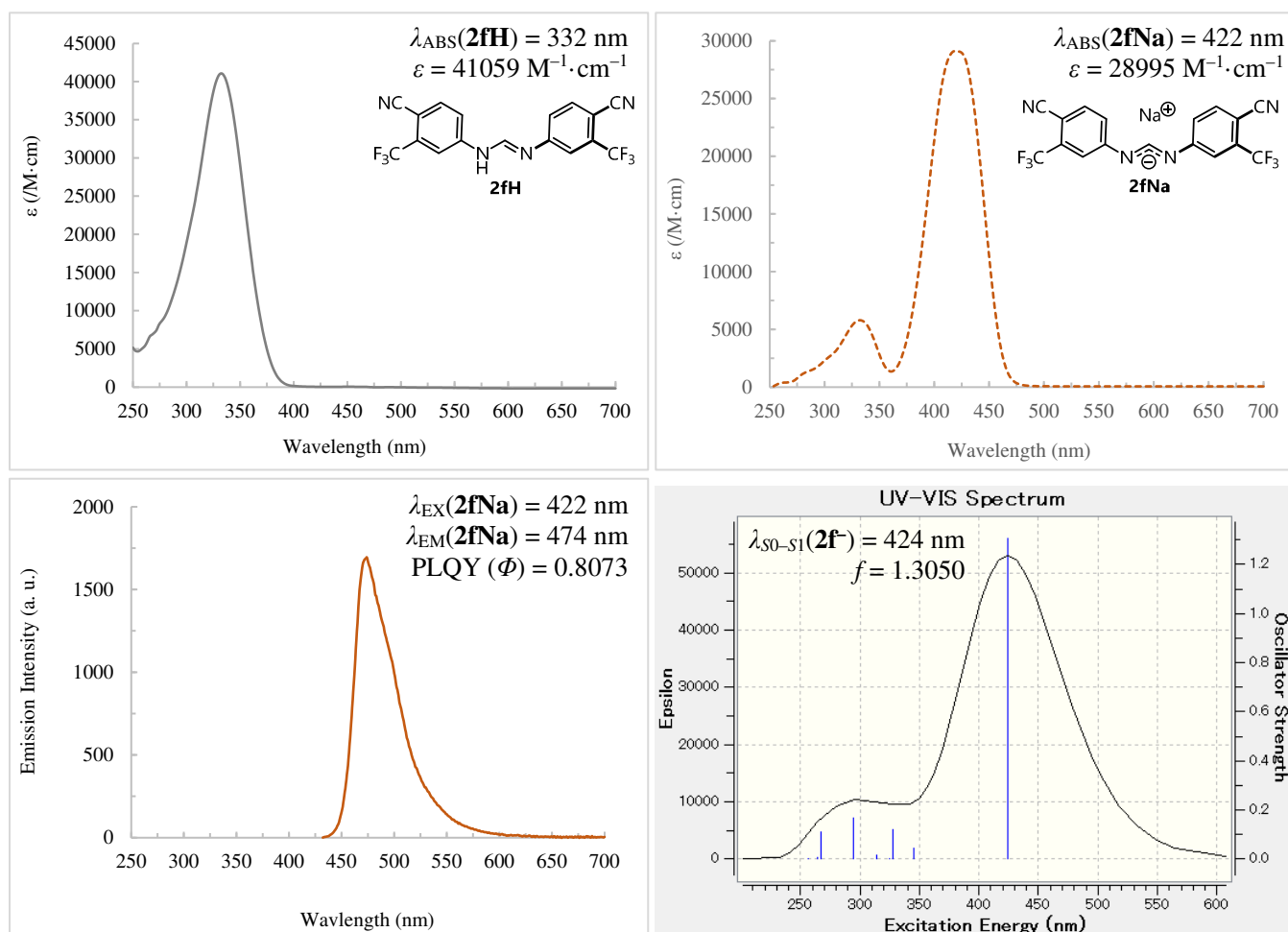


Figure S12. (Top, left) UV-Vis absorption spectrum of **2fH** in THF ($1.0 \times 10^{-5} \text{ M}$). (Top, right) UV-Vis absorption spectra of **2fNa** in THF ($1.0 \times 10^{-4} \text{ M}$). (Bottom, left) emission spectra of **2fNa** in THF ($1.0 \times 10^{-4} \text{ M}$). (Bottom, right) DFT-based simulation of UV-Vis spectrum, the excitation energies, and the oscillator strengths for the optimized geometry of **2f-**.

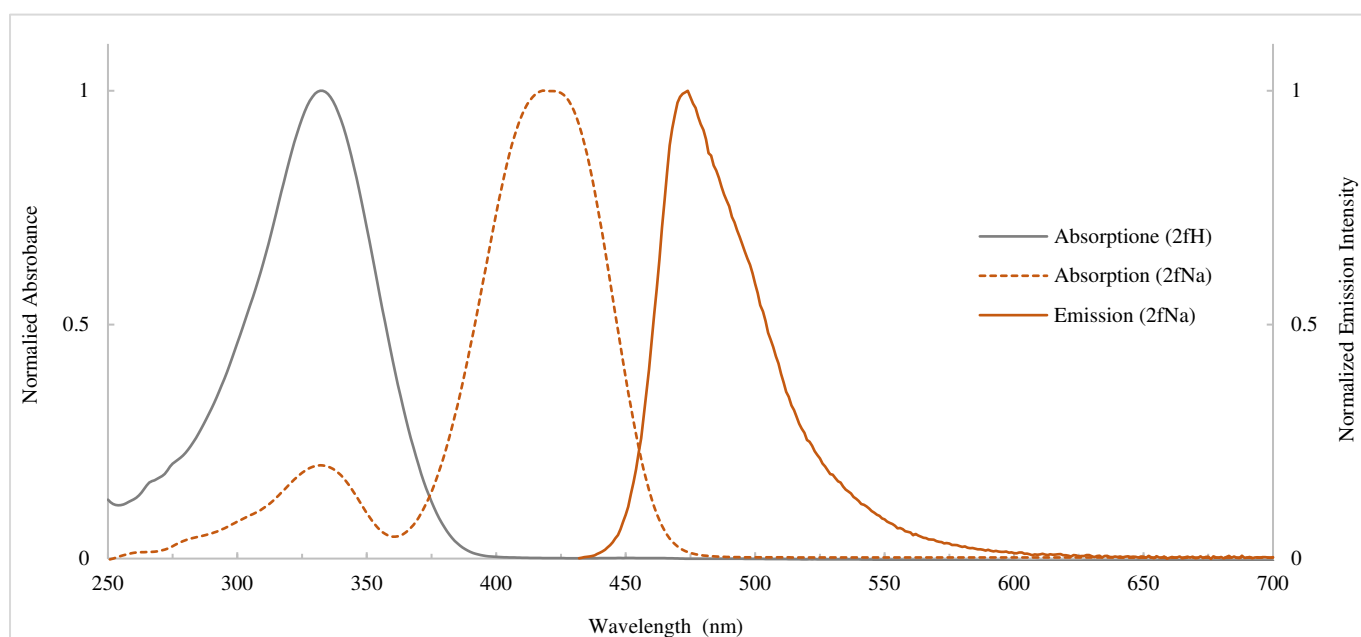


Figure S13. Normalized absorption and emission spectra of **2fH** and **2fNa** in THF.

For **2gH** and **2gNa**:

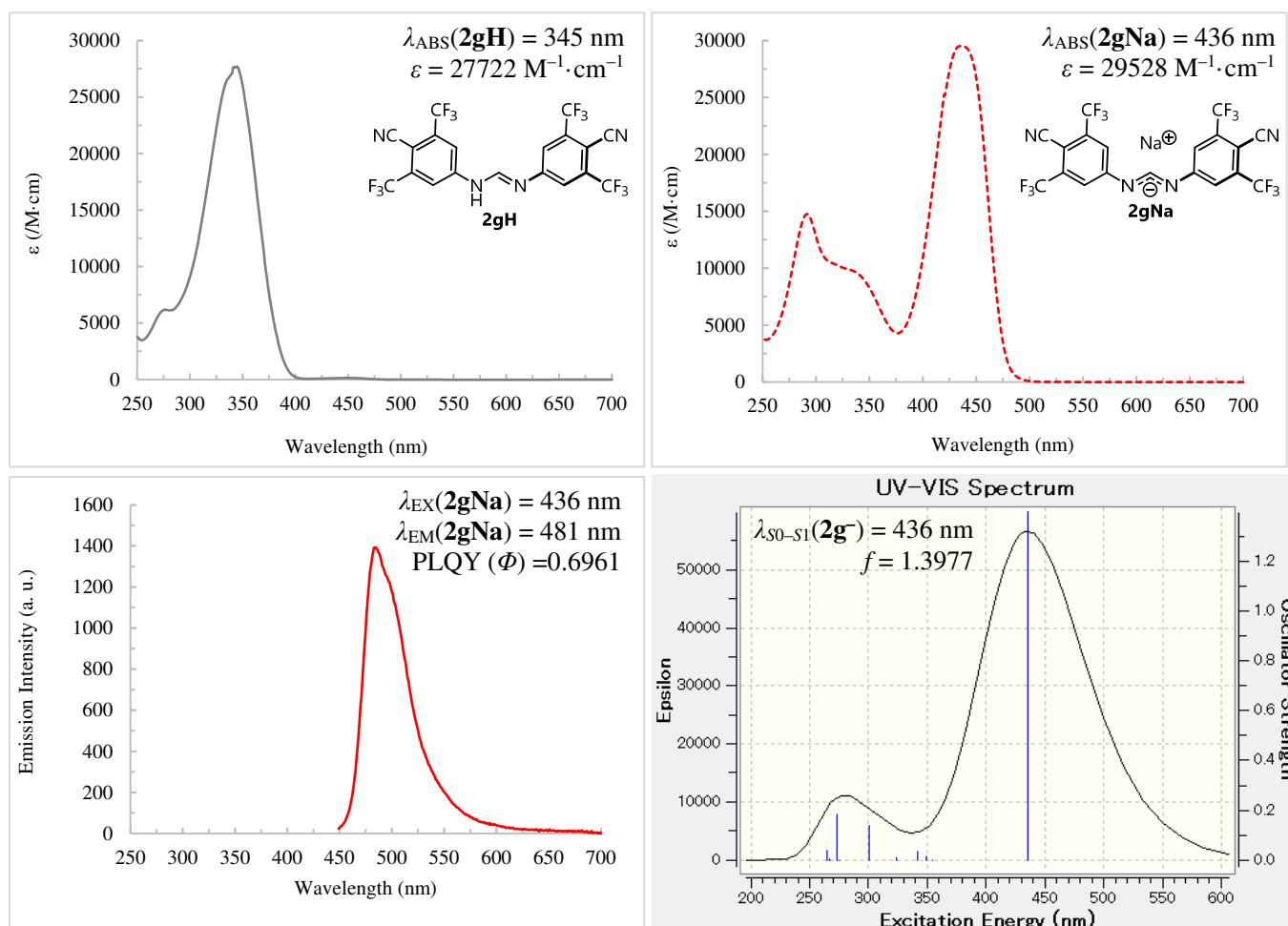


Figure S14. (Top, left) UV-Vis absorption spectrum of **2gH** in THF (1.0×10^{-5} M). (Top, right) UV-Vis absorption spectra of **2gNa** in THF (1.0×10^{-4} M). (Bottom, left) emission spectra of **2gNa** in THF (1.0×10^{-4} M). (Bottom, right) DFT-based simulation of UV-Vis spectrum, the excitation energies, and the oscillator strengths for the optimized geometry of **2g⁻**.

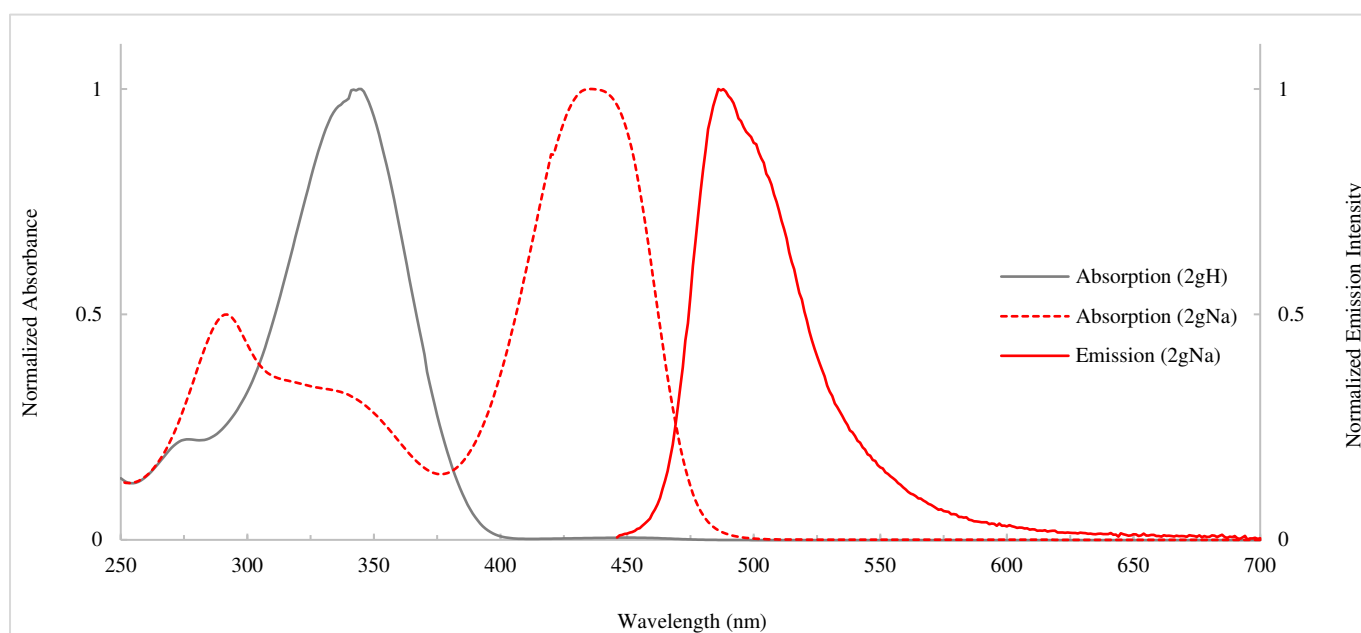
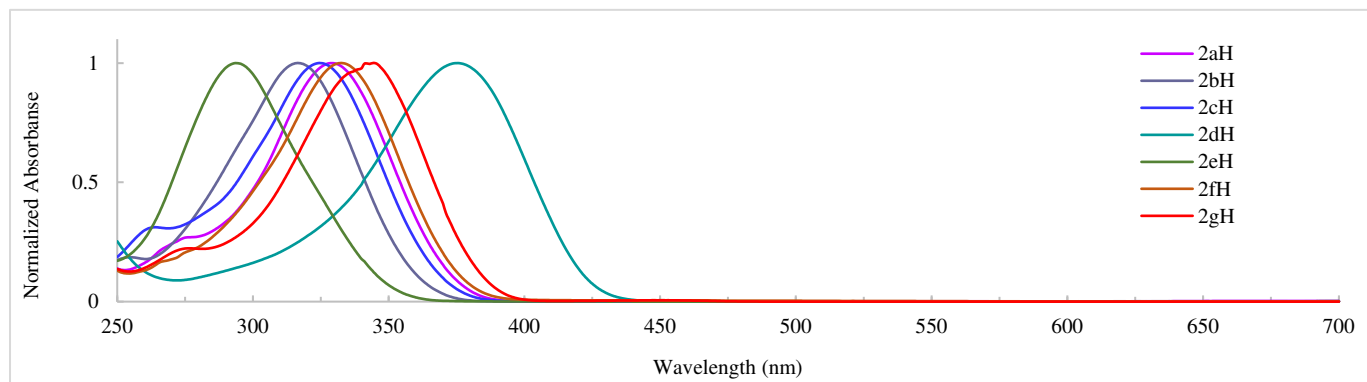
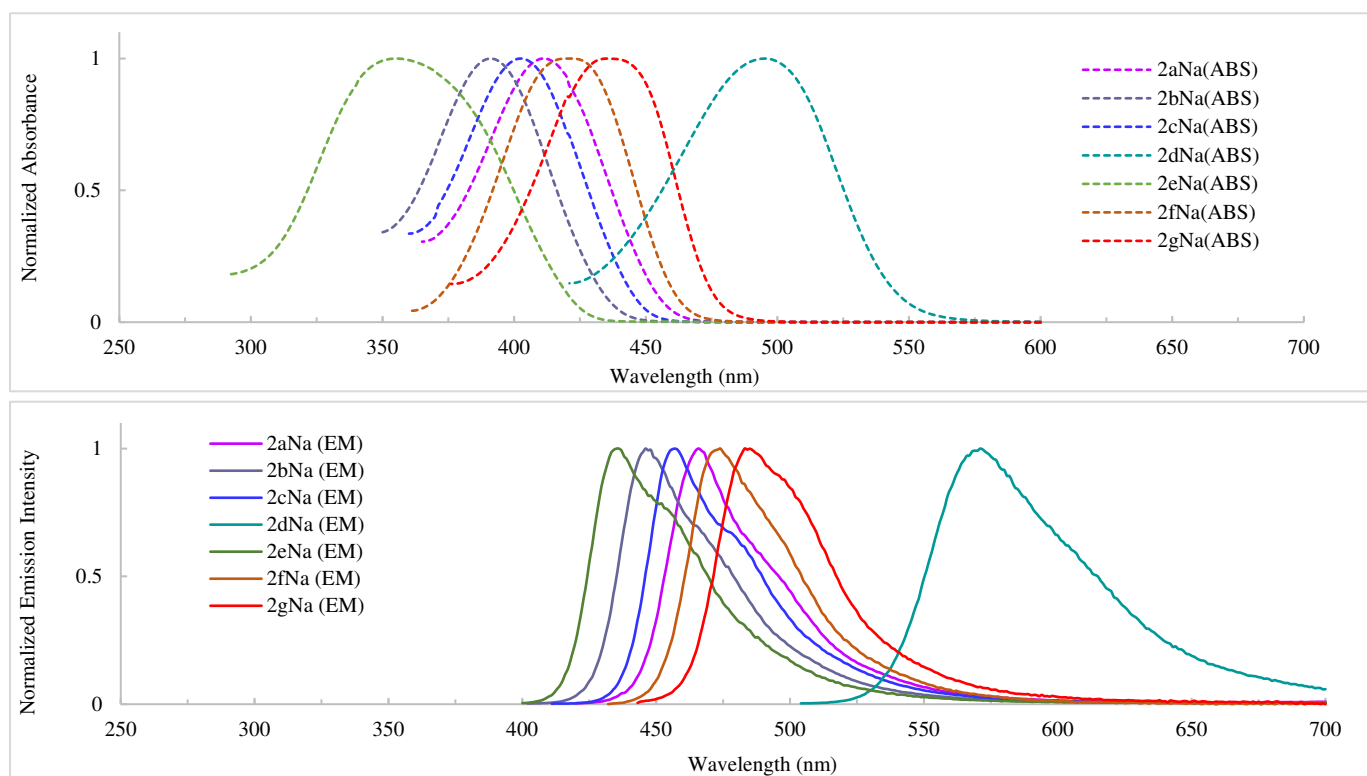


Figure S15. Normalized absorption and emission spectra of **2gH** and **2gNa** in THF.

Table S1. Summary of Photophysical Properties of **2aH–2gH** and **2aNa–2gNa** in THF.

amidine	ϵ ($M^{-1}\cdot cm^{-1}$)	λ_{ABS} (nm)	amidinate	ϵ ($M^{-1}\cdot cm^{-1}$)	λ_{ABS} (nm)	λ_{EM} (nm)	$\Delta\nu$ (cm^{-1})	Φ (%)
2aH	30703	329	2aNa	25362	411	471	3099	78
2bH	39982	317	2bNa	14764	391	446	3154	67
2cH	71929	325	2cNa	26284	402	457	2994	76
2dH	45306	375	2dNa	34286	495	568	2596	21
2eH	30122	294	2eNa	19887	355	436	5233	24
2fH	41059	332	2fNa	28995	422	474	2600	81
2gH	27722	345	2gNa	29528	436	481	2146	65

2aH–2gH: 1.0×10^{-5} M, **2aNa–2gNa:** 1.0×10^{-4} M.

**Figure S16.** Normalized absorption of **2aH–2gH** in THF.**Figure S17.** (Top) normalized absorption spectra of **2aNa–2gNa** in THF. (Bottom) normalized emission spectra of **2aNa–2gNa**.

(E) Cation Effects on the Absorption & Emission Spectra

For **2gNa** in THF (1.0×10^{-5} M):

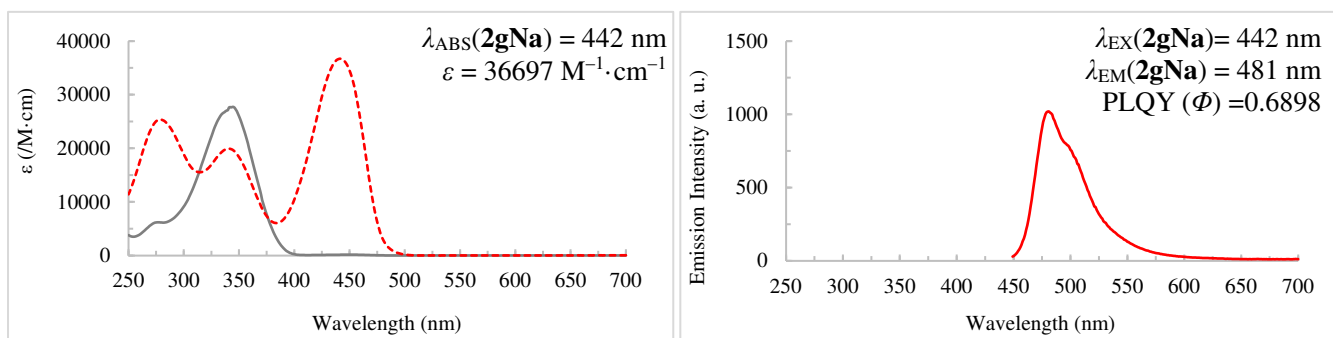


Figure S18. (Left) UV-Vis absorption spectrum of **2gH** and **2gNa**. (Right) emission spectrum of **2gNa**.

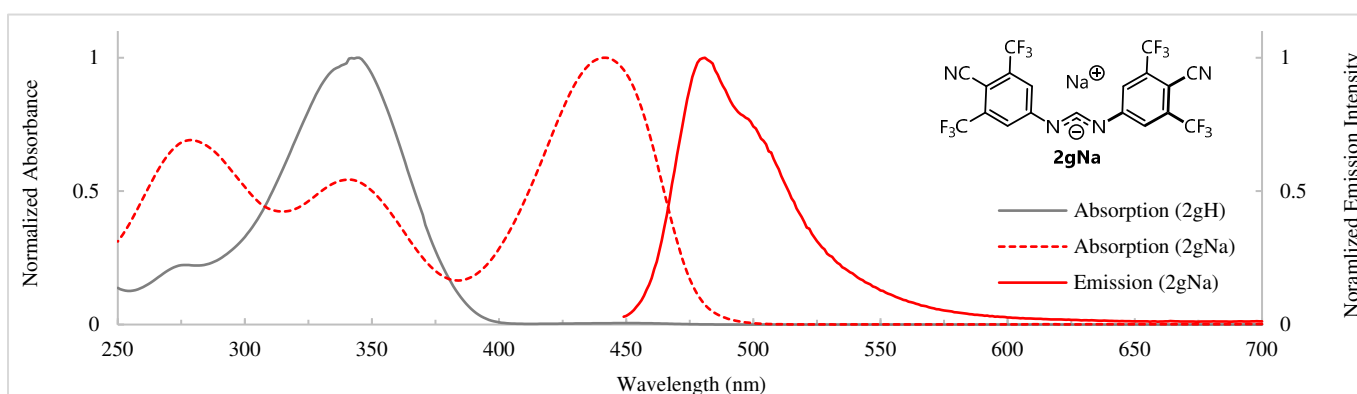


Figure S19. Normalized absorption and emission spectra of **2gH** and **2gNa** in THF.

For **2gLi** in THF (1.0×10^{-5} M):

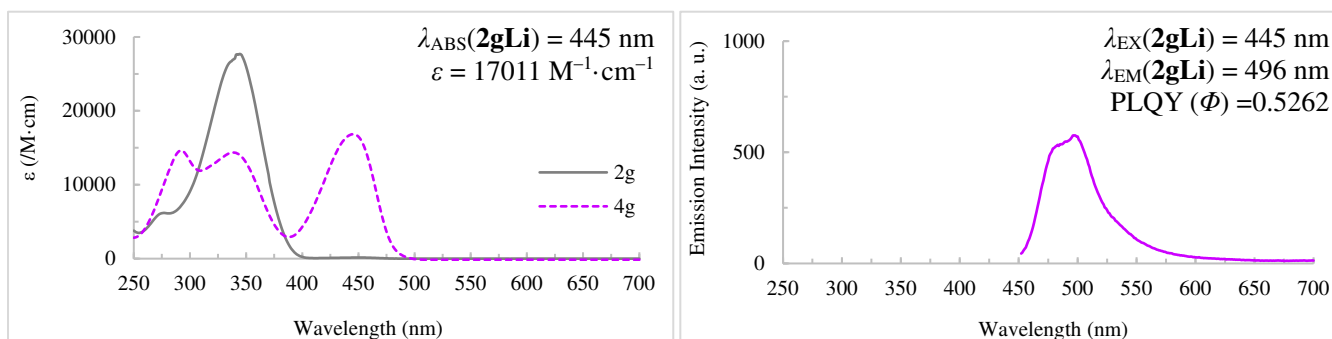


Figure S20. (Left) UV-Vis absorption spectrum of **2gH** and **2gLi**. (Right) emission spectrum of **2gLi**.

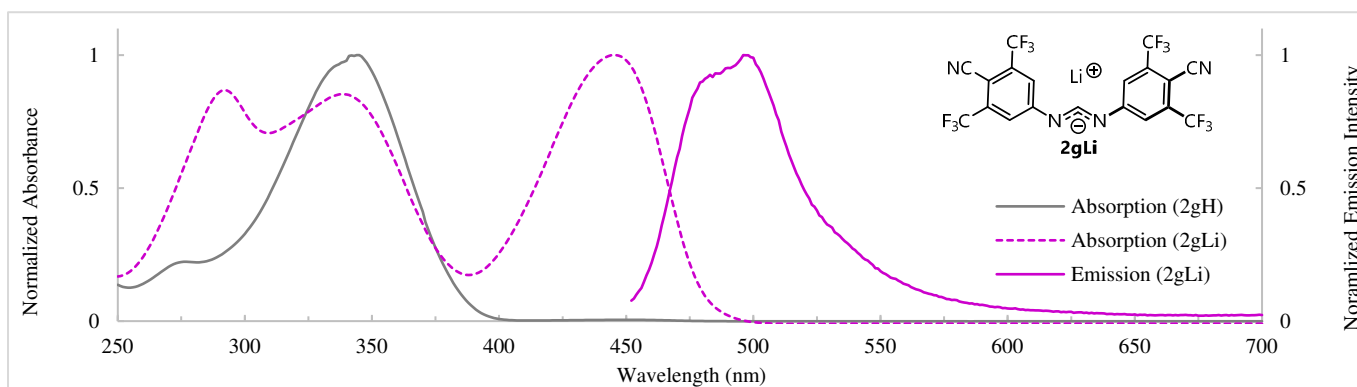


Figure S21. Normalized absorption and emission spectra of **2gH** and **2gLi** in THF.

For **2gNa(15c5)** in THF (1.0×10^{-5} M):

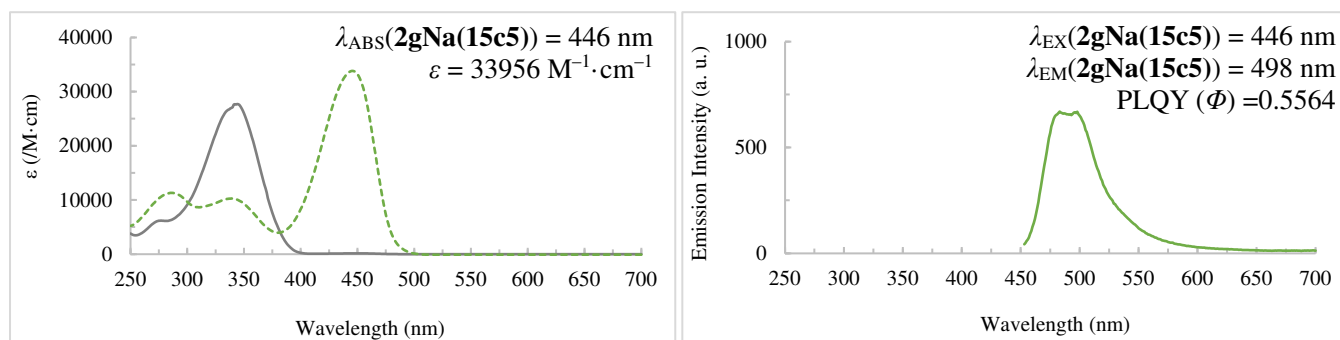


Figure S22. (Left) UV-Vis absorption spectrum of **2gH** and **2gNa(15c5)**. (Right) emission spectrum of **2gNa(15c5)**.

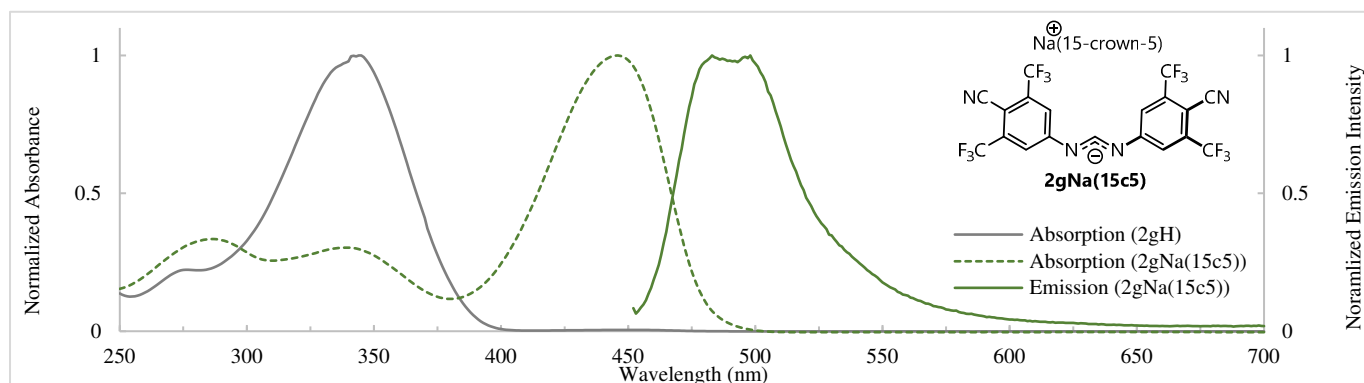


Figure S23. Normalized absorption and emission spectra of **2gH** and **2gNa(15c5)** in THF.

For **2gK** in THF (1.0×10^{-5} M):

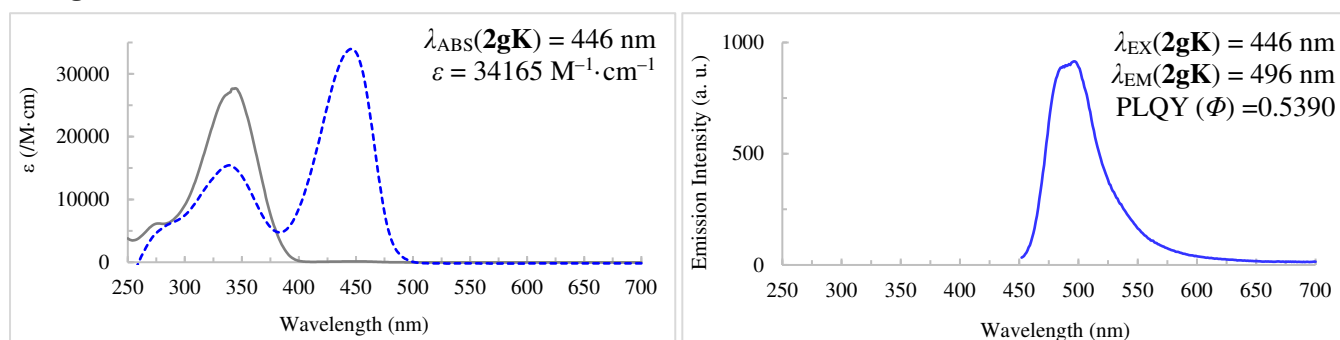


Figure S24. (Left) UV-Vis absorption spectrum of **2gH** and **2gK**. (Right) emission spectrum of **2gK**.

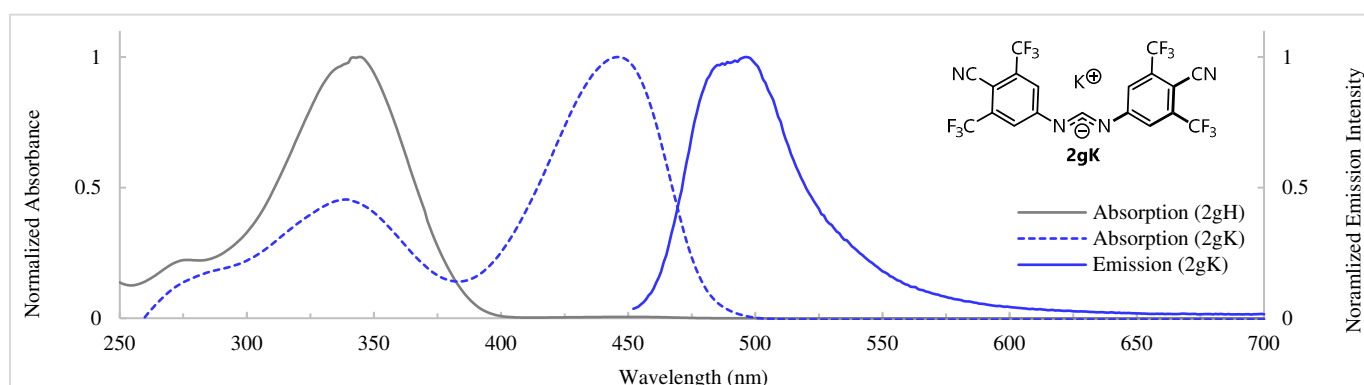


Figure S25. Normalized absorption and emission spectra of **2gH** and **2gK** in THF.

For **2gHdbu** in THF (1.0×10^{-5} M):

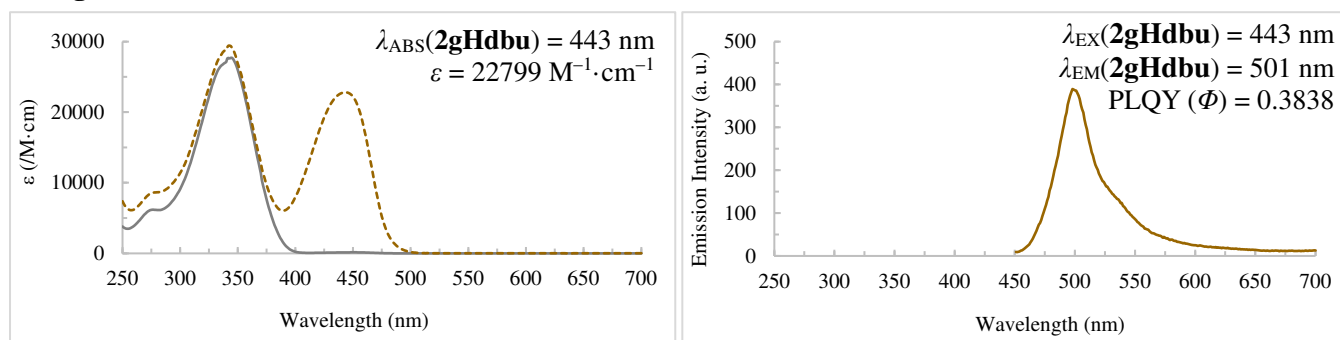


Figure S26. (Left) UV-Vis absorption spectrum of **2gH** and **2gHdbu**. (Right) emission spectrum of **2gHdbu**.

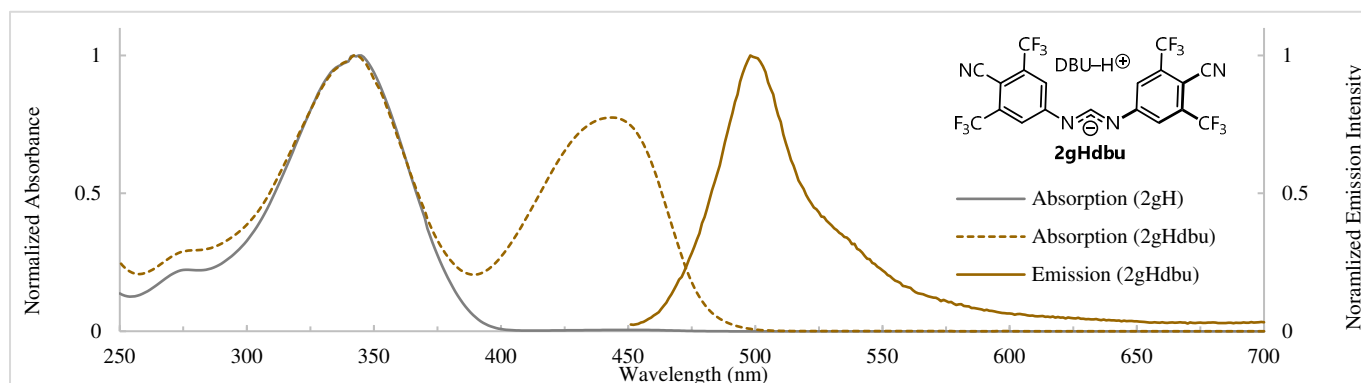


Figure S27. Normalized absorption and emission spectra of **2gH** and **2gHdbu** in THF.

Table S2. Summary of Photophysical Properties of **2gM** in THF.

cation	2gM	ϵ ($M^{-1}\cdot cm^{-1}$)	λ_{ABS} (nm)	λ_{EM} (nm)	$\Delta\nu$ (cm^{-1})	Φ (%)
Li ⁺	2gLi	17011	445	496	2311	53
Na ⁺	2gNa	36697	442	481	1834	69
[Na(15-crown-5)] ⁺	2gNa(15c5)	33955	446	498	2341	56
K ⁺	2gK	34165	446	496	2260	54
DBU-H ⁺	2gHdbu	22799	443	498	2493	38

2gM: 1.0×10^{-5} M

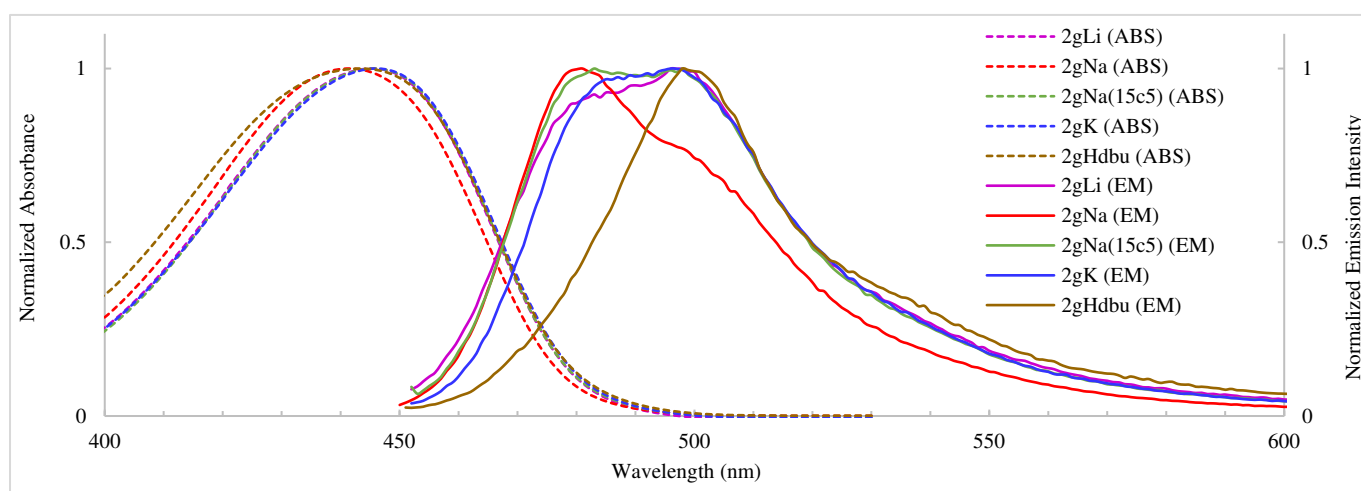


Figure S28. Normalized absorption and emission spectra of **2gNa-2gHdbu** in THF.

(F) Solid-State Emission Properties

Table S3. Solid-State Emission of **2gNa–2gDBUH**.

cation	2gM	λ_{EX} (nm)	λ_{EM} (nm)	Φ (%)
Li ⁺	2gLi	445	498	9
Na	2gNa	442	504	14
Na(thf) ₂ (OH ₂)	2gNa(xt)	442	498	14
[Na(15-crown-5)] ⁺	2gNa(15c5)	446	524	29
K ⁺	2gK	446	499	13
DBU–H ⁺	2gHdbu	443	538	14

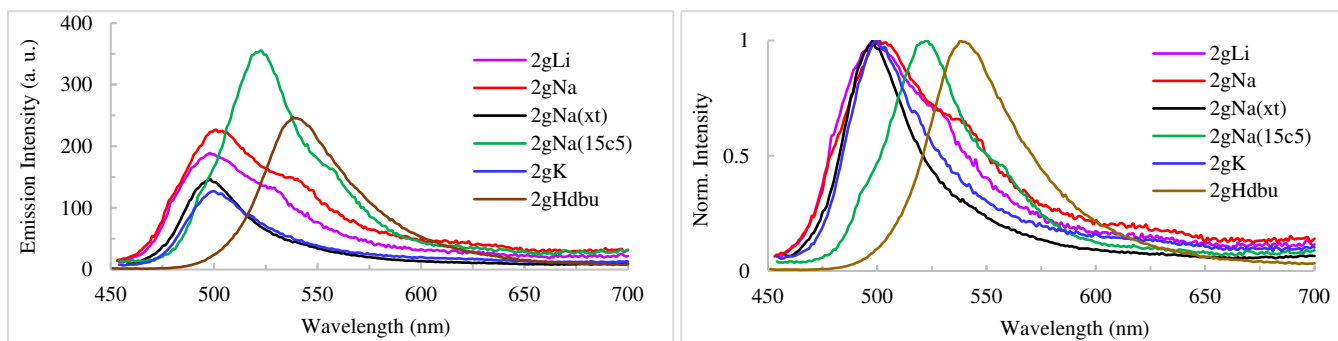


Figure S29. (Left) solid-state emission spectra of **2gM**. (Right) normalized spectra.

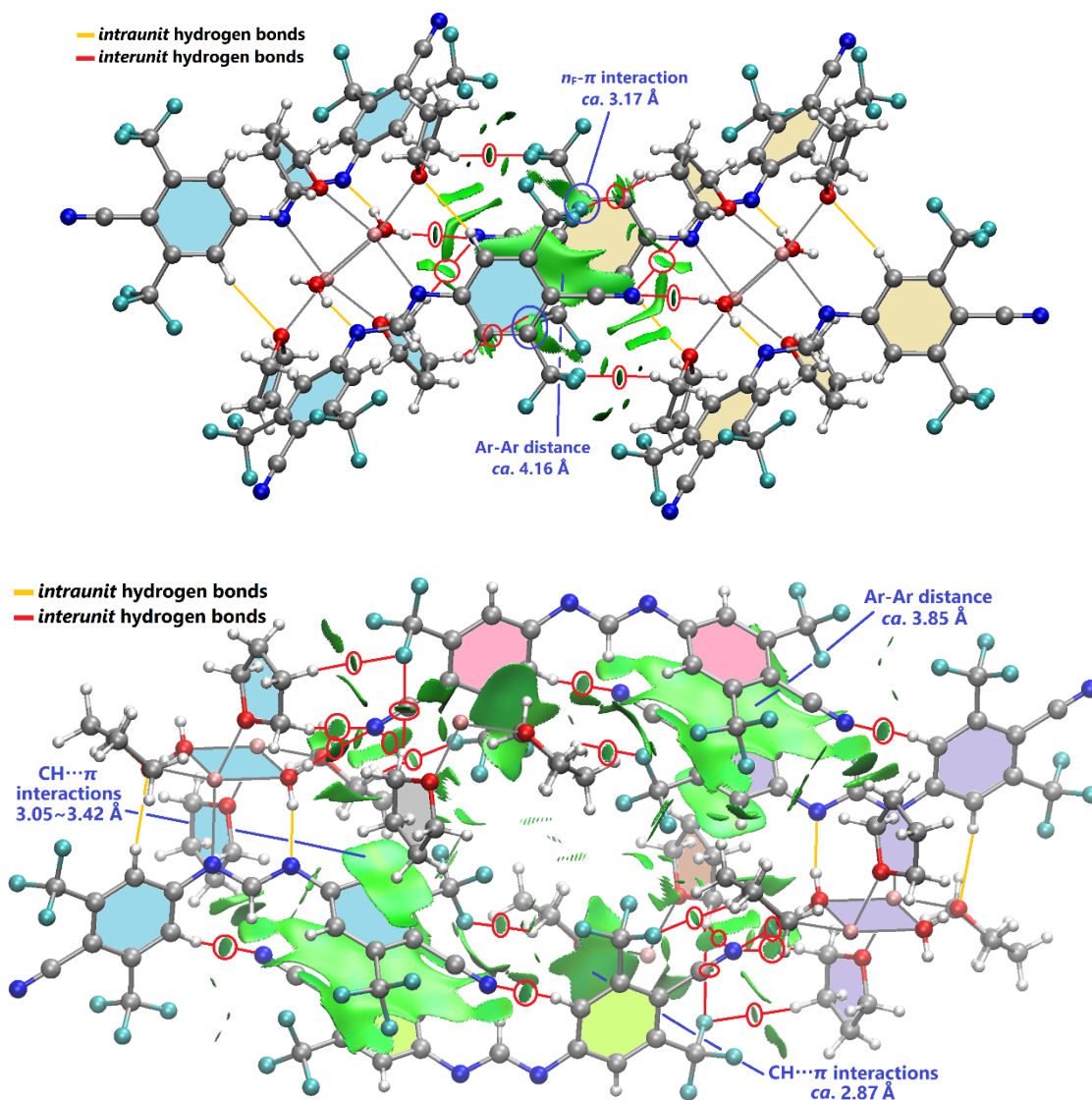


Figure S30. Mappings of intra- and intermolecular interactions of **[2gNa(thf)₂(OH₂)₂]** in the crystal structures. (Top) Interunit interactions of “X axis”. (Bottom) Interunit interactions of “Y and Z axes”.

(G) Solvent Effects on the Absorption & Emission

Table S4. Photophysical Properties of **2gNa(15c5)** in Various Solvents.

solvent	ϵ_r	ϵ ($M^{-1}\cdot cm^{-1}$)	λ_{ABS} (nm)	λ_{EM} (nm)	$\Delta\nu$ (cm^{-1})	Φ (%)	τ (ns)
toluene	2.38	14999	432	474	2078	91	-
CHCl ₃	4.81	11615	430	478	2362	80	-
THF	7.58	33956	446	498	2341	56	1.54
MeCN	35.9	94224	449	497	2126	0.56	3.37
DMSO	46.5	59932	459	509	2164	4.3	-

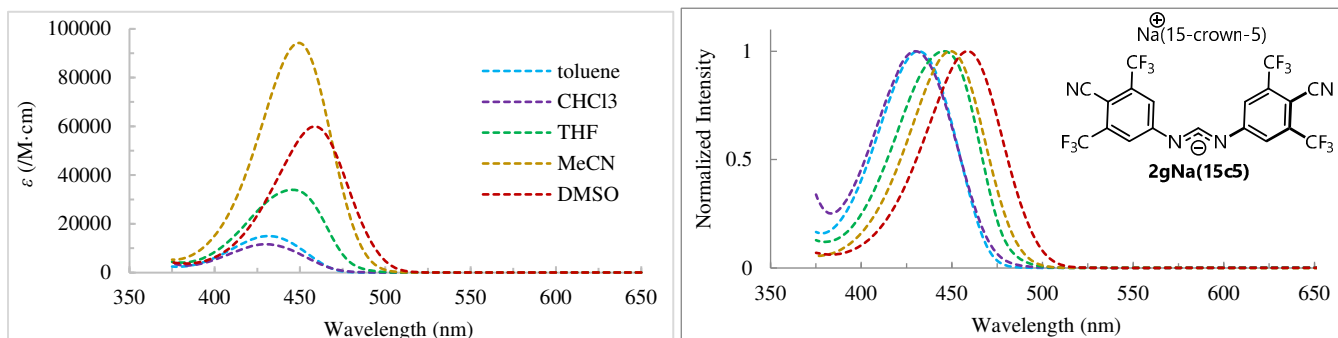


Figure S31. (Left) UV-Vis absorption spectra of **2gNa(15c5)** in various solvents (1.0×10^{-5} M). (Right) normalized spectra.

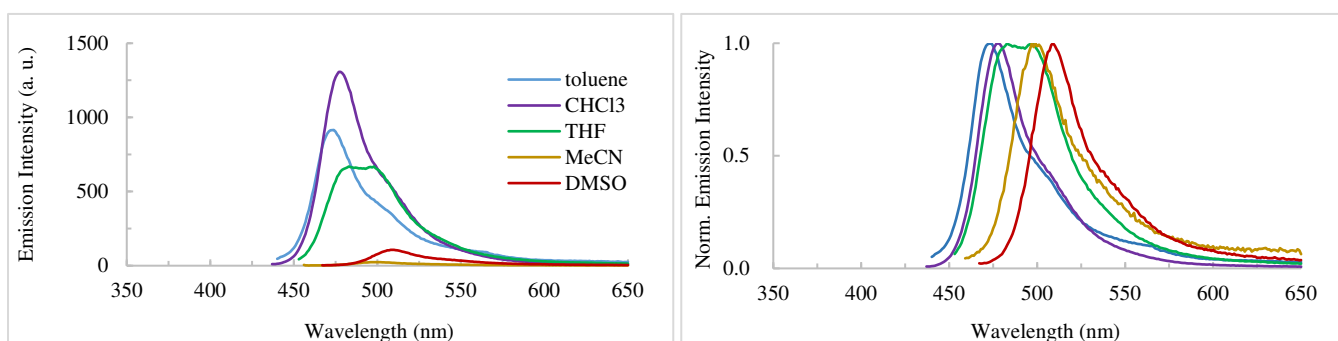


Figure S32. (Left) Emission spectra of **2gNa(15c5)** in various solvents (1.0×10^{-5} M). (Right) normalized spectra.

Table S5. Lippert-Mataga plot for **2gNa(15c5)**.

solvent	ϵ_r	n	Δf	λ_{ABS} (nm)	ν_{ABS} (cm^{-1})	λ_{EM} (nm)	ν_{EM} (cm^{-1})	$\Delta\nu$ (cm^{-1})
toluene	2.38	1.496	0.013504	431.5	23175.0	474.0	21097.0	2077.9
CHCl ₃	4.81	1.443	0.149202	429.5	23282.9	478.0	20920.5	2362.4
THF	7.58	1.408	0.209297	446.0	22421.5	498.0	20080.3	2341.2
MeCN	35.9	1.344	0.304587	449.5	22246.9	497.0	20120.7	2126.2
DMSO	46.5	1.477	0.263734	458.5	21810.3	509.0	19646.4	2163.9

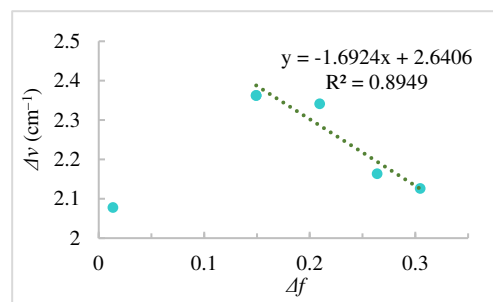
Lippert-Mataga equation:

$$\Delta\nu = \frac{2(\Delta\mu)^2}{hca^3} \Delta f + const. \quad (\text{eq. 1})$$

$$\Delta\nu = \nu_{ABS} - \nu_{EM} \quad (\text{eq. 2})$$

$$\Delta\mu = \mu_{EX} - \mu_{GR} \quad (\text{eq. 3})$$

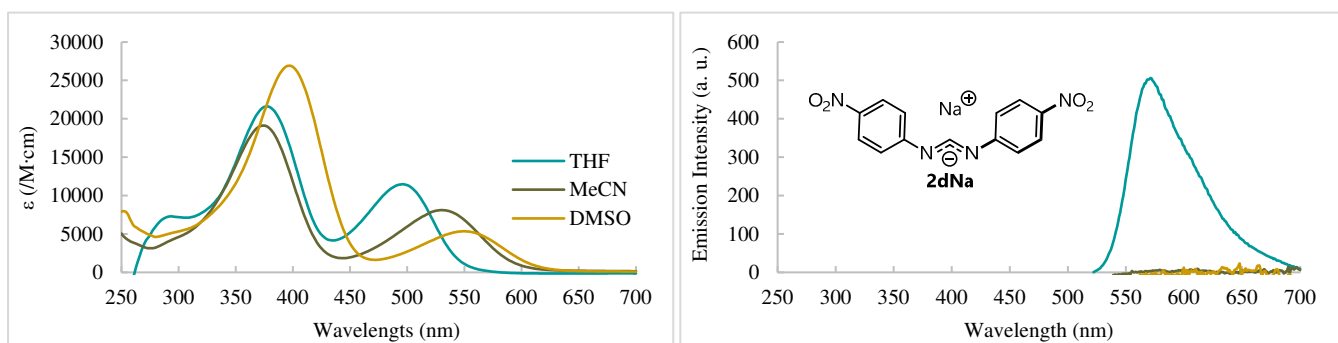
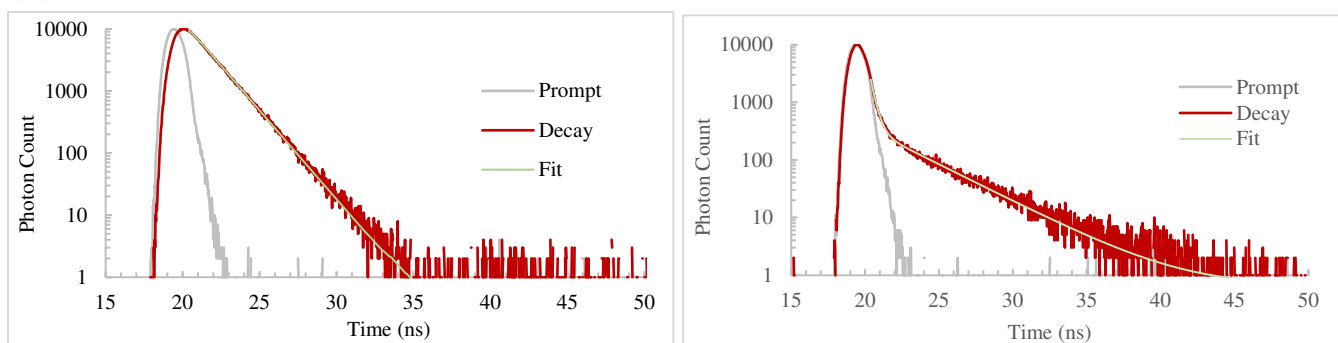
$$\Delta f = \frac{\epsilon - 1}{2\epsilon + 1} - \frac{n^2 - 1}{2n^2 + 1} \quad (\text{eq. 4})$$



(ϵ_r : dielectric constant, n : refractive index, h : Planck constant (6.6256×10^{-27}), c : speed of light (2.9979×10^{10} cm/s), a : Onsager radius (for **2g**: 7.22 \AA)^{S8}, μ : dipole moment (for **2gNa(15c5)** anion: $\mu_{EX} = 0.07$ Debye, $\mu_{GR} = 0.99$ Debye).

Table S6. Photophysical Properties of **2dNa** in Solvents.

solvent	ϵ_r	ϵ ($M^{-1}\cdot cm^{-1}$)	λ_{ABS} (nm)	λ_{EM} (nm)	$\Delta\nu$ (cm^{-1})	Φ (%)
THF	7.58	11469	469	571	3809	56
MeCN	35.9	8102	530	—	—	<0.1
DMSO	46.5	5346	550	—	—	<0.1

**Figure S33.** (Left) UV-Vis absorption of **2dNa** in solvents (1.0×10^{-5} M). (Right) emission spectra of **2dNa** (1.0×10^{-4} M).**(H) Emission Lifetimes**

$$\tau = 1.54 \text{ ns (100\%), } \chi^2 = 1.096$$

$$\tau_1 = 0.32 \text{ ns (38.7\%), } \tau_2 = 3.37 \text{ ns (61.3\%), } \chi^2 = 1.195$$

Figure S34. (Left) emission decay of **2gNa(15c5)** in THF (1.0×10^{-5} M, argon-bubbled). (Right) emission decay of **2gNa(15c5)** in MeCN (1.0×10^{-5} M, argon-bubbled).*

*The emission in MeCN would be a prompt fluorescence (no delayed emission), though it appears to exhibit biexponential decay. The emission was extremely weak in MeCN, thus overlapping to the measurement threshold.

(I) Temperature Dependence of Photoluminescence

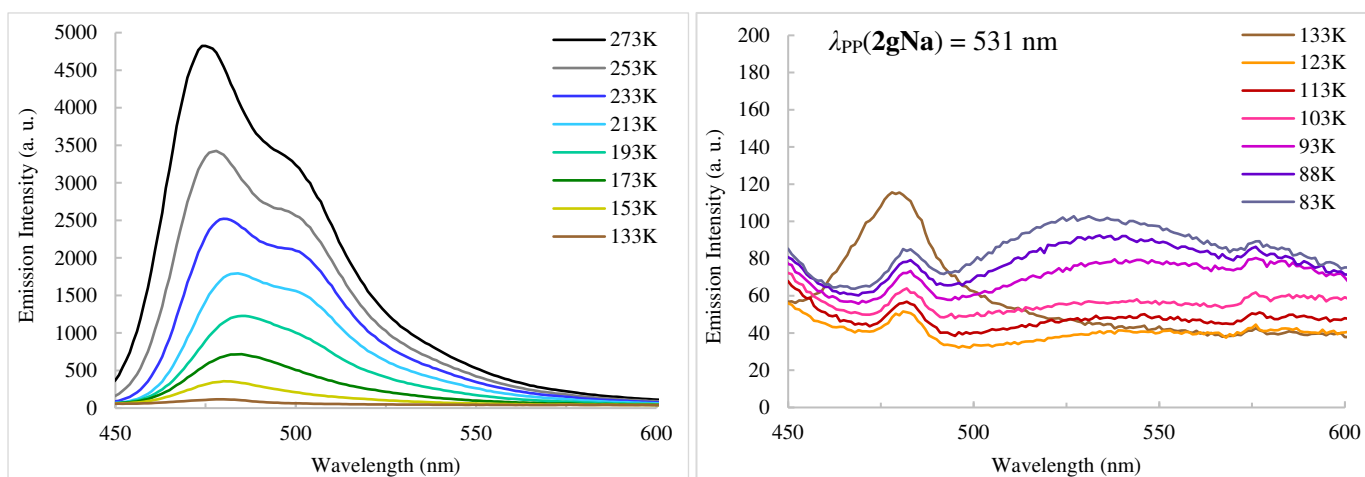


Figure S35. Variable-temperature emission spectra of **2gNa** in 2MeTHF (1.0×10^{-5} M) at 273–133 K (left) and 133–83 K (right) under 421 nm photoexcitation.

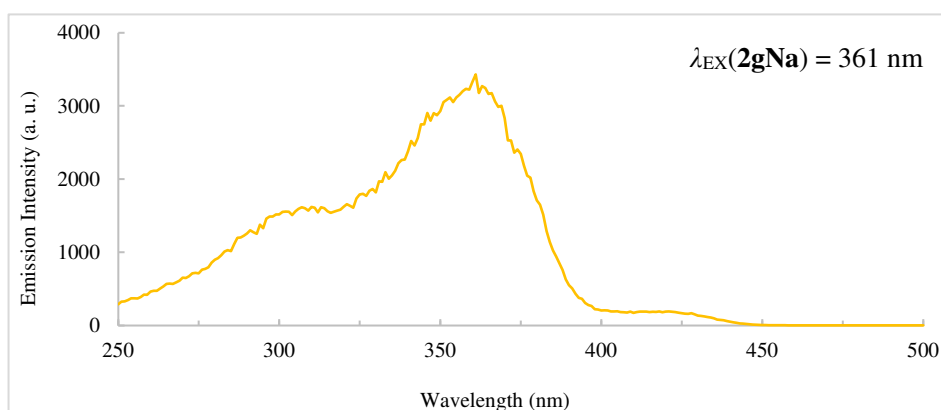


Figure S36. Excitation spectrum of **2gNa** in 2MeTHF (1.0×10^{-5} M) at 77 K corresponding to the phosphorescence with the emission maximum at 531 nm.

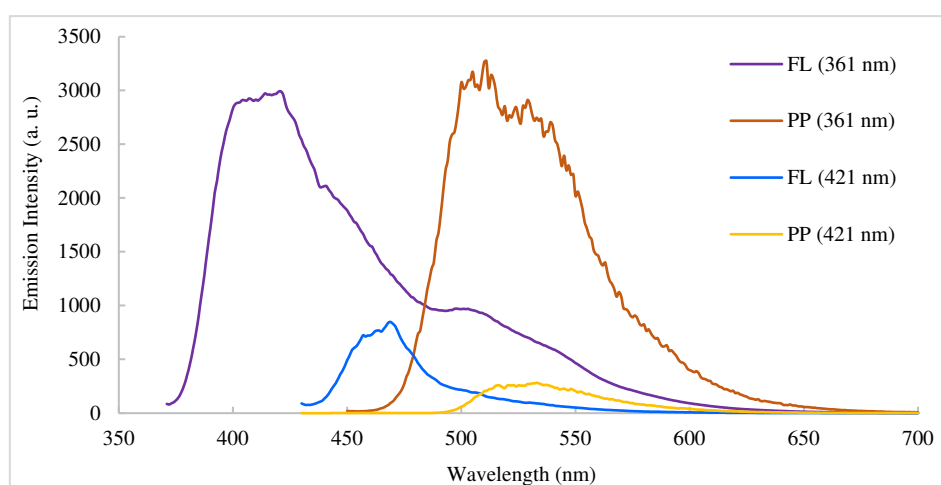


Figure S37. Fluorescence (FL) and phosphorescence spectra of **2gNa** in 2MeTHF at 77 K upon 361- and 421-nm irradiation (delay: 10 ms). FL: fluorescence, PP: phosphorescence.

(J) Computational Details

All quantum chemical calculations were performed using Gaussian 09 program package.^{S9} All the optimized geometries, frequencies, and zero-point energies were calculated using B3LYP^{S10} functional including a D3 version of Grimme's dispersion with Becke-Johnson damping (D3(BJ)).^{S11} The geometry optimizations and frequency calculations were carried out with 6-31+G(d,p) basis set. The geometry optimizations were performed without any symmetry constraint followed by analytical frequency calculations to confirm that a minimum had been reached. A single-point energy calculations were conducted with the polarized valence triple- ζ basis set 6-311++G(2d,p) basis set. Solvent effects (THF; $\epsilon = 7.58$) were introduced for all calculations by means of the polarizable continuum models implemented in Gaussian 09. SMD^{S12} model was employed for the single-point calculations at the geometries that optimized with IEFPCM^{S13} model for all the minima.

The electronic energies and the Gibbs energies at 298.15 K and 1 atm were obtained by adding the thermal energy corrections and the Gibbs energy corrections derived from the analytical frequency calculations to the single-point energies, respectively. The energy levels of the frontier orbitals (HOMO and LUMO(+ x) orbitals), excitation energies, absorption (or emission) wavelengths, and the oscillator strengths were estimated by the time-dependent (TD) calculation of each optimized ground-state geometries at TD-B3LYP-D3(BJ)/6-311++G(2d,p)/SMD(THF). For the S_1 excited states, the same levels of theory were used to estimate the above parameters against each optimized excited-state geometries at TD-B3LYP-D3(BJ)/6-31+G(d,p)/IEFPCM(THF). These calculations involve a certain margin error.

(J-1) Frontier Orbital Energies, Excitation Parameters, and NBO Analysis of *N,N'*-Diarylformamidinate Anions

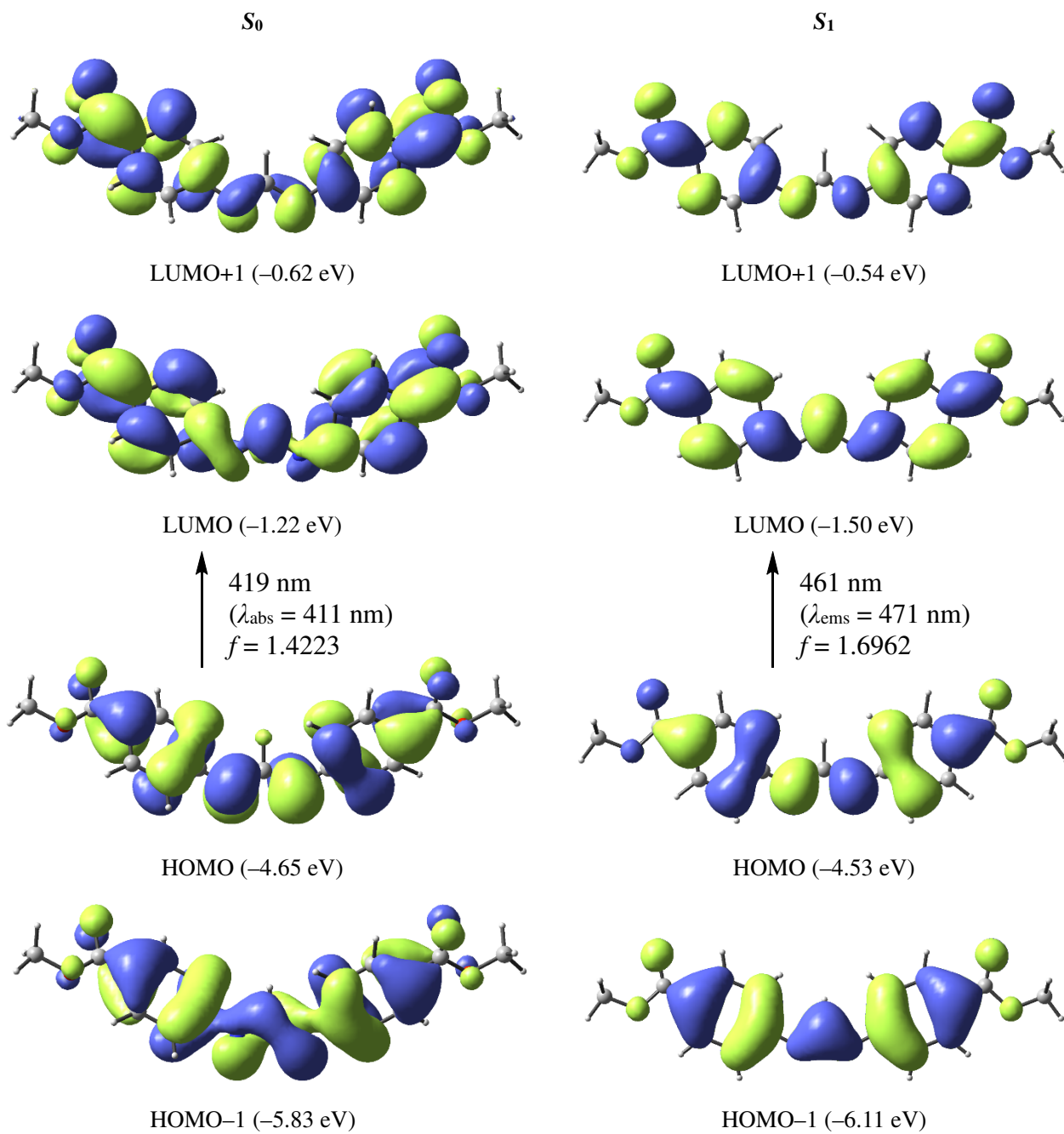


Figure S38. S_0 - and S_1 -state MOs, orbital energies, excitation energies, and oscillator strengths of $2a^-$.

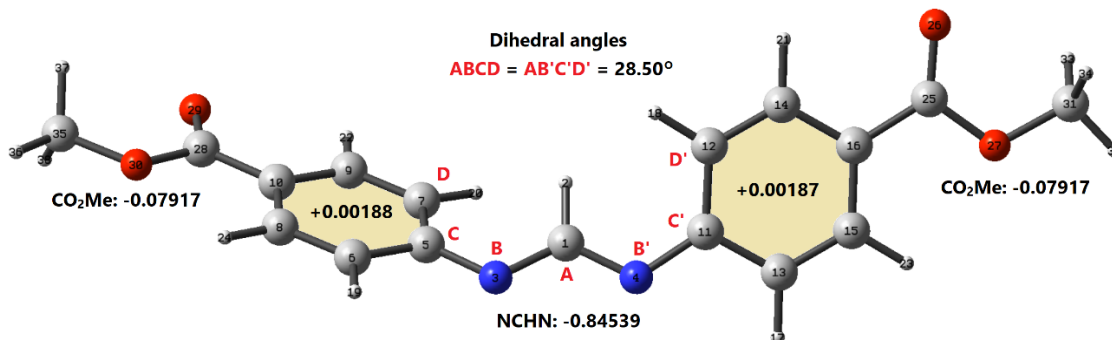


Figure S39. Dihedral angles and the sum of natural atomic charges of diazaallyl, aryl, and electron-withdrawing groups of $2a^-$ (S_0).

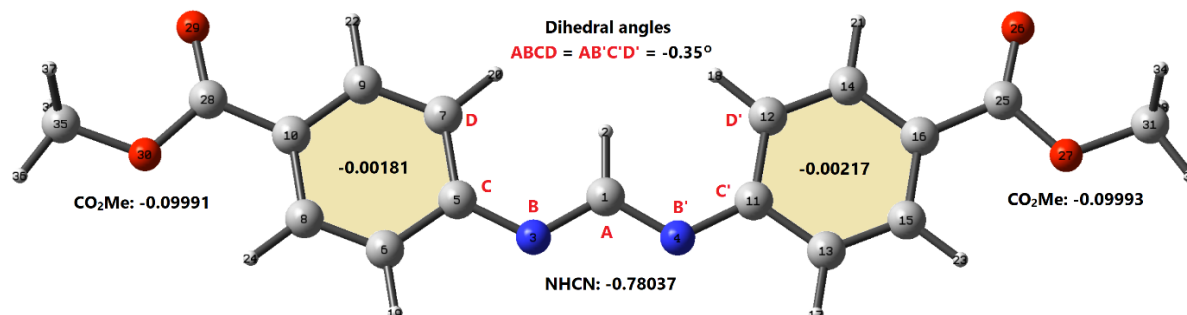


Figure S40. Dihedral angles and the sum of natural atomic charges of diazaallyl, aryl, and electron-withdrawing groups of $2a^-$ anion (S_1).

Table S7. Natural atomic charges of $2a^-$ at the S_0 and S_1 states.

S_0						S_1					
NCHN	NPA (δ)	Ar1	NPA (δ)	Ar2	NPA (δ)	NCHN	NPA (δ)	Ar1	NPA (δ)	Ar2	NPA (δ)
C 1	0.30242	C 5	0.18412	C 11	0.18412	C 1	0.41673	C 5	0.18079	C 11	0.18080
H 2	0.12598	C 6	-0.24335	C 12	-0.27349	H 2	0.12652	C 6	-0.24566	C 12	-0.30353
N 3	-0.63689	C 7	-0.27349	C 13	-0.24336	N 3	-0.66181	C 7	-0.30354	C 13	-0.24573
N 4	-0.63690	C 8	-0.16339	C 14	-0.15211	N 4	-0.66181	C 8	-0.16150	C 14	-0.07839
		C 9	-0.15211	C 15	-0.16339			C 9	-0.07840	C 15	-0.16160
		C 10	-0.22617	C 16	-0.22617			C 10	-0.25840	C 16	-0.25844
		H 17	0.21453	H 19	0.21453			H 17	0.21479	H 19	0.21477
		H 18	0.21612	H 20	0.21612			H 18	0.20916	H 20	0.20915
		H 21	0.22321	H 22	0.22321			H 21	0.21780	H 22	0.21780
		H 23	0.22241	H 24	0.22241			H 23	0.22315	H 24	0.22300
		C 28	0.80590	C 25	0.80590			C 28	0.79675	C 25	0.79676
		O 29	-0.66638	O 26	-0.66638			O 29	-0.67399	O 26	-0.67399
		O 30	-0.56894	O 27	-0.56894			O 30	-0.56917	O 27	-0.56917
		C 35	-0.21239	C 31	-0.21239			C 35	-0.21306	C 31	-0.21305
		H 36	0.19010	H 32	0.19010			H 36	0.18931	H 32	0.18931
		H 37	0.18632	H 33	0.18632			H 37	0.18508	H 33	0.18508
		H 38	0.18622	H 34	0.18622			H 38	0.18515	H 34	0.18515
sum	-0.84539	sum	-0.07729	sum	-0.7730	sum	-0.78037	sum	-0.10174	sum	-0.10208
		aryl	-0.00188	aryl	-0.00187			aryl	-0.00181	aryl	-0.00217
		EWG	-0.07917	EWG	-0.07917			EWG	-0.09993	EWG	-0.09991

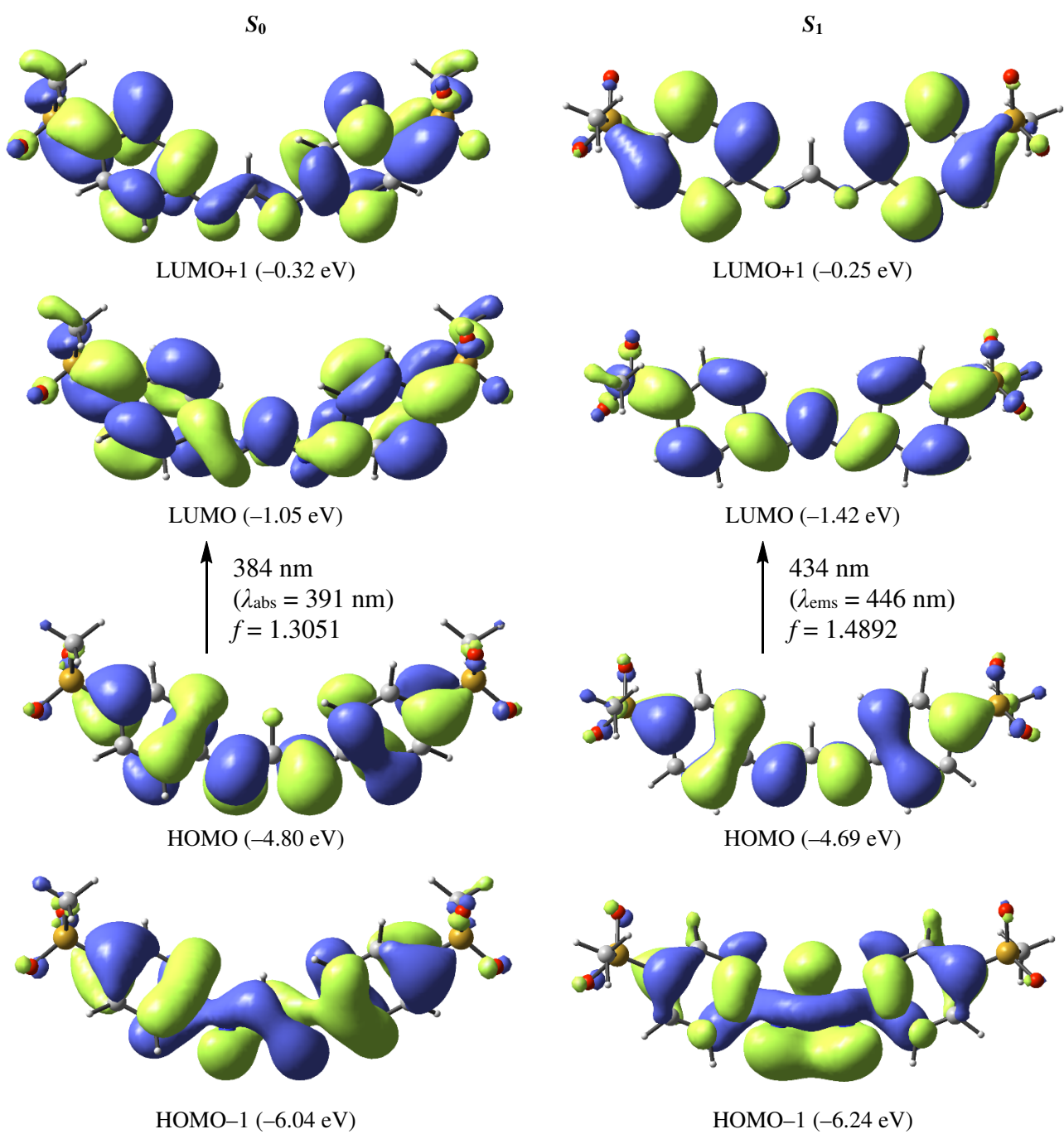


Figure S41. S_0 - and S_1 -state MOs, orbital energies, excitation energies, and oscillator strengths of **2b⁻**.

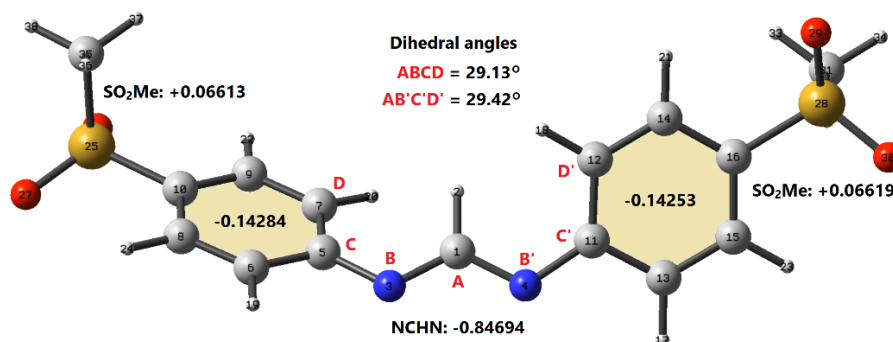


Figure S42. Dihedral angles and the sum of natural atomic charges of diazaallyl, aryl, and electron-withdrawing groups of **2b⁻** (S_0).

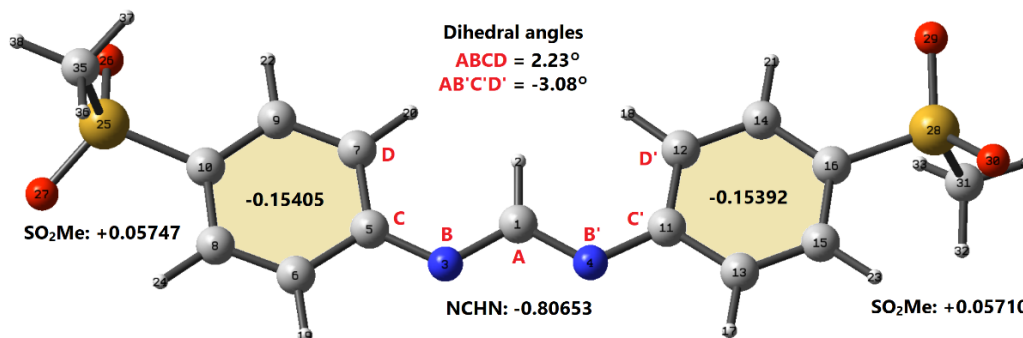


Figure S43. Dihedral angles and the sum of natural atomic charges of diazaallyl, aryl, and electron-withdrawing groups of **2b⁻** (S_1).

Table S8. Natural atomic charges of **2b⁻** at the S_0 and S_1 states.

S_0						S_1					
NCHN	NPA (δ)	Ar1	NPA (δ)	Ar2	NPA (δ)	NCHN	NPA (δ)	Ar1	NPA (δ)	Ar2	NPA (δ)
C	1	0.30418	C	5	0.18376	C	11	0.18379	C	5	0.18642
H	2	0.12465	C	6	-0.23248	C	12	-0.26494	C	6	-0.23633
N	3	-0.63802	C	7	-0.26511	C	13	-0.23249	C	7	-0.26274
N	4	-0.63775	C	8	-0.18681	C	14	-0.18124	C	8	-0.18148
			C	9	-0.18118	C	15	-0.18674	C	9	-0.18282
			C	10	-0.36420	C	16	-0.36395	C	10	-0.37626
			H	17	0.21939	H	19	0.21932	H	17	0.21950
			H	18	0.21975	H	20	0.21970	H	18	0.21440
			H	21	0.23179	H	22	0.23180	H	21	0.23346
			H	23	0.23225	H	24	0.23222	H	23	0.23180
			S	28	2.10294	S	25	2.10298	S	28	2.10069
			O	29	-0.98460	O	26	-0.98470	O	29	-0.98667
			O	30	-0.98415	O	27	-0.98412	O	30	-0.98633
			C	35	-0.78732	C	31	-0.78727	C	35	-0.78538
			H	36	0.23831	H	32	0.23834	H	36	0.23663
			H	37	0.23791	H	33	0.23790	H	37	0.23652
			H	38	0.24304	H	34	0.24306	H	38	0.24201
sum	-0.84694	sum	-0.07671	sum	-0.07634	sum	-0.80653	sum	-0.09658	sum	-0.09682
		aryl	-0.14284	aryl	-0.14253			aryl	-0.15405	aryl	-0.15392
		EWG	0.06613	EWG	0.06619			EWG	0.05747	EWG	0.05710

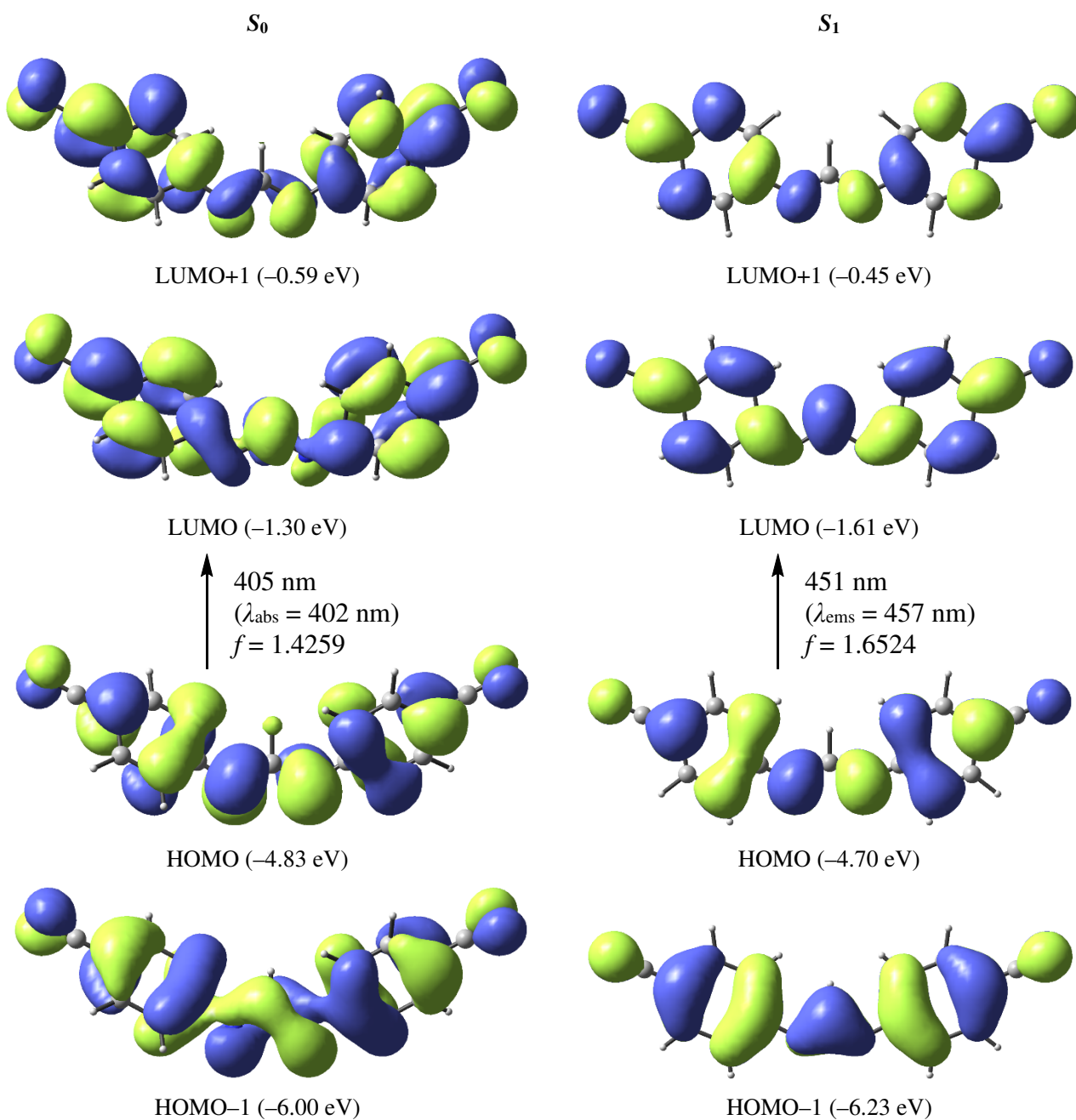


Figure S44. S_0 - and S_1 -state MOs, orbital energies, excitation energies, and oscillator strengths of $2c^-$.

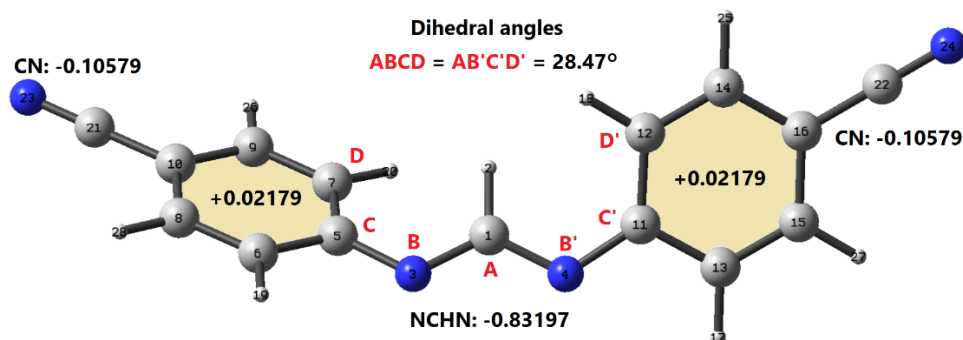


Figure S45. Dihedral angles and the sum of natural atomic charges of diazaallyl, aryl, and electron-withdrawing groups of $2c^-$ (S_0).

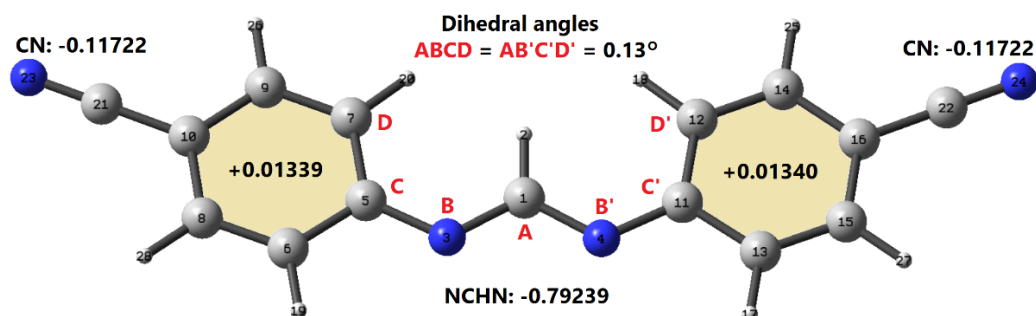


Figure S46. Dihedral angles and the sum of natural atomic charges of diazaallyl, aryl, and electron-withdrawing groups of $2c^-$ (S_1).

Table S9. Natural atomic charges of $2c^-$ at the S_0 and S_1 states.

S_0						S_1					
NCHN	NPA (δ)	Ar1	NPA (δ)	Ar2	NPA (δ)	NCHN	NPA (δ)	Ar1	NPA (δ)	Ar2	NPA (δ)
C	1	0.30516	C	5	0.18639	C	1	0.31500	C	5	0.18845
H	2	0.12759	C	6	-0.23413	C	2	0.13595	C	6	-0.23790
N	3	-0.63236	C	7	-0.26689	N	3	-0.62167	C	7	-0.26360
N	4	-0.63236	C	8	-0.15019	N	4	-0.62167	C	8	-0.14674
			C	9	-0.14309				C	9	-0.14402
			C	10	-0.26131				C	10	-0.26613
			H	19	0.22178				H	19	0.22098
			H	20	0.22126				H	20	0.21592
			C	22	0.34453				C	22	0.34074
			N	24	-0.45032				N	24	-0.45796
			H	26	0.22364				H	26	0.22205
			H	28	0.22433				H	28	0.22438
sum	-0.83197	sum	-0.08400	sum	-0.08400	sum	-0.79239	sum	-0.10383	sum	-0.10382
		aryl	0.02179	aryl	0.02179			aryl	0.01339	aryl	0.01340
		EWG	-0.10579	EWG	-0.10579			EWG	-0.11722	EWG	-0.11722

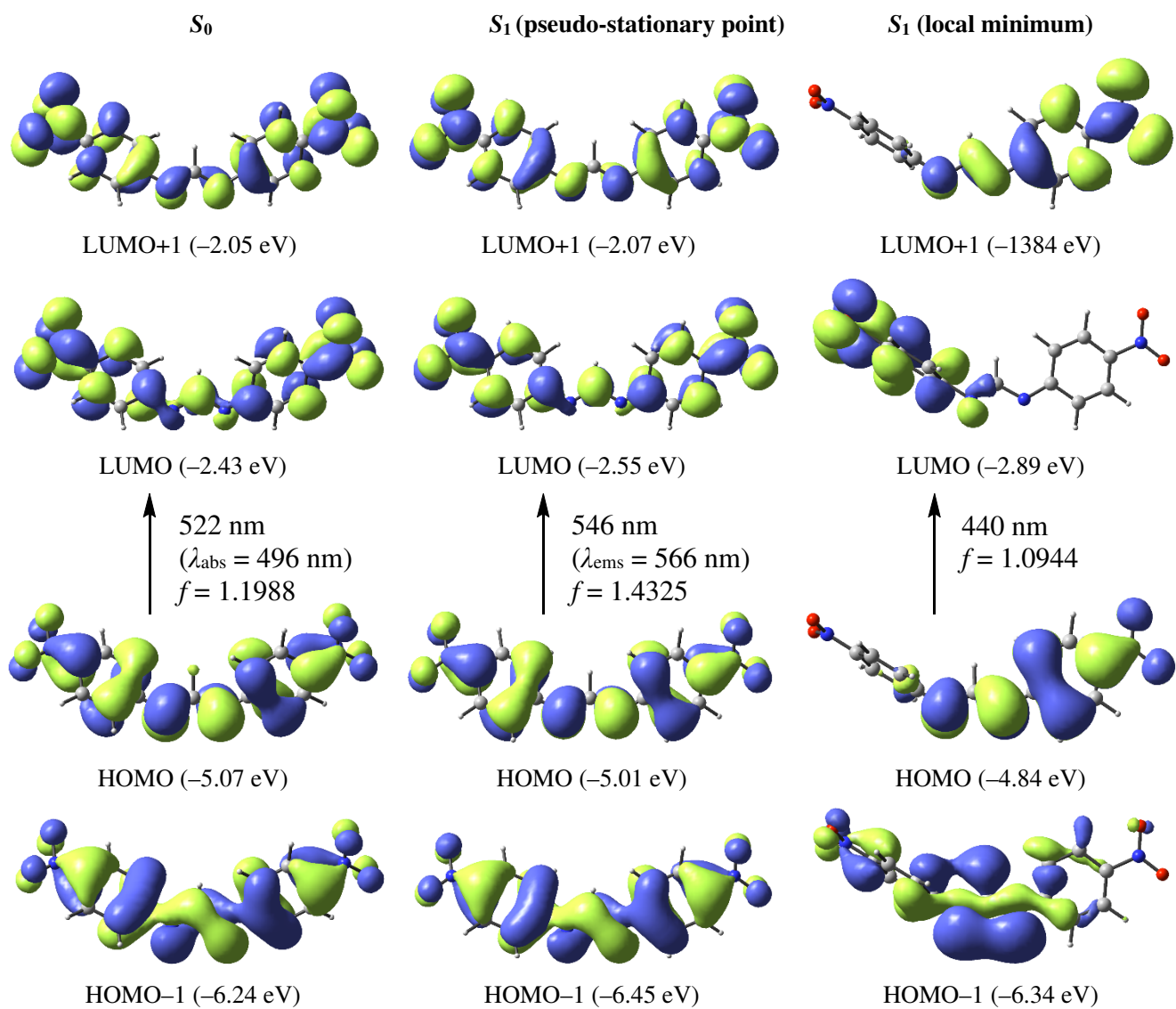


Figure S47. S_0 - and S_1 -state MOs, orbital energies, excitation energies, and oscillator strengths of **2d⁻**.

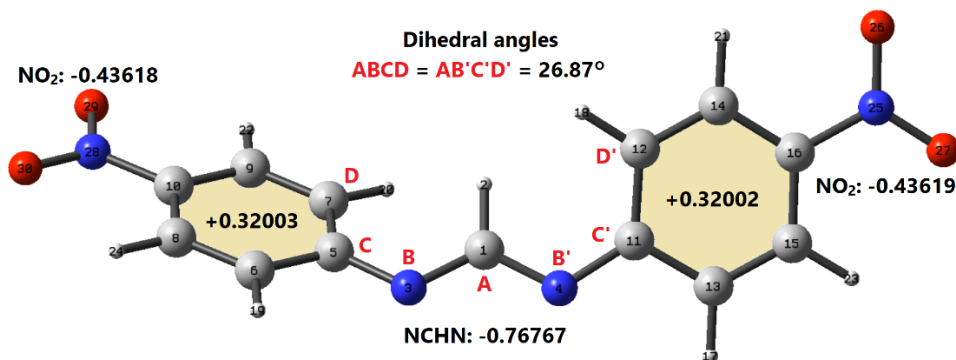


Figure S48. Dihedral angles and the sum of natural atomic charges of diazaallyl, aryl, and electron-withdrawing groups of $2d^-$ (S_0).

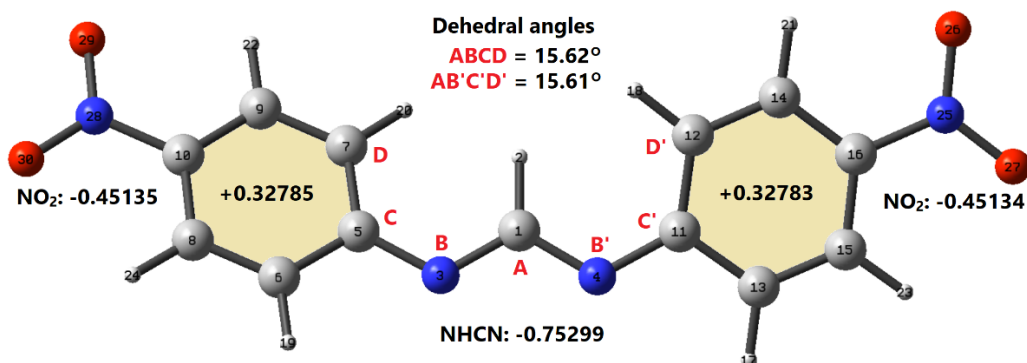


Figure S49. Dihedral angles and the sum of natural atomic charges of diazaallyl, aryl, and electron-withdrawing groups of $2d^-$ (pseudo-stationary point at S_1).

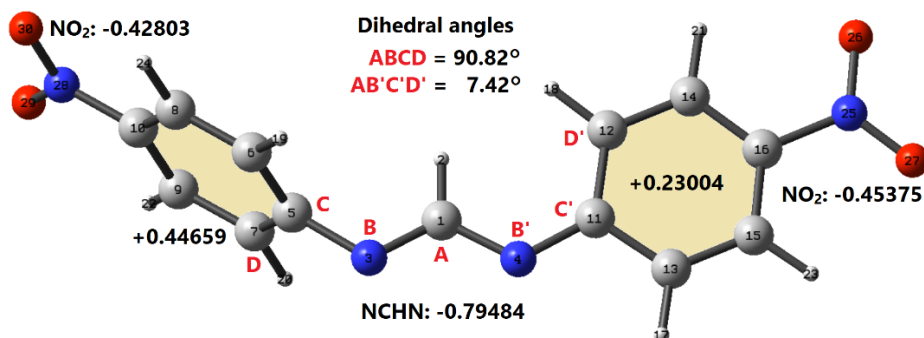


Figure S50. Dihedral angles and the sum of natural atomic charges of diazaallyl, aryl, and electron-withdrawing groups of $2d^-$ (local minimum at S_1).

Table S10. Natural atomic charges of **2d⁻** at the S_0 and S_1 (a pseudo-stationary point and a local minimum) states.

S_0						S_1 (a pseudo-stationary point)					
NCHN	NPA (δ)	Ar1	NPA (δ)	Ar2	NPA (δ)	NCHN	NPA (δ)	Ar1	NPA (δ)	Ar2	NPA (δ)
C	1	0.30981	C	5	0.19839	C	11	0.19839	C	11	0.19277
H	2	0.13514	C	6	-0.22588	C	12	-0.25843	C	12	-0.25387
N	3	-0.60631	C	7	-0.25843	C	13	-0.22588	C	13	-0.22266
N	4	-0.60631	C	8	-0.17585	C	14	-0.16821	C	14	-0.16775
			C	9	-0.16821	C	15	-0.17585	C	15	-0.17447
			C	10	0.02355	C	16	0.02355	C	16	0.02814
			H	19	0.22402	H	17	0.22402	H	19	0.22498
			H	20	0.22293	H	18	0.22292	H	20	0.22053
			H	22	0.23956	H	21	0.23956	H	22	0.23949
			H	24	0.23995	H	23	0.23995	H	24	0.24067
			N	28	0.47420	N	25	0.47420	N	28	0.46527
			O	29	-0.45545	O	26	-0.45545	O	29	-0.45871
			O	30	-0.45494	O	27	-0.45493	O	30	-0.45791
sum	-0.76767	sum	-0.11616	sum	-0.11616	sum	-0.75299	sum	-0.12350	sum	-0.12351
		aryl	0.32003	aryl	0.32002			aryl	0.32785	aryl	0.32783
		EWG	-0.43619	EWG	-0.43618			EWG	-0.45135	EWG	-0.45134

S_1 (a local minimum)								
NCHN	NPA (δ)	Ar1	NPA (δ)	Ar2	NPA (δ)			
C	1	0.30126	C	5	0.21516	C	11	0.19728
H	2	0.13743	C	6	-0.23364	C	12	-0.27610
N	3	-0.57591	C	7	-0.23384	C	13	-0.23729
N	4	-0.65762	C	8	-0.14610	C	14	-0.17874
			C	9	-0.14598	C	15	-0.18955
			C	10	0.03995	C	16	0.00696
			H	19	0.23273	H	17	0.21907
			H	20	0.23284	H	18	0.21435
			H	22	0.24276	H	21	0.23626
			H	24	0.24271	H	23	0.23780
			N	28	0.44543	N	25	0.48002
			O	29	-0.43666	O	26	-0.46726
			O	30	-0.43680	O	27	-0.46651
sum	-0.79484	sum	0.01856	sum	-0.22371			
		aryl	0.44659	aryl	0.23004			
		EWG	-0.42803	EWG	-0.45375			

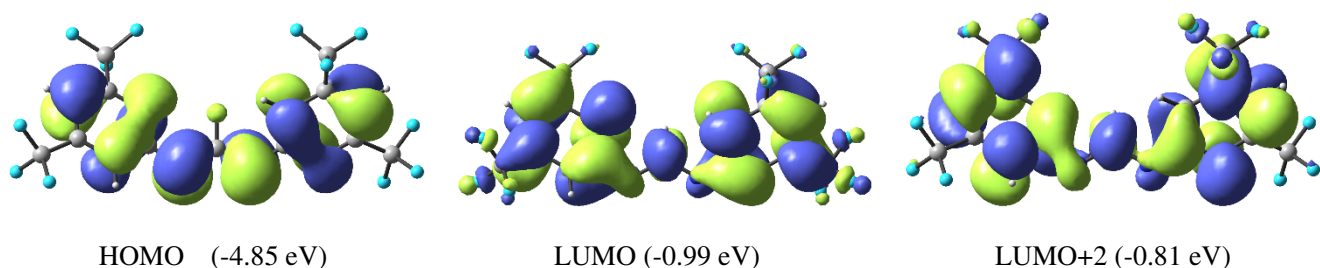


Figure S51. Frontier orbitals for the ground state (S_0) of $2e^-$.

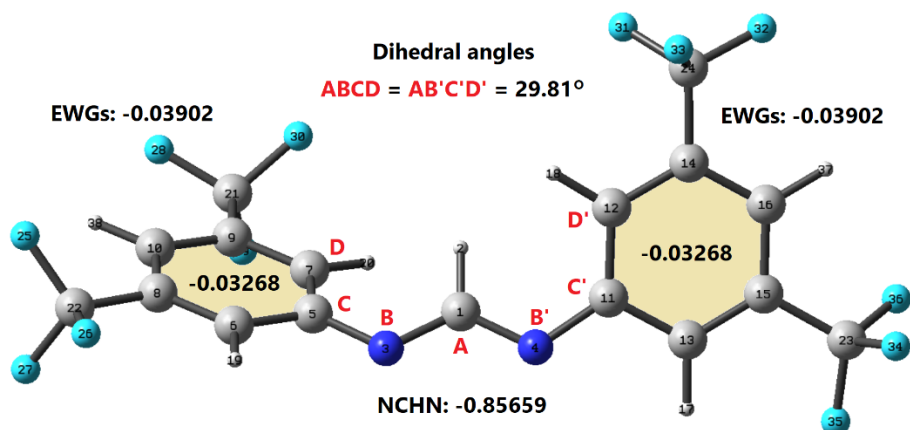


Figure S52. Dihedral angles and the sum of natural atomic charges of diazaallyl, aryl, and electron-withdrawing groups of $2e^-$ (S_0).

Table S11. Natural atomic charges of $2e^-$ at the S_0 state.

		S_0			
NCHN	NPA (δ)	Ar1	NPA (δ)	Ar2	NPA (δ)
C	1	0.30255	C	5	0.16823
H	2	0.12508	C	6	-0.17870
N	3	-0.64211	C	7	-0.22101
N	4	-0.64211	C	8	-0.15311
			C	9	-0.14664
			C	10	-0.20924
			H	19	0.23490
			H	20	0.23155
			C	21	1.09014
			C	22	1.09040
			F	25	-0.37099
			F	26	-0.36551
			F	27	-0.37329
			F	28	-0.36781
			F	29	-0.37229
			F	30	-0.36967
			H	38	0.24134
sum	-0.85659	sum	-0.07170	sum	-0.07170
		aryl	-0.03268	aryl	-0.03268
		EWG	-0.03902	EWG	-0.03902

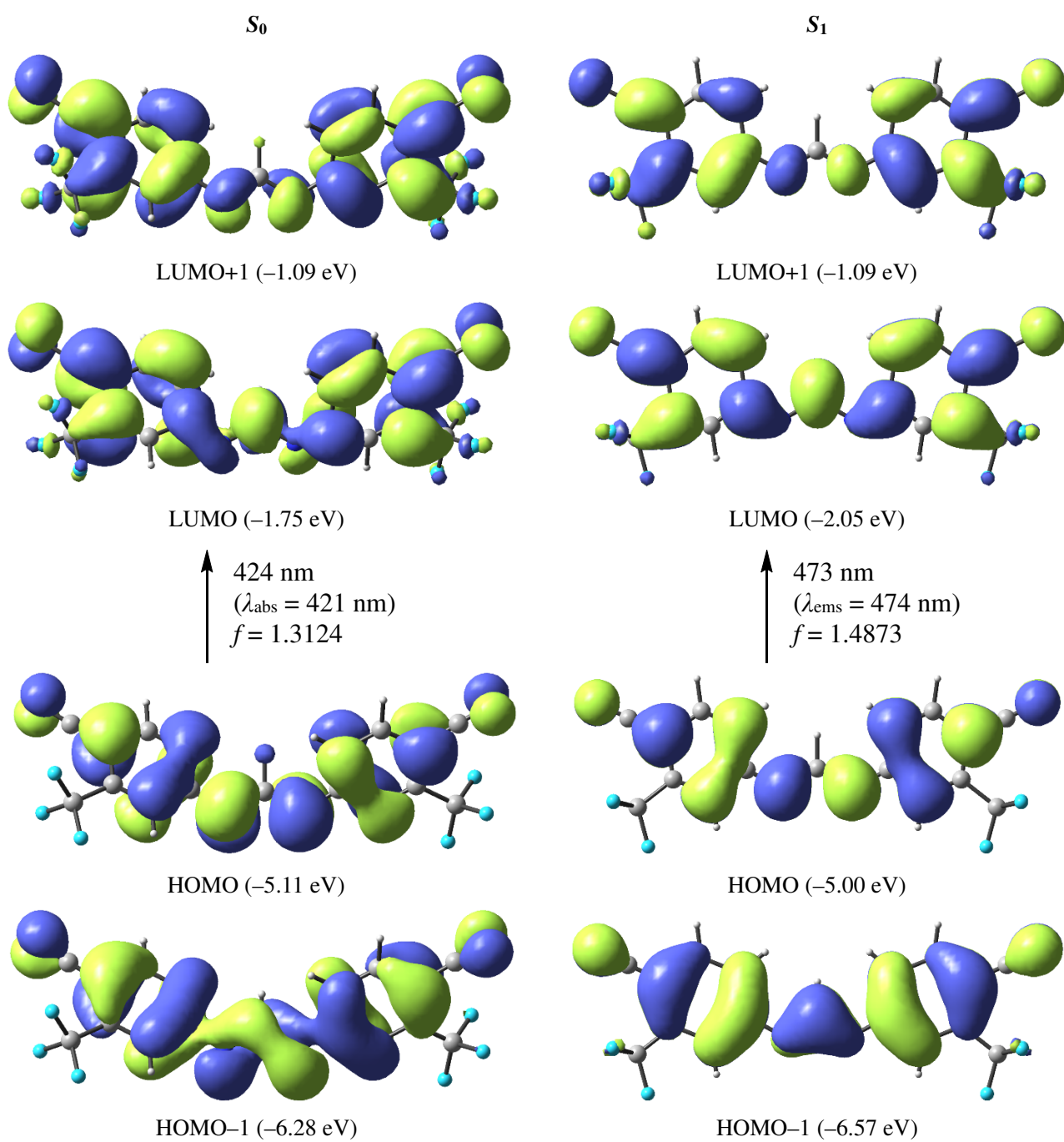


Figure S53. S_0 - and S_1 -state MOs, orbital energies, excitation energies, and oscillator strengths of $2\mathbf{f}^-$.

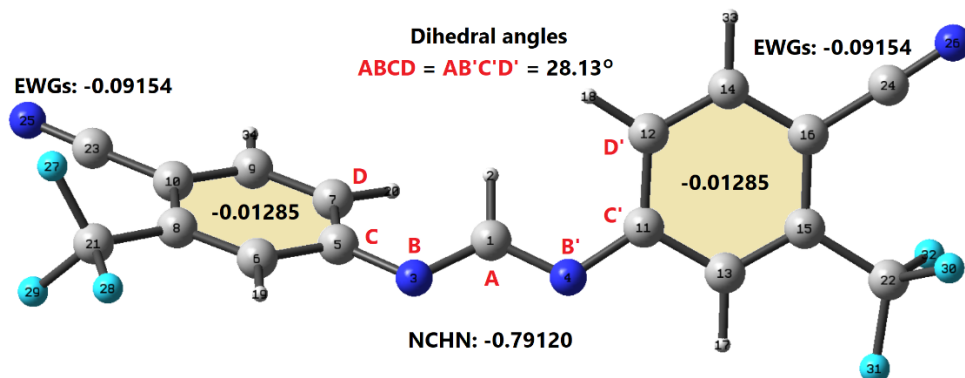


Figure S54. Dihedral angles and the sum of natural atomic charges of diazaallyl, aryl, and electron-withdrawing groups of $2f^- (S_0)$.

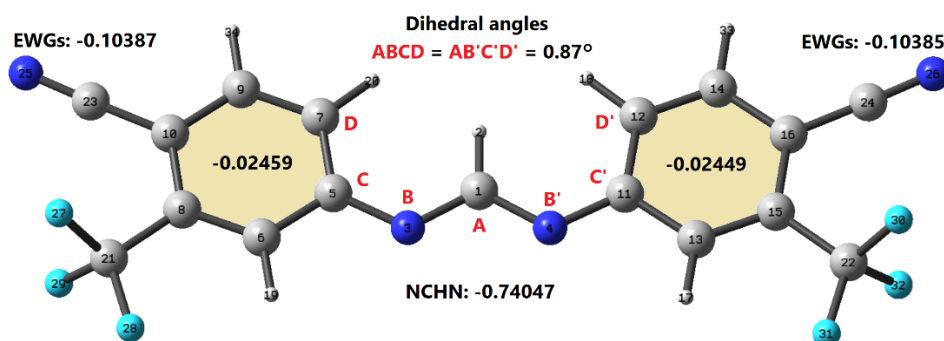


Figure S55. Dihedral angles and the sum of natural atomic charges of diazaallyl, aryl, and electron-withdrawing groups of $2f^- (S_1)$.

Table S12. Natural atomic charges of $2f^-$ at the S_0 and S_1 states.

		S_0				S_1					
NCHN	NPA (δ)	Ar1	NPA (δ)	Ar2	NPA (δ)	NCHN	NPA (δ)	Ar1	NPA (δ)	Ar2	NPA (δ)
C	1	0.31055	C	5	0.19177	C	1	0.40670	C	5	0.18121
H	2	0.13237	C	6	-0.19014	C	2	0.12782	C	6	-0.18479
N	3	-0.61706	C	7	-0.24855	C	3	-0.63750	C	7	-0.24301
N	4	-0.61706	C	8	-0.10396	C	4	-0.63749	C	8	-0.10983
			C	9	-0.12827	C	5	-0.13193	C	9	-0.10980
			C	10	-0.23177	C	6	-0.23152	C	10	-0.23153
			H	17	0.24025	C	7	0.24397	H	17	0.24402
			H	18	0.22702	H	18	0.22196	H	18	0.22196
			C	22	1.08851	C	21	1.08757	C	21	1.08758
			C	24	0.33003	C	22	1.08757	C	22	1.08757
			N	26	-0.41698	C	23	0.32637	C	23	0.32637
			F	30	-0.36570	N	26	-0.42214	N	26	-0.42214
			F	31	-0.36128	F	30	-0.36727	F	30	-0.36727
			F	32	-0.36612	F	27	-0.36612	F	27	-0.36722
			F	32	-0.36612	F	28	-0.36128	F	28	-0.36117
			H	33	0.23080	F	29	-0.36570	F	29	-0.36727
					H	34	0.23080	H	33	0.22935	
sum	-0.79120	sum	-0.10439	sum	-0.10439	sum	-0.74047	sum	-0.12846	sum	-0.12846
		aryl	-0.01285	aryl	-0.01285			aryl	-0.02459	aryl	-0.02459
		EWG	-0.09154	EWG	-0.09154			EWG	-0.10387	EWG	-0.10387

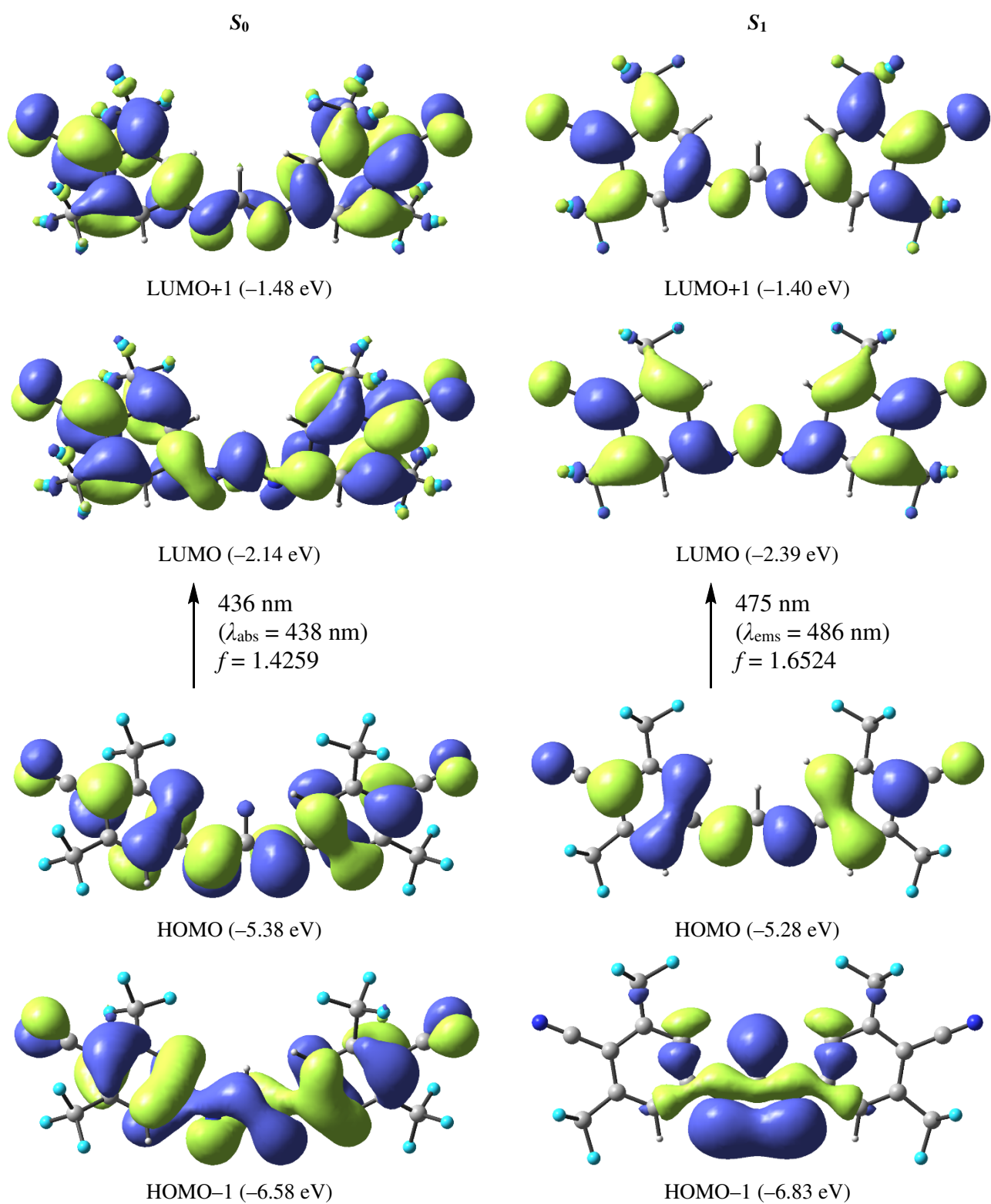


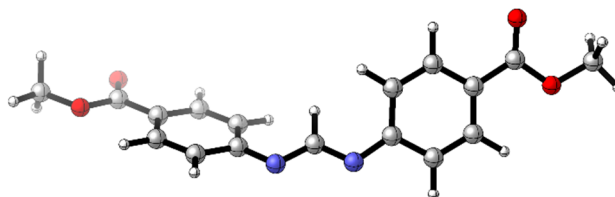
Figure S56. S_0 - and S_1 -state MOs, orbital energies, excitation energies, and oscillator strengths of $2g^-$.

Table S14. Summary of the calculated photoexcitation parameters

	state	frontier orbitals	E_{EX} (eV)	wavelengths (nm)			λ_{EM}	oscillator strength f
				calcd. $\lambda_{S_0-S_1}$	λ_{ABS}	calcd. $\lambda_{S_1-S_0}$		
2a⁻	S_0	HOMO/LUMO	2.96	419	411	—	—	1.4223
	S_1	HOMO/LUMO	2.69	—	—	461	471	1.6962
2b⁻	S_0	HOMO/LUMO	3.22	385	391	—	—	1.3051
	S_1	HOMO/LUMO	2.85	—	—	434	446	1.4892
2c⁻	S_0	HOMO/LUMO	3.07	403	402	—	—	1.4259
	S_1	HOMO/LUMO	2.75	—	—	451	457	1.6524
2d⁻	S_0	HOMO/LUMO	2.39	519	496	—	—	1.1988
	S_1	HOMO/LUMO	2.27	—	—	546	566	1.4325
2e⁻	S_0	HOMO/LUMO	3.27	379	—	—	—	0.1734
		HOMO/LUMO+2	3.48	356	355	—	436	0.8568
2f⁻	S_0	HOMO/LUMO	2.94	424	421	—	—	1.3124
	S_1	HOMO/LUMO	2.62	—	—	473	474	1.4873
2g⁻	S_0	HOMO/LUMO	2.87	436	438	—	—	1.3913
	S_1	HOMO/LUMO	2.70	—	—	475	486	1.6759

(J-2) Cartesian Coordinates of DFT-Optimized States

Singlet ground state (S_0) of $2a^-$



$E_{298}(\text{B3LYP}) = -1067.49364381$ Hartree

$E_{298}(\text{TD-B3LYP}) = -1067.38452088$ Hartree

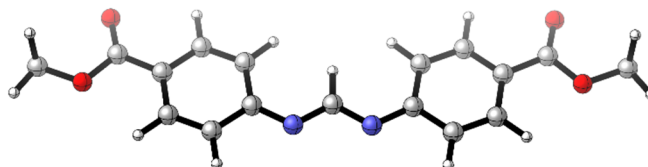
$G_{298}(\text{B3LYP}) = -1067.56759381$ Hartree

$G_{298}(\text{TD-B3LYP}) = -1067.45847088$ Hartree

-1 1

C	0.000042	1.220719	-0.000634	H	-3.790630	-1.611825	1.429885
H	0.000066	0.116603	-0.000275	H	3.790814	-1.612650	-1.429214
N	1.157712	1.852775	0.128877	H	-5.559413	1.355406	-1.125707
N	-1.157656	1.852645	-0.130550	H	5.559411	1.356215	1.124613
C	2.322971	1.131197	0.016491	C	-6.091238	-0.964626	0.258756
C	3.483054	1.621847	0.674305	O	-6.257780	-1.996619	0.903746
C	2.475851	-0.053545	-0.759755	O	-7.102607	-0.389278	-0.441129
C	4.696746	0.960126	0.600691	C	6.091313	-0.964760	-0.258251
C	3.693170	-0.713401	-0.829225	O	6.257908	-1.997150	-0.902591
C	4.825439	-0.228521	-0.148571	O	7.102602	-0.389036	0.441441
C	-2.322892	1.131107	-0.017665	C	-8.374592	-1.057369	-0.383657
C	-2.475713	-0.053153	0.759330	H	-9.043607	-0.460133	-1.002224
C	-3.483018	1.621325	-0.675727	H	-8.292597	-2.072520	-0.779140
C	-3.693029	-0.712961	0.829314	H	-8.740316	-1.097814	0.645114
C	-4.696708	0.959656	-0.601594	C	8.374563	-1.057223	0.384570
C	-4.825353	-0.228501	0.148452	H	9.043505	-0.459660	1.002898
H	-3.390056	2.534285	-1.255895	H	8.292449	-2.072139	0.780630
H	-1.635871	-0.430072	1.333105	H	8.740454	-1.098287	-0.644118
H	3.390048	2.535179	1.253880				
H	1.636047	-0.430819	-1.333354				

Singlet excited state (S_1) of $2a^-$



$E_{298}(\text{B3LYP}) = -1067.49025005$ Hartree

$E_{298}(\text{TD-B3LYP}) = -1067.39146512$ Hartree

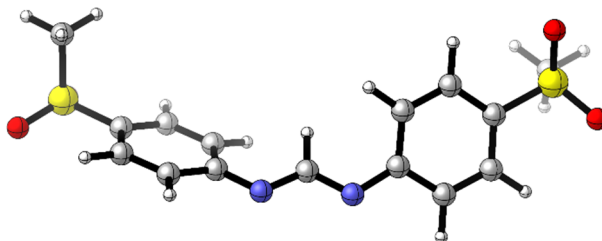
$G_{298}(\text{B3LYP}) = -1067.56074105$ Hartree

$G_{298}(\text{TD-B3LYP}) = -1067.46195612$ Hartree

-1 1

C	0.000003	0.749196	-0.000068	H	4.023943	-2.198059	0.097586
H	0.000004	-0.344069	0.000014	H	-4.023927	-2.198085	-0.097382
N	-1.148132	1.435631	-0.034781	H	5.650880	1.796069	0.127222
N	1.148136	1.435640	0.034546	H	-5.649878	1.796034	-0.127464
C	-2.359330	0.807542	-0.064602	C	6.330624	-0.881030	0.130054
C	-3.515227	1.646817	-0.088807	O	6.569698	-2.094437	0.132308
C	-2.585068	-0.613123	-0.070619	O	7.335765	0.044996	0.142881
C	-4.795128	1.130215	-0.111313	C	-6.330614	-0.881068	-0.129983
C	-3.866923	-1.124302	-0.093999	O	-6.569683	-2.094476	-0.132107
C	-5.003470	-0.277533	-0.112629	O	-7.335757	0.044954	-0.142892
C	2.359336	0.807559	0.064447	C	8.672928	-0.474865	0.158134
C	2.585079	-0.613105	0.070630	H	9.325115	0.398397	0.164794
C	3.515230	1.646841	0.088559	H	8.841741	-1.081996	1.051388
C	3.866935	-1.124276	0.094079	H	8.861527	-1.083326	-0.730276
C	4.795132	1.130245	0.111139	C	-8.672919	-0.474913	-0.158046
C	5.003479	-0.277502	0.112620	H	-9.325109	0.398346	-0.164792
H	3.352857	2.720626	0.086175	H	-8.841756	-1.082152	-1.051221
H	1.750143	-1.303743	0.056775	H	-8.861491	-1.083268	0.730443
H	-3.352858	2.720603	-0.086551				
H	-1.750130	-1.303757	-0.056692				

Singlet ground state (S_0) of $2b^-$



$E_{298}(\text{B3LYP}) = -1787.63044753$ Hartree

$E_{298}(\text{TD-B3LYP}) = -1787.51193383$ Hartree

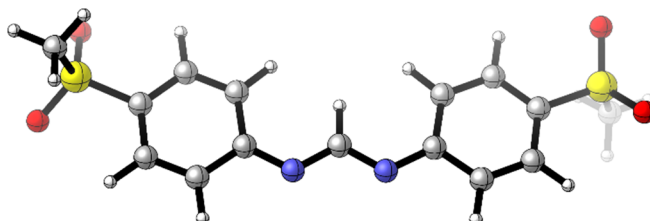
$G_{298}(\text{B3LYP}) = -1787.70787953$ Hartree

$G_{298}(\text{TD-B3LYP}) = -1787.58936583$ Hartree

-1 1

C	-0.028481	-0.934253	-0.543316	H	3.729904	0.831890	2.138480
H	-0.023411	0.043745	-0.029450	H	-3.762955	2.305735	-0.591711
N	-1.191876	-1.535877	-0.742925	H	5.555169	-0.573542	-1.499567
N	1.129173	-1.449143	-0.930331	H	-5.616159	-1.477245	0.301884
C	-2.348392	-0.824430	-0.529424	S	-6.337610	1.317754	0.243763
C	-3.522998	-1.545808	-0.184256	O	-6.350000	2.614847	-0.477617
C	-2.473781	0.585808	-0.684357	O	-7.459495	0.371213	0.024192
C	-4.731919	-0.907035	0.038084	S	6.297187	0.952587	0.836777
C	-3.682240	1.231872	-0.459124	O	6.319434	1.087987	2.314646
C	-4.811527	0.488217	-0.094289	O	7.411522	0.232339	0.171835
C	2.291977	-0.876977	-0.471885	C	6.258805	2.620175	0.150601
C	2.427708	-0.208752	0.778444	H	6.169794	2.544934	-0.933684
C	3.461304	-1.005040	-1.269156	H	5.407202	3.149888	0.578628
C	3.641046	0.335963	1.177585	H	7.198285	3.099585	0.432506
C	4.675103	-0.466116	-0.874587	C	-6.295860	1.690998	2.007742
C	4.764927	0.212083	0.351273	H	-6.217066	0.752138	2.556845
H	3.379352	-1.536951	-2.211598	H	-5.437365	2.334032	2.204185
H	1.580198	-0.153806	1.452626	H	-7.230003	2.203977	2.244602
H	-3.448202	-2.624386	-0.091018				
H	-1.622208	1.167144	-1.020122				

Singlet excited state (S_1) of $2b^-$



$E_{298}(\text{B3LYP}) = -1787.62632704$ Hartree

$E_{298}(\text{TD-B3LYP}) = -1787.52146094$ Hartree

$G_{298}(\text{B3LYP}) = -1787.69941004$ Hartree

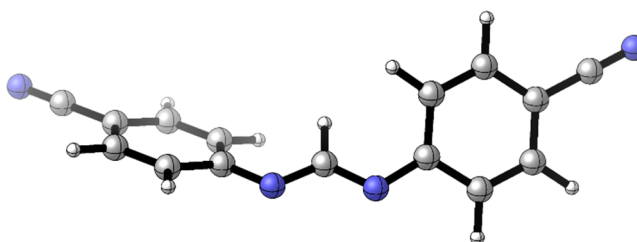
$G_{298}(\text{TD-B3LYP}) = -1787.59454394$ Hartree

-1 1

C	0.011399	0.849946	-0.007706	H	-1.714361	-1.207049	-0.054740
H	0.016711	-0.238994	0.072550	H	3.371682	2.818316	-0.176228
N	1.158222	1.541056	-0.096221	H	1.735419	-1.201281	-0.112361
N	-1.141487	1.536753	-0.002157	H	-3.978362	-2.128536	0.025919
C	2.364528	0.910796	-0.124723	H	4.002788	-2.116822	-0.102989
C	3.526175	1.743715	-0.154810	H	-5.650196	1.854237	0.216529
C	2.575190	-0.517539	-0.112499	H	5.671117	1.871456	-0.187241
C	4.804382	1.220859	-0.154747	S	6.588523	-0.874644	-0.012894
C	3.853200	-1.042295	-0.109943	O	6.551142	-2.286507	-0.476487
C	4.973430	-0.187658	-0.132032	O	7.560491	0.059158	-0.639469
C	-2.345691	0.902749	0.033143	S	-6.568051	-0.891391	0.083590
C	-2.553970	-0.525843	0.005357	O	-6.503031	-2.310573	0.520940
C	-3.507938	1.732519	0.101427	O	-7.506261	0.030026	0.776945
C	-3.830092	-1.053975	0.046436	C	-7.057071	-0.906910	-1.657227
C	-4.783674	1.206152	0.148057	H	-7.035450	0.118153	-2.029277
C	-4.949973	-0.202675	0.128156	H	-6.357685	-1.538870	-2.205823
H	-3.355495	2.807323	0.125390	H	-8.069213	-1.315064	-1.702265

C	6.980109	-0.920281	1.752010	H	6.251854	-1.562890	2.248352
H	6.934863	0.097871	2.140553	H	7.988835	-1.328255	1.847241

Singlet ground state (S_0) of $2e^-$



$E_{298}(\text{B3LYP}) = -796.21197985$ Hartree

$E_{298}(\text{TD-B3LYP}) = -796.09943089$ Hartree

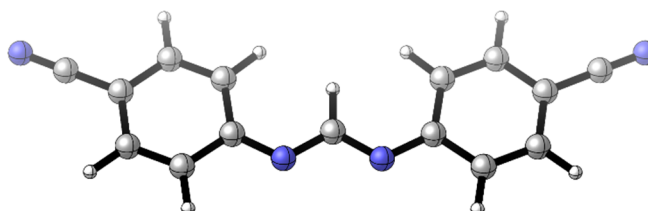
$G_{298}(\text{B3LYP}) = -796.27277885$ Hartree

$G_{298}(\text{TD-B3LYP}) = -796.16022989$ Hartree

-1 1

C	-0.000011	-0.912777	-0.000193	C	4.820659	0.526624	0.046865
H	0.000002	0.191384	0.000104	H	3.358585	-2.232446	-1.326993
N	-1.154052	-1.545330	0.154327	H	1.663299	0.734926	1.299526
N	1.154015	-1.545276	-0.155055	H	-3.358644	-2.233080	1.325871
C	-2.320889	-0.825974	0.066114	H	-1.663273	0.735654	-1.299049
C	-3.465322	-1.320097	0.749047	C	-6.070196	1.206536	-0.099193
C	-2.490036	0.358067	-0.707721	C	6.070251	1.206289	0.099975
C	-4.681359	-0.663018	0.703147	N	-7.095493	1.764810	-0.139210
C	-3.706363	1.021084	-0.755045	N	7.095571	1.764497	0.140313
C	-4.820631	0.526792	-0.046472	H	3.810233	1.919040	1.356074
C	2.320871	-0.825996	-0.066465	H	-3.810165	1.919881	-1.354934
C	2.490053	0.357625	0.708004	H	5.535248	-1.057205	-1.244882
C	3.465288	-1.319782	-0.749669	H	-5.535272	-1.057721	1.244408
C	3.706403	1.020573	0.755696				
C	4.681348	-0.662769	-0.703407				

Singlet excited state (S_1) of $2e^-$



$E_{298}(\text{B3LYP}) = -796.20838020$ Hartree

$E_{298}(\text{TD-B3LYP}) = -796.10744435$ Hartree

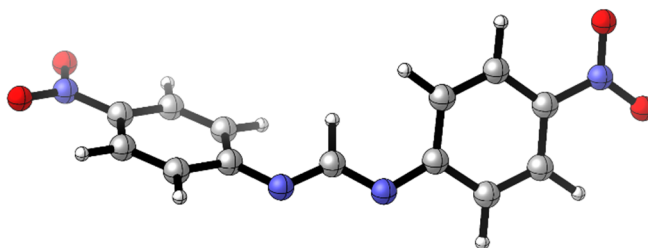
$G_{298}(\text{B3LYP}) = -796.26651320$ Hartree

$G_{298}(\text{TD-B3LYP}) = -796.16557735$ Hartree

-1 1

C	0.000001	-0.637895	0.000002	C	-4.989893	0.397989	0.064281
H	0.000001	0.454658	0.000007	H	-3.359638	-2.608422	0.063577
N	1.149814	-1.326444	-0.020945	H	-1.738108	1.413756	0.012518
N	-1.149813	-1.326444	0.020942	H	3.359639	-2.608422	-0.063595
C	2.357074	-0.698384	-0.035938	H	1.738109	1.413756	-0.012495
C	3.517207	-1.534262	-0.058255	C	6.292623	0.948101	-0.076944
C	2.575628	0.727151	-0.029258	C	-6.292622	0.948101	0.076951
C	4.794486	-1.016157	-0.071995	N	7.375138	1.400747	-0.088159
C	3.852216	1.248227	-0.042832	N	-7.375137	1.400747	0.087168
C	4.989895	0.397989	-0.064276	H	-3.997004	2.324199	0.036861
C	-2.357073	-0.698384	0.035940	H	3.997006	2.324198	-0.036836
C	-2.575626	0.727151	0.029273	H	-5.655955	-1.675306	0.088297
C	-3.517206	-1.534261	0.058247	H	5.655956	-1.675306	-0.088312
C	-3.852214	1.248228	0.042847				
C	-4.794485	-1.016157	0.071988				

Singlet ground state (S_0) of $2d^-$



$E_{298}(\text{B3LYP}) = -1020.81488623$ Hartree

$E_{298}(\text{TD-B3LYP}) = -1020.72768105$ Hartree

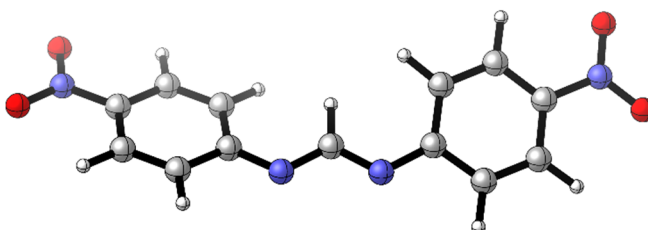
$G_{298}(\text{B3LYP}) = -1020.87972223$ Hartree

$G_{298}(\text{TD-B3LYP}) = -1020.79251705$ Hartree

-1 1

C	-0.000006	-1.025977	-0.000030	H	3.345463	-2.426462	-1.280991
H	-0.000002	0.076281	0.000028	H	1.676215	0.642457	1.253128
N	-1.150401	-1.665612	0.154796	H	-3.345478	-2.426567	1.280797
N	1.150385	-1.665605	-0.154923	H	-1.676219	0.642600	-1.253015
C	-2.321735	-0.965894	0.068740	H	3.854751	1.784939	1.300468
C	-3.465618	-1.501300	0.727569	H	-3.854744	1.785109	-1.300219
C	-2.501978	0.236519	-0.680226	H	5.547377	-1.275278	-1.206436
C	-4.689462	-0.865995	0.688224	H	-5.547381	-1.275353	1.206382
C	-3.725921	0.876395	-0.725599	N	6.087913	0.998051	0.082375
C	-4.823131	0.333673	-0.035761	O	6.190412	2.058310	0.731770
C	2.321724	-0.965906	-0.068787	O	7.053556	0.500037	-0.530409
C	2.501974	0.236427	0.680304	N	-6.087903	0.998120	-0.082187
C	3.465608	-1.501254	-0.727665	O	-6.190397	2.058443	-0.731478
C	3.725923	0.876287	0.725753	O	-7.053545	0.500058	0.530561
C	4.689458	-0.865966	-0.688243				
C	4.823133	0.333625	0.035868				

Stationary point geometry for singlet excited state (S_1) of $2d^-$



$E_{298}(\text{B3LYP}) = -1020.81310026$ Hartree

$E_{298}(\text{TD-B3LYP}) = -1020.72963015$ Hartree

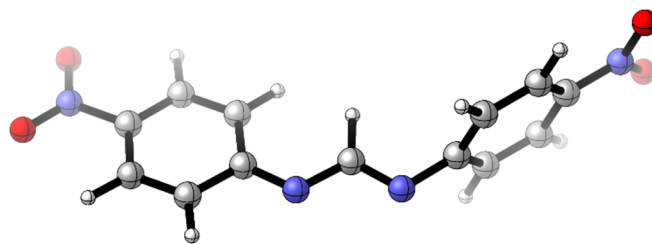
$G_{298}(\text{B3LYP}) = -1020.87681726$ Hartree

$G_{298}(\text{TD-B3LYP}) = -1020.79334715$ Hartree

-1 1

C	0.000003	-0.865657	0.000015	H	-1.715097	1.079462	-0.722313
H	0.000008	0.229940	-0.000014	H	3.349376	-2.666885	-0.678548
N	1.145177	-1.539045	-0.054856	H	1.715114	1.079433	0.722410
N	-1.145182	-1.539037	0.054921	H	-3.965973	2.062887	-0.706064
C	2.349743	-0.877174	-0.018525	H	3.965988	2.062869	0.706111
C	3.496876	-1.632780	-0.386320	H	-5.630175	-1.654605	0.683342
C	2.549820	0.477016	0.384649	H	5.630159	-1.654591	-0.683413
C	4.763326	-1.075968	-0.392705	N	-6.227587	0.854803	0.002896
C	3.814204	1.038583	0.390998	O	-6.351246	2.060013	-0.340309
C	4.923411	0.268257	-0.006151	O	-7.210421	0.145618	0.343013
C	-2.349740	-0.877167	0.018562	N	6.227585	0.854806	-0.002943
C	-2.549811	0.477033	-0.384592	O	6.351251	2.060014	0.340282
C	-3.496885	-1.632782	0.386313	O	7.210413	0.145628	-0.343100
C	-3.814195	1.038595	-0.390967				
C	-4.763335	-1.075975	0.392668				
C	-4.923411	0.268257	0.006133				
H	-3.349390	-2.666892	0.678529				

Local minimum for singlet excited state (S_1) of $2d^-$



$E_{298}(\text{B3LYP}) = -1020.79940902$ Hartree

$E_{298}(\text{TD-B3LYP}) = -1020.74396349$ Hartree

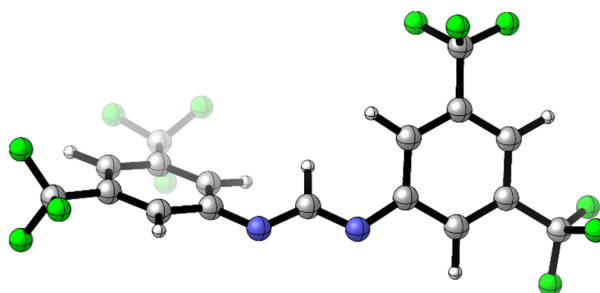
$G_{298}(\text{B3LYP}) = -1020.85677502$ Hartree

$G_{298}(\text{TD-B3LYP}) = -1020.80132949$ Hartree

-1 1

C	0.053053	-0.127528	-0.906171	H	-3.413915	0.065715	-2.656634
H	0.127514	0.014926	0.178277	H	2.396947	-2.385637	-0.594091
N	1.117385	-0.272461	-1.622420	H	2.604746	1.877461	-1.060762
N	-1.165300	-0.131654	-1.529309	H	-5.655399	0.179252	-1.552552
C	2.350056	-0.253867	-0.891257	H	4.777865	1.903215	0.154836
C	2.915093	-1.446733	-0.424161	H	-3.760315	-0.146709	2.299113
C	3.031644	0.952049	-0.686241	H	4.572296	-2.357862	0.617989
C	4.134130	-1.438368	0.252527	N	-6.113056	0.092629	1.075226
C	4.250353	0.972795	-0.009367	O	-7.116972	0.190381	0.359634
C	4.812650	-0.224967	0.468571	O	-6.153100	0.045902	2.310431
C	-2.305158	-0.085563	-0.810788	N	6.044961	-0.209365	1.152680
C	-3.509612	0.025076	-1.578240	O	6.643756	0.922832	1.347828
C	-2.423888	-0.151525	0.618790	O	6.551591	-1.327341	1.567316
C	-4.746447	0.088406	-0.973272				
C	-3.661858	-0.093974	1.222964				
C	-4.811312	0.029717	0.426429				
H	-1.547703	-0.262151	1.242678				

Singlet ground state (S_0) of $2e^-$



$E_{298}(\text{B3LYP}) = -1960.27638370$ Hartree

$E_{298}(\text{TD-B3LYP}) = -1960.15629633$ Hartree

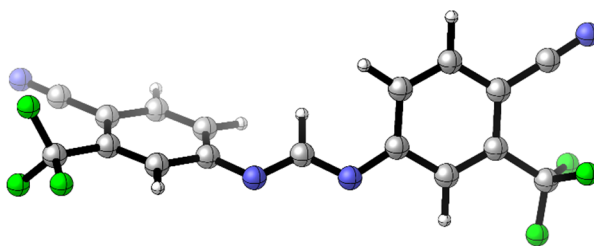
$G_{298}(\text{B3LYP}) = -1960.37011370$ Hartree

$G_{298}(\text{TD-B3LYP}) = -1960.25002633$ Hartree

-1 1

C	0.000119	1.245267	-0.000591	C	-3.795014	-1.900433	1.729837
H	0.000005	0.139422	0.000056	C	-5.893286	1.456765	-1.320437
N	-1.157842	1.874506	-0.129992	C	5.893609	1.457251	1.318821
N	1.158209	1.874421	0.128074	C	3.794479	-1.903354	-1.727189
C	-2.318336	1.142381	-0.014445	F	-6.596573	0.473039	-1.947609
C	-3.472350	1.608505	-0.694169	F	-5.601240	2.387181	-2.261249
C	-2.468201	-0.021189	0.779210	F	-6.772500	2.047687	-0.456967
C	-4.679496	0.926914	-0.613697	F	-4.920960	-2.625149	1.511571
C	-3.690820	-0.693940	0.841389	F	-3.806262	-1.564515	3.053644
C	-4.813605	-0.240612	0.151484	F	-2.745744	-2.753300	1.572888
C	2.318552	1.141924	0.013369	F	2.745774	-2.756506	-1.567890
C	2.468174	-0.022624	-0.778894	F	4.920994	-2.627245	-1.509169
C	3.472679	1.608637	0.692499	F	3.804073	-1.569261	-3.051463
C	3.690664	-0.695688	-0.840294	F	6.772579	2.047501	0.454639
C	4.679690	0.926715	0.612818	F	5.601713	2.388463	2.258897
C	4.813552	-0.241761	-0.150958	F	6.597110	0.474121	1.946674
H	3.384017	2.508877	1.288966	H	5.757464	-0.767591	-0.209092
H	1.632291	-0.384119	-1.366411	H	-5.757624	-0.766188	0.210226
H	-3.383496	2.508007	-1.291720				
H	-1.632396	-0.382149	1.367162				

Singlet ground state (S_0) of $2f^-$



$E_{298}(\text{B3LYP}) = -1470.51814305$ Hartree

$E_{298}(\text{TD-B3LYP}) = -1470.41076136$ Hartree

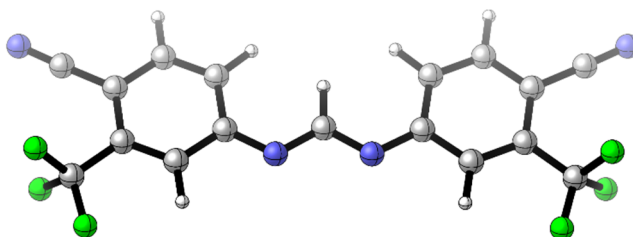
$G_{298}(\text{B3LYP}) = -1470.59770905$ Hartree

$G_{298}(\text{TD-B3LYP}) = -1470.49032736$ Hartree

-1 1

C	-0.000028	-0.424459	-0.000093	H	-3.487862	-1.768084	0.842052
H	-0.000041	0.679369	-0.000060	H	-1.484671	1.220927	-1.522778
N	-1.162250	-1.059950	-0.003945	C	-5.995299	-0.790472	0.624891
N	1.162209	-1.059923	0.003722	C	5.995252	-0.790330	-0.625092
C	-2.304131	-0.348931	-0.260439	C	-6.000966	1.675175	-0.981550
C	-3.526897	-0.857798	0.256936	C	6.000877	1.675233	0.981477
C	-2.378467	0.829746	-1.050628	N	-6.976701	2.272730	-1.209064
C	-4.732145	-0.217030	0.041544	N	6.976602	2.272792	1.209024
C	-3.586484	1.473962	-1.265261	F	-6.612694	0.084513	1.466653
C	-4.787104	0.976099	-0.724865	F	-5.782331	-1.923093	1.333626
C	2.304075	-0.348896	0.260255	F	-6.908661	-1.099652	-0.336836
C	2.378391	0.829742	1.050506	F	6.908618	-1.099545	0.336621
C	3.526851	-0.857715	-0.257145	F	5.782303	-1.922919	-1.333885
C	3.586397	1.473967	1.265174	F	6.612635	0.084708	-1.466807
C	4.732088	-0.216938	-0.041718	H	3.618978	2.371856	1.873328
C	4.787026	0.976152	0.724755	H	-3.619081	2.371883	-1.873367
H	3.487832	-1.767971	-0.842309				
H	1.484587	1.220883	1.522674				

Singlet Excited state (S_1) of $2f^-$



$E_{298}(\text{B3LYP}) = -1470.51468198$ Hartree

$E_{298}(\text{TD-B3LYP}) = -1470.41842354$ Hartree

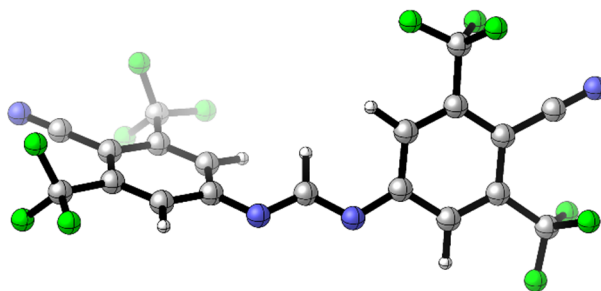
$G_{298}(\text{B3LYP}) = -1470.59113798$ Hartree

$G_{298}(\text{TD-B3LYP}) = -1470.49487954$ Hartree

-1 1

C	0.000000	-0.037099	-0.000005	H	-1.726188	2.026675	-0.109498
H	0.000000	1.055220	-0.000001	C	-5.960284	-1.324519	-0.194677
N	-1.145986	-0.724249	-0.045485	C	5.960285	-1.324515	0.194679
N	1.145987	-0.724249	0.045473	C	-6.263332	1.614976	-0.256610
C	-2.350013	-0.084599	-0.095834	C	6.263330	1.614980	0.256618
C	-3.500619	-0.917808	-0.122028	N	-7.309333	2.139975	-0.303372
C	-2.561850	1.338764	-0.124784	N	7.309329	2.139982	0.303385
C	-4.782309	-0.402734	-0.171634	F	-6.804156	-1.117142	0.859638
C	-3.839191	1.855385	-0.176850	F	-5.610131	-2.632335	-0.154822
C	-4.981440	1.017635	-0.201676	F	-6.726222	-1.162694	-1.314477
C	2.350013	-0.084598	0.095826	F	6.726218	-1.162691	1.314482
C	2.561848	1.338766	0.124778	F	5.610132	-2.632332	0.154821
C	3.500620	-0.917806	0.122022	F	6.804160	-1.117137	-0.859632
C	3.839189	1.855387	0.176850	H	3.985754	2.930247	0.200150
C	4.782309	-0.402731	0.171633	H	-3.985757	2.930245	-0.200147
C	4.981439	1.017638	0.201679				
H	3.342544	-1.989125	0.099982				
H	1.726186	2.026676	0.109491				
H	-3.341543	-1.989127	-0.099990				

Singlet ground state (S_0) of $2g^-$



$E_{298}(\text{B3LYP}) = -2144.81847078$ Hartree

$E_{298}(\text{TD-B3LYP}) = -2144.71389236$ Hartree

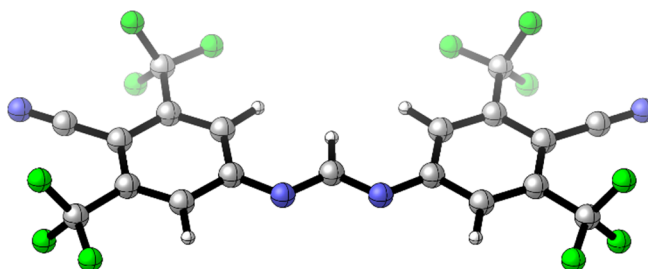
$G_{298}(\text{B3LYP}) = -2144.91645578$ Hartree

$G_{298}(\text{TD-B3LYP}) = -2144.81187736$ Hartree

-1 1

C	0.000022	-1.159376	0.000040	C	5.946486	-1.606689	-0.964767
H	0.000015	-0.056160	0.000016	C	-5.946436	-1.606713	0.964870
N	1.157364	-1.799430	-0.070312	C	-3.746897	1.994336	-1.825237
N	-1.157312	-1.799441	0.070420	C	6.099776	0.864254	0.556290
C	2.317820	-1.101613	0.105793	C	-6.099754	0.864162	-0.556295
C	3.503906	-1.633206	-0.462075	N	7.127765	1.400263	0.671702
C	2.447211	0.091199	0.867828	N	-7.127748	1.400157	-0.671731
C	4.723316	-0.999435	-0.322247	F	6.518153	-0.764119	-1.865648
C	3.669239	0.727953	1.005632	F	5.671320	-2.753445	-1.625501
C	4.842994	0.208158	0.411587	F	6.906653	-1.903639	-0.049451
C	-2.317777	-1.101645	-0.105714	F	4.187985	3.047713	1.088164
C	-2.447181	0.091133	-0.867802	F	4.600248	1.871036	2.875322
C	-3.503856	-1.633225	0.462177	F	2.548732	2.354673	2.338786
C	-3.669217	0.727867	-1.005634	F	-2.548730	2.354537	-2.338864
C	-4.723274	-0.999475	0.322323	F	-4.187982	3.047620	-1.088264
C	-4.842966	0.208085	-0.411565	F	-4.600245	1.870861	-2.875369
H	-3.427517	-2.555003	1.024429	F	-6.906603	-1.903712	0.049569
H	-1.584955	0.499483	-1.377116	F	-5.671258	-2.753439	1.625652
H	3.427577	-2.555008	-1.024287	F	-6.518109	-0.764111	1.865716
H	1.584979	0.499562	1.377123				
C	3.746905	1.994458	1.825181				

Singlet excited state (S_1) of $2g^-$



$E_{298}(\text{B3LYP}) = -2144.81515281$ Hartree

$E_{298}(\text{TD-B3LYP}) = -2144.71922541$ Hartree

$G_{298}(\text{B3LYP}) = -2144.91128581$ Hartree

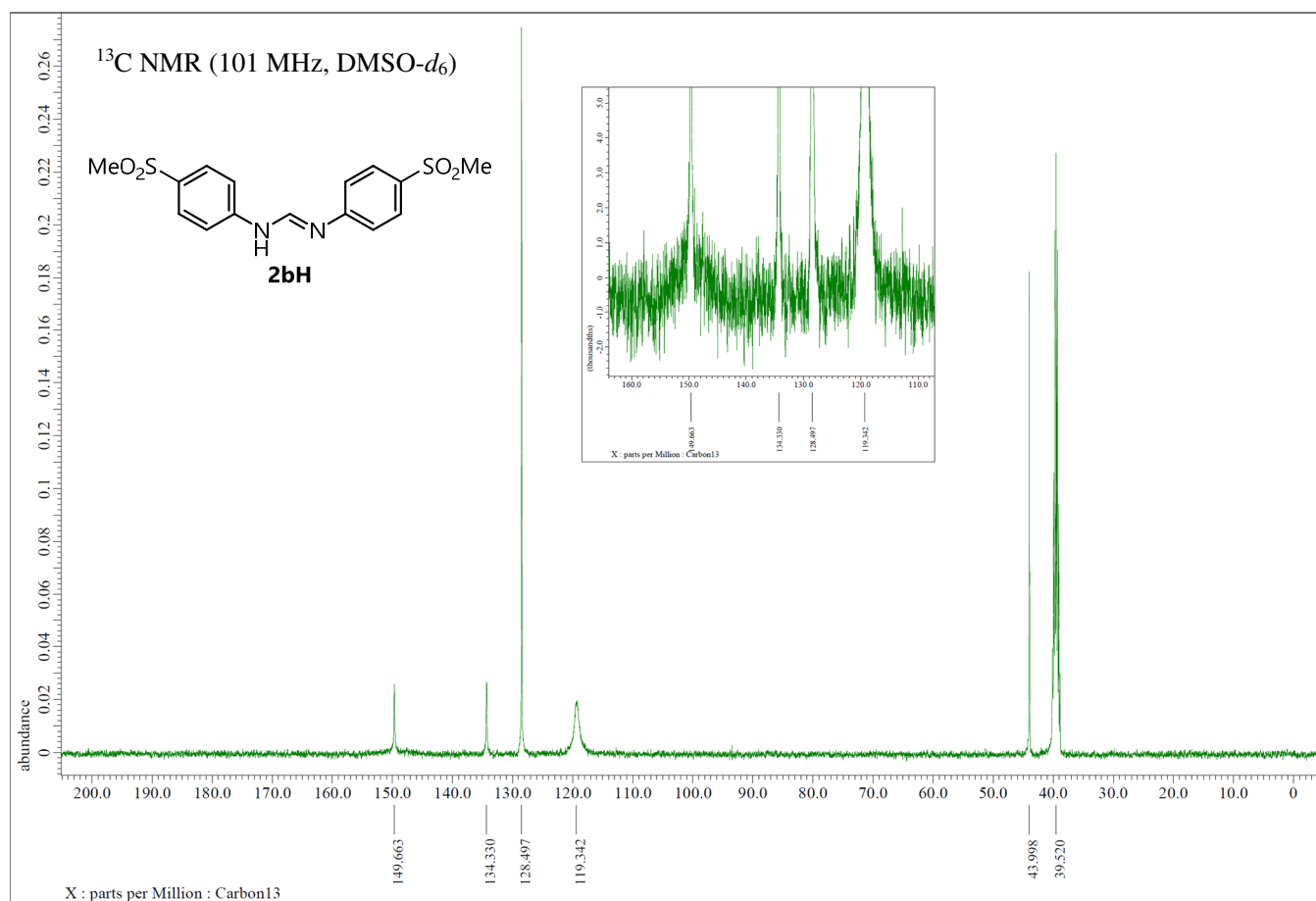
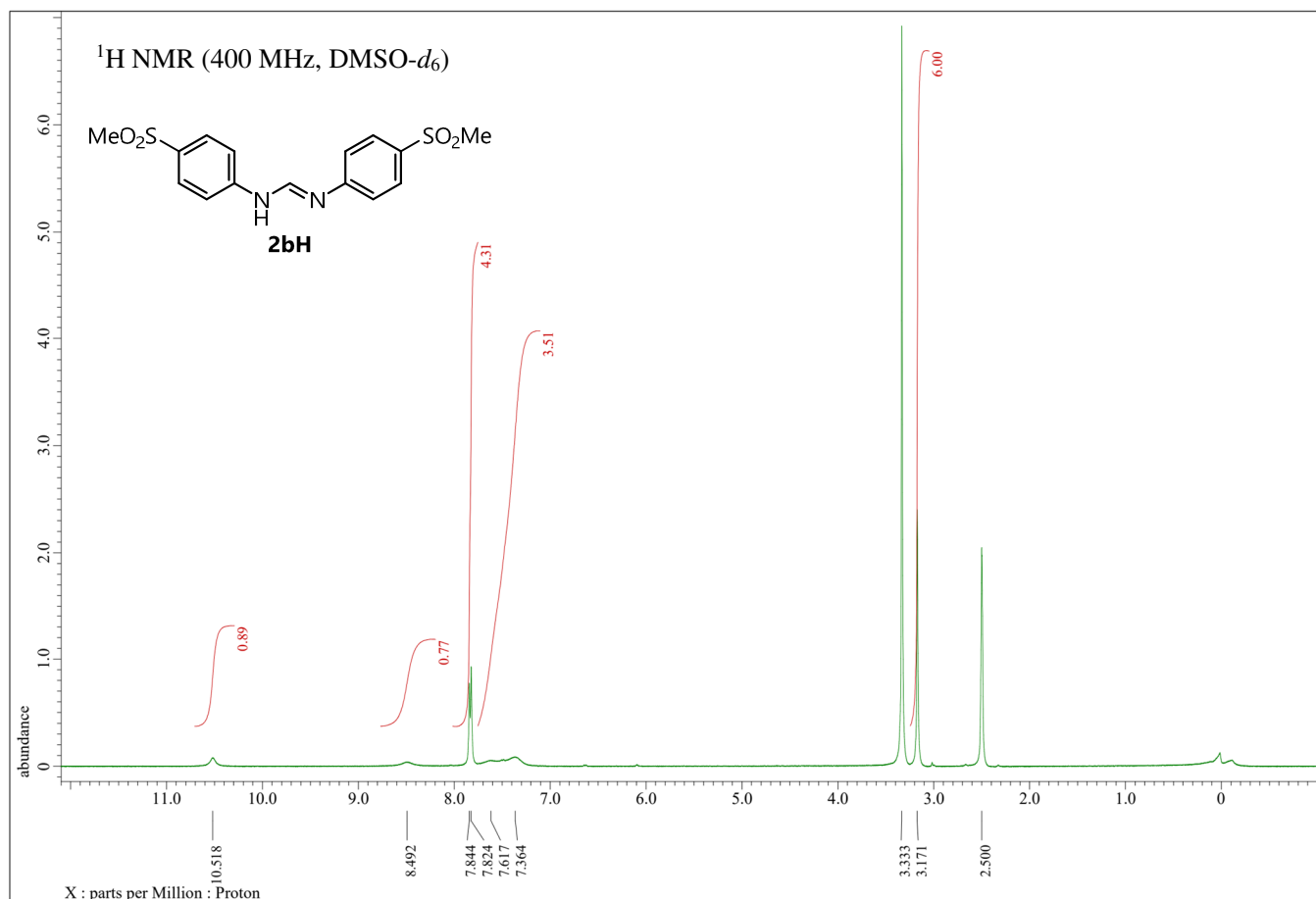
$G_{298}(\text{TD-B3LYP}) = -2144.81535841$ Hartree

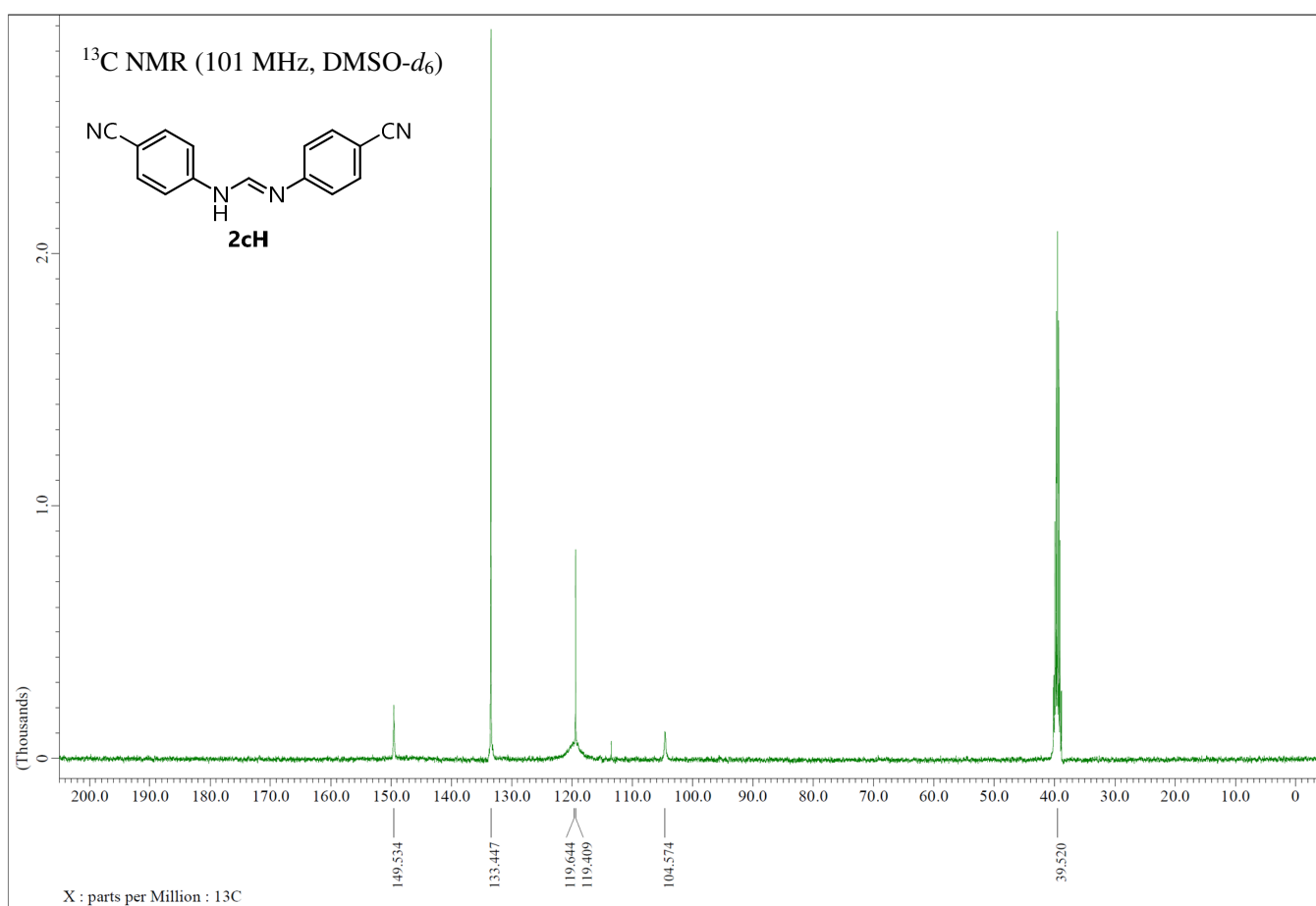
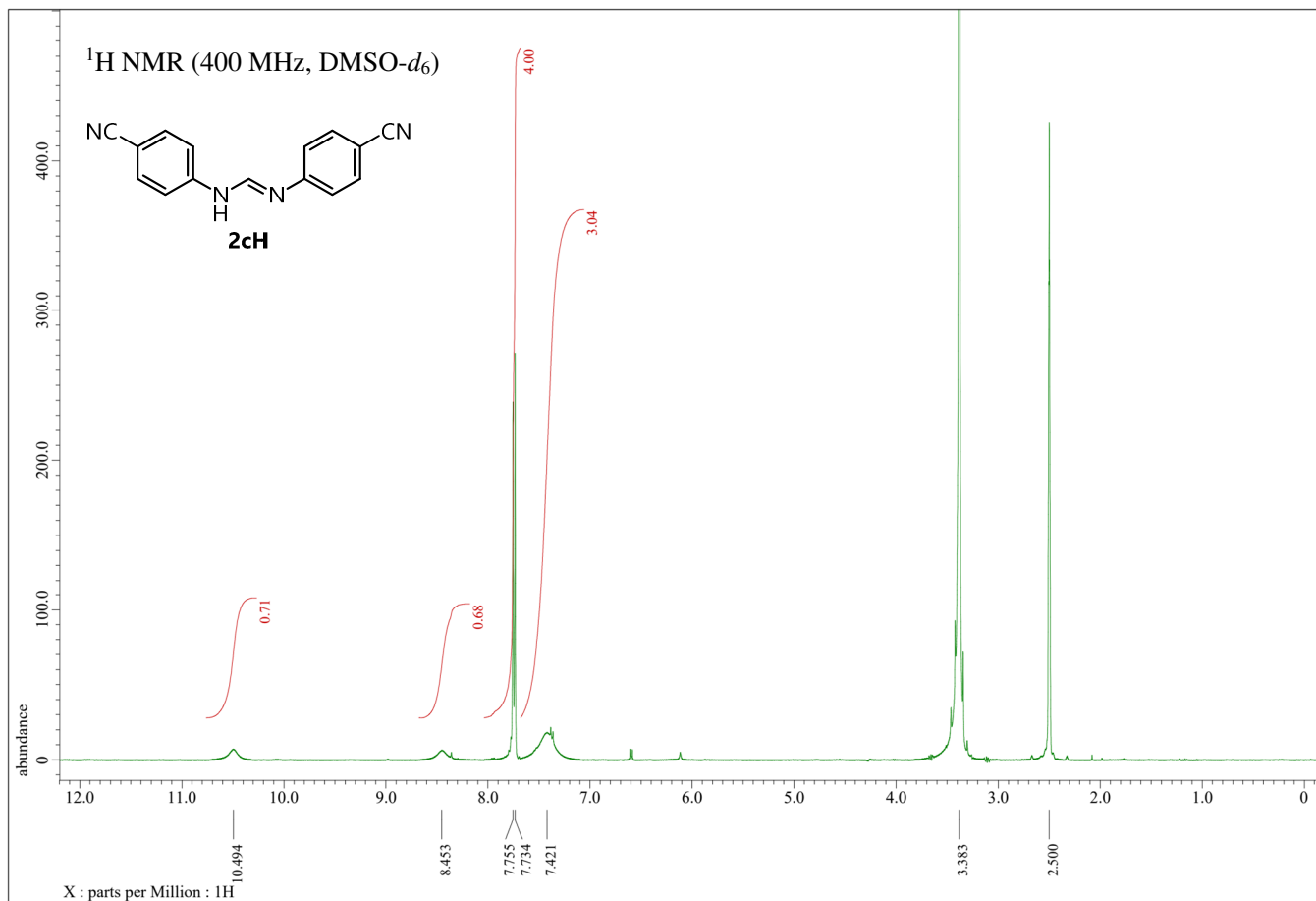
-1 1

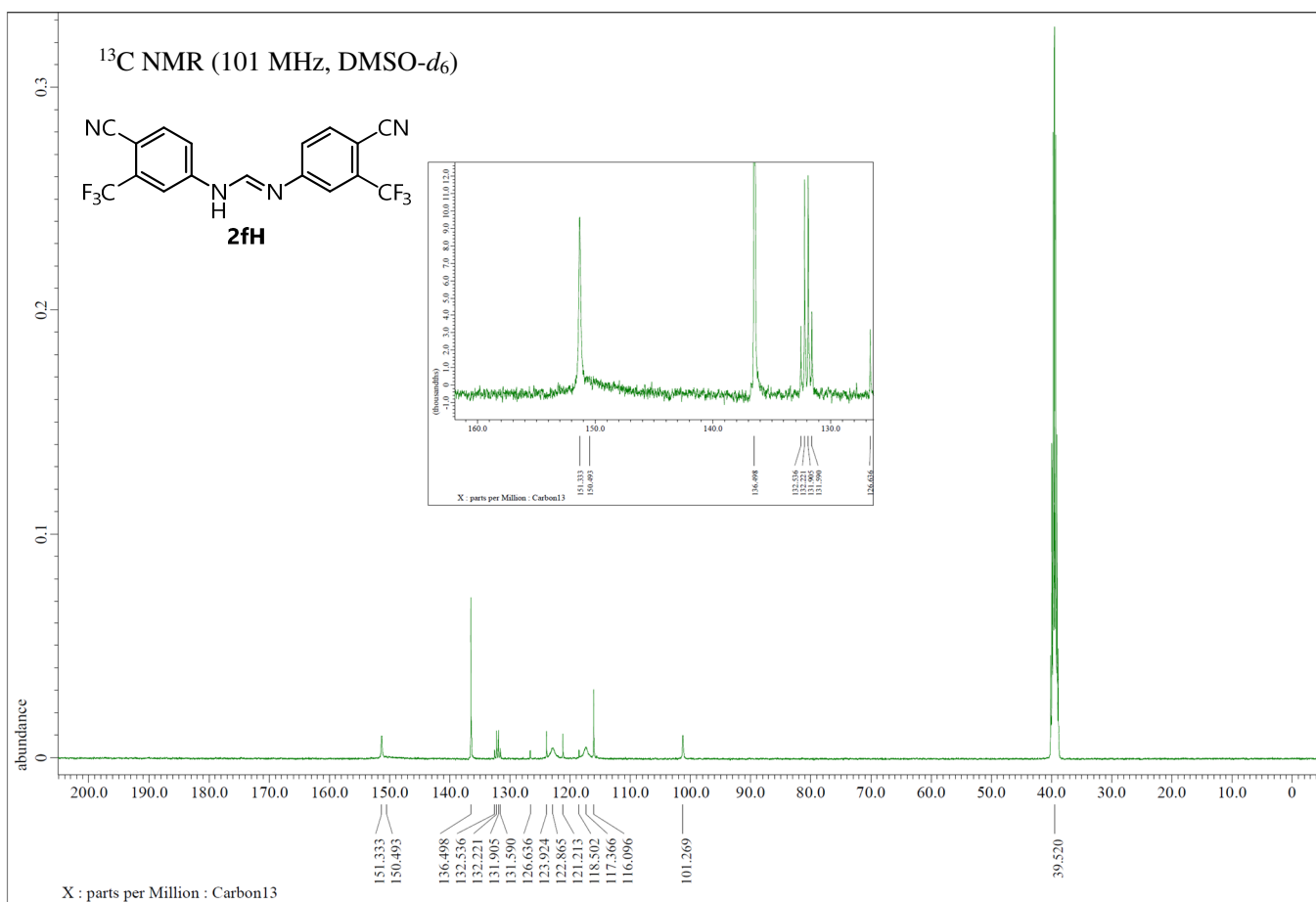
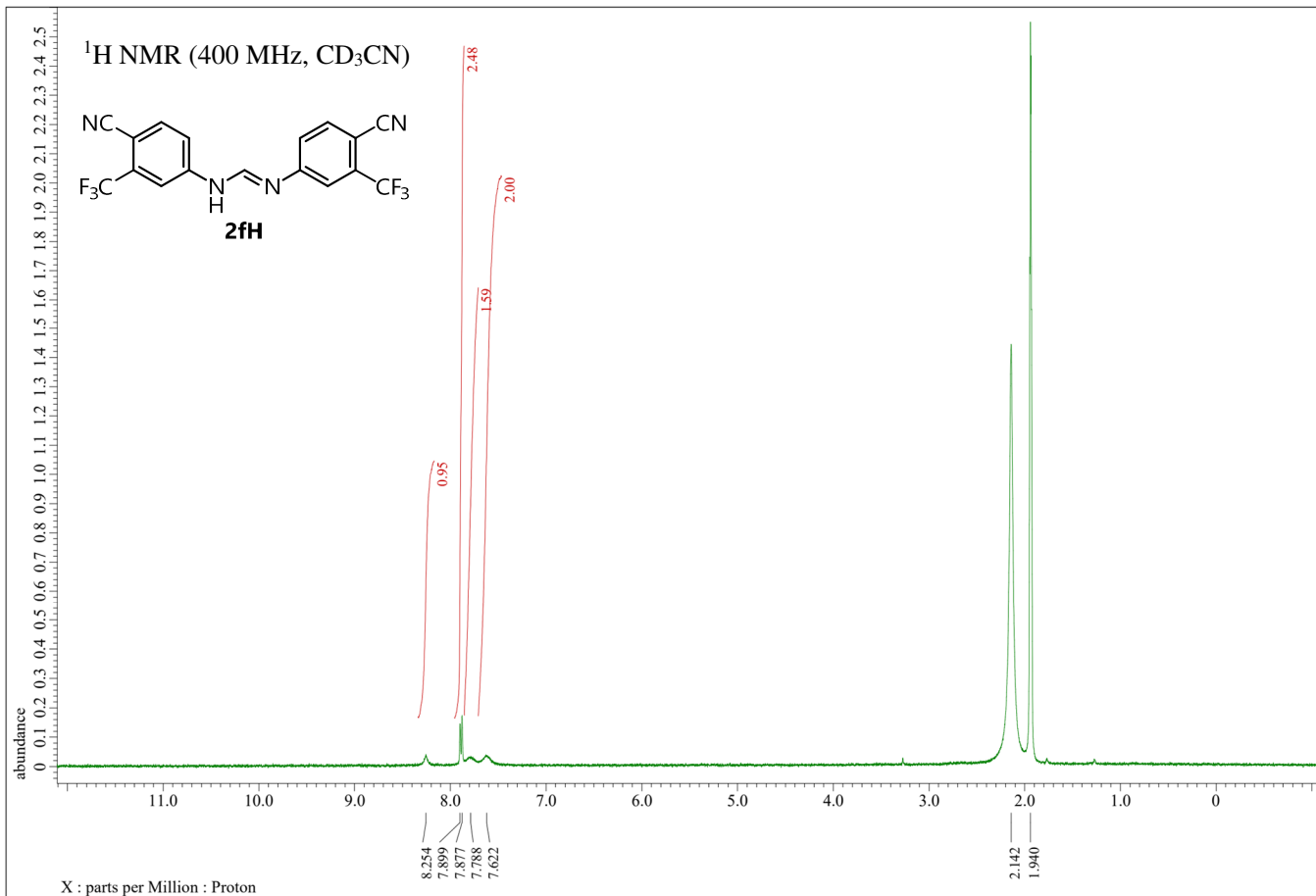
C	0.000000	0.873730	-0.000031	C	5.009969	-0.136340	-0.004020
H	0.000000	-0.219516	0.000049	H	3.331059	2.855079	-0.003861
N	-1.143600	1.563270	0.000874	H	1.754079	-1.166745	0.000934
N	1.143599	1.563270	-0.001015	H	-3.331059	2.855079	0.003778
C	-2.356101	0.940498	0.001588	H	-1.754079	-1.166745	-0.001095
C	-3.498756	1.785236	0.003343	C	-4.054510	-2.482686	0.001310
C	-2.584297	-0.475145	0.000648	C	-5.950432	2.221704	0.006454
C	-4.781876	1.279180	0.004549	C	5.950432	2.221705	-0.006394
C	-3.864497	-0.986048	0.001830	C	4.054510	-2.482686	-0.001324
C	-5.009969	-0.136340	0.004057	C	-6.321066	-0.668640	0.005812
C	2.356101	0.940498	-0.001689	C	6.321066	-0.668640	-0.005682
C	2.584297	-0.475145	-0.000746	N	-7.407726	-1.102390	0.007327
C	3.498756	1.785236	-0.003406	N	7.407726	-1.102390	-0.007118
C	3.864498	-0.986048	-0.001861	F	-6.753205	2.049064	-1.081178
C	4.781876	1.279180	-0.004541	F	-5.572917	3.521288	0.006205

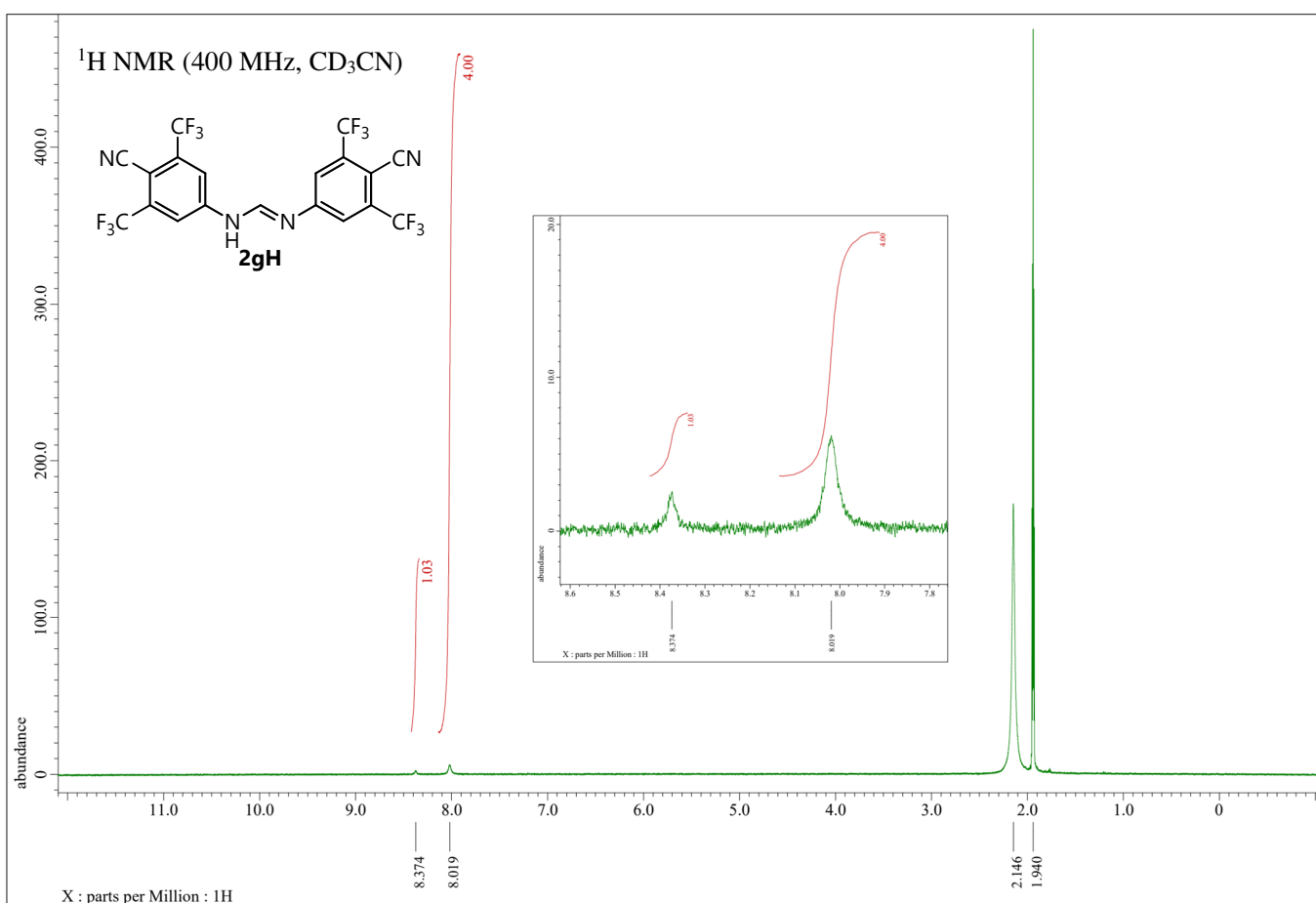
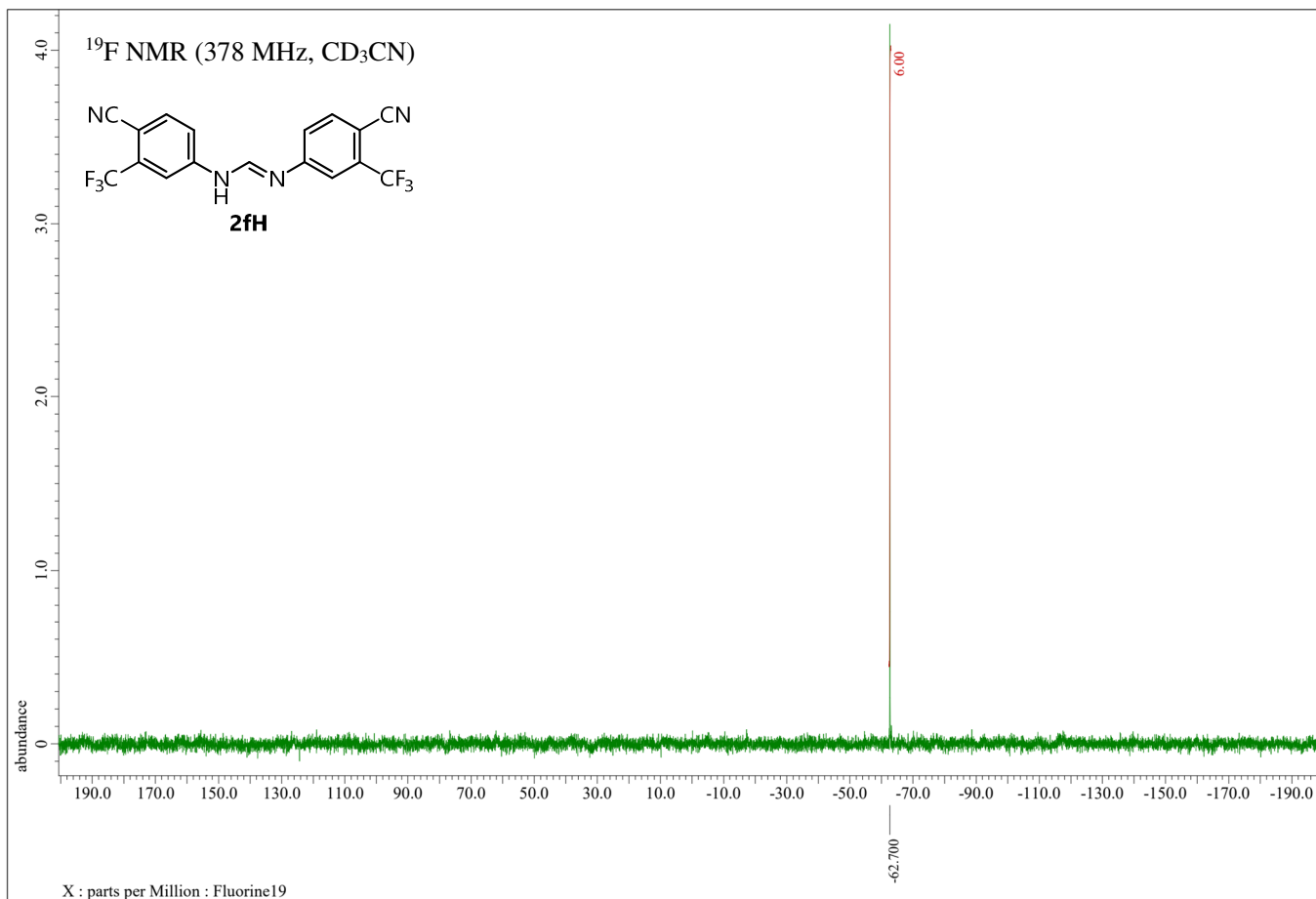
F	-6.750045	2.048566	1.096341	F	4.743712	-2.908849	-1.092891
F	-4.751792	-2.907283	-1.085663	F	6.750122	2.048532	-1.096219
F	-4.743550	-2.908852	1.092979	F	5.572916	3.521289	-0.006213
F	-2.880914	-3.156993	-0.003600	F	6.753128	2.049099	1.081300
F	2.880914	-3.156993	0.003412				
F	4.751632	-2.907285	1.085752				

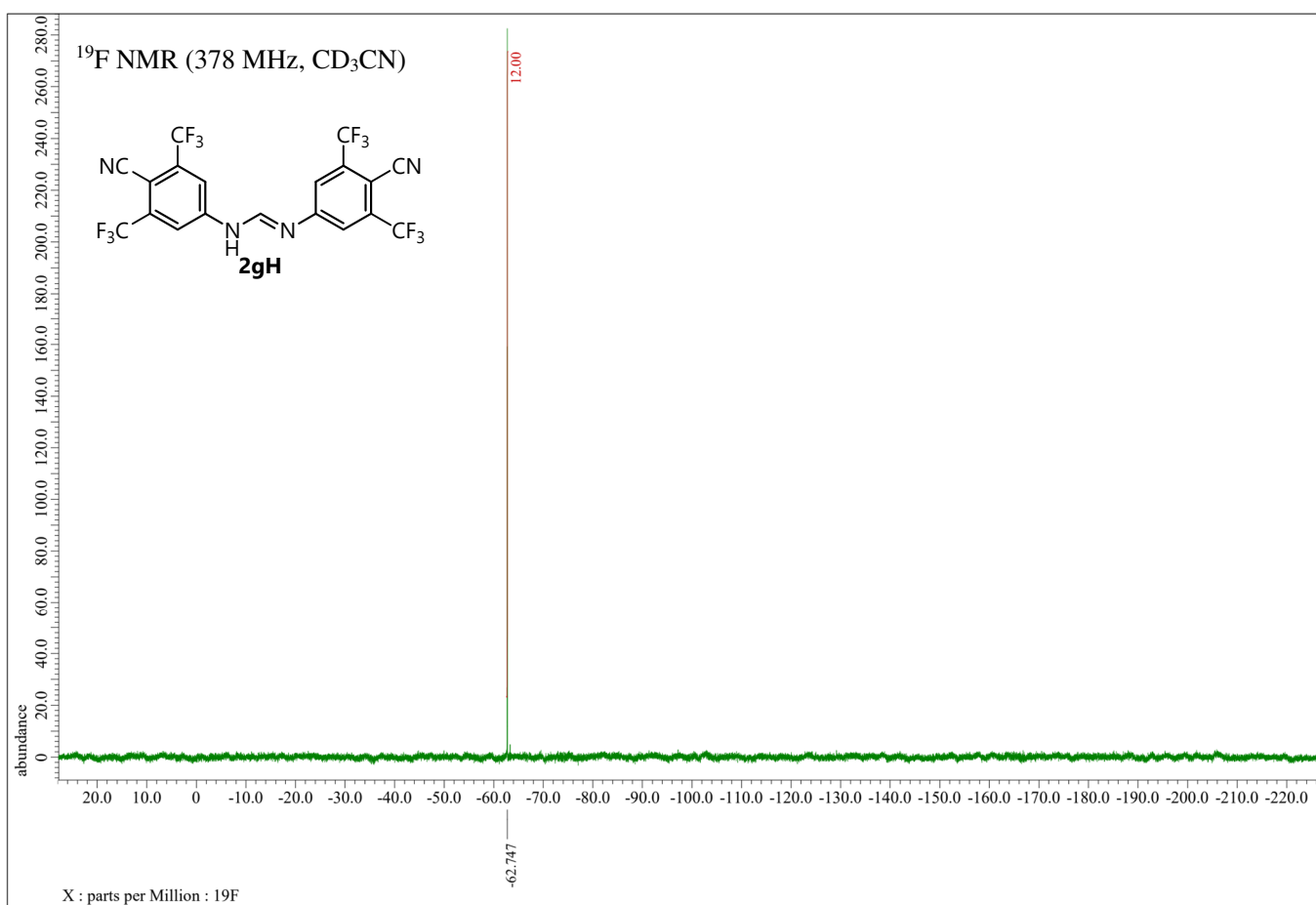
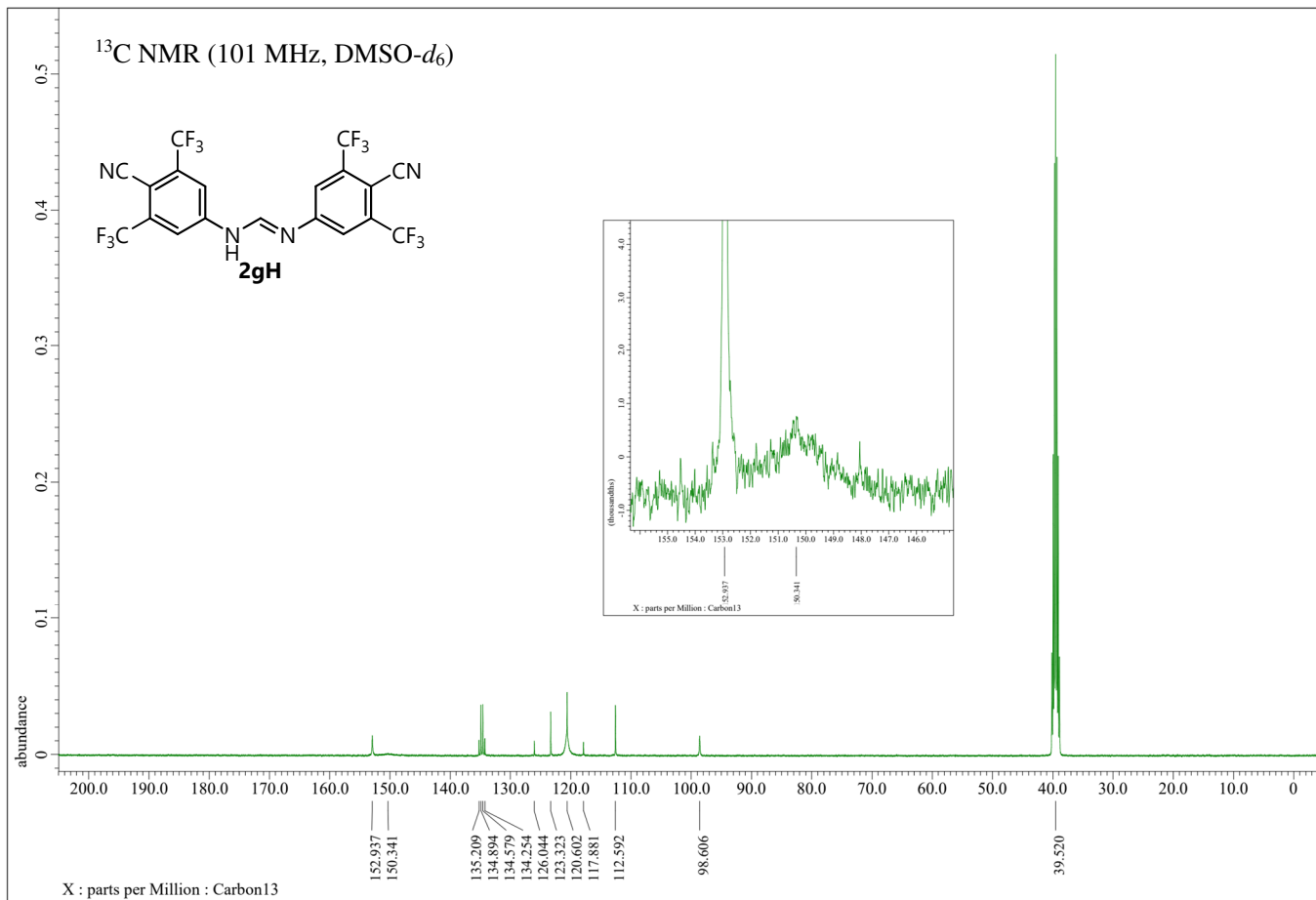
(K) Copies of NMR Spectra

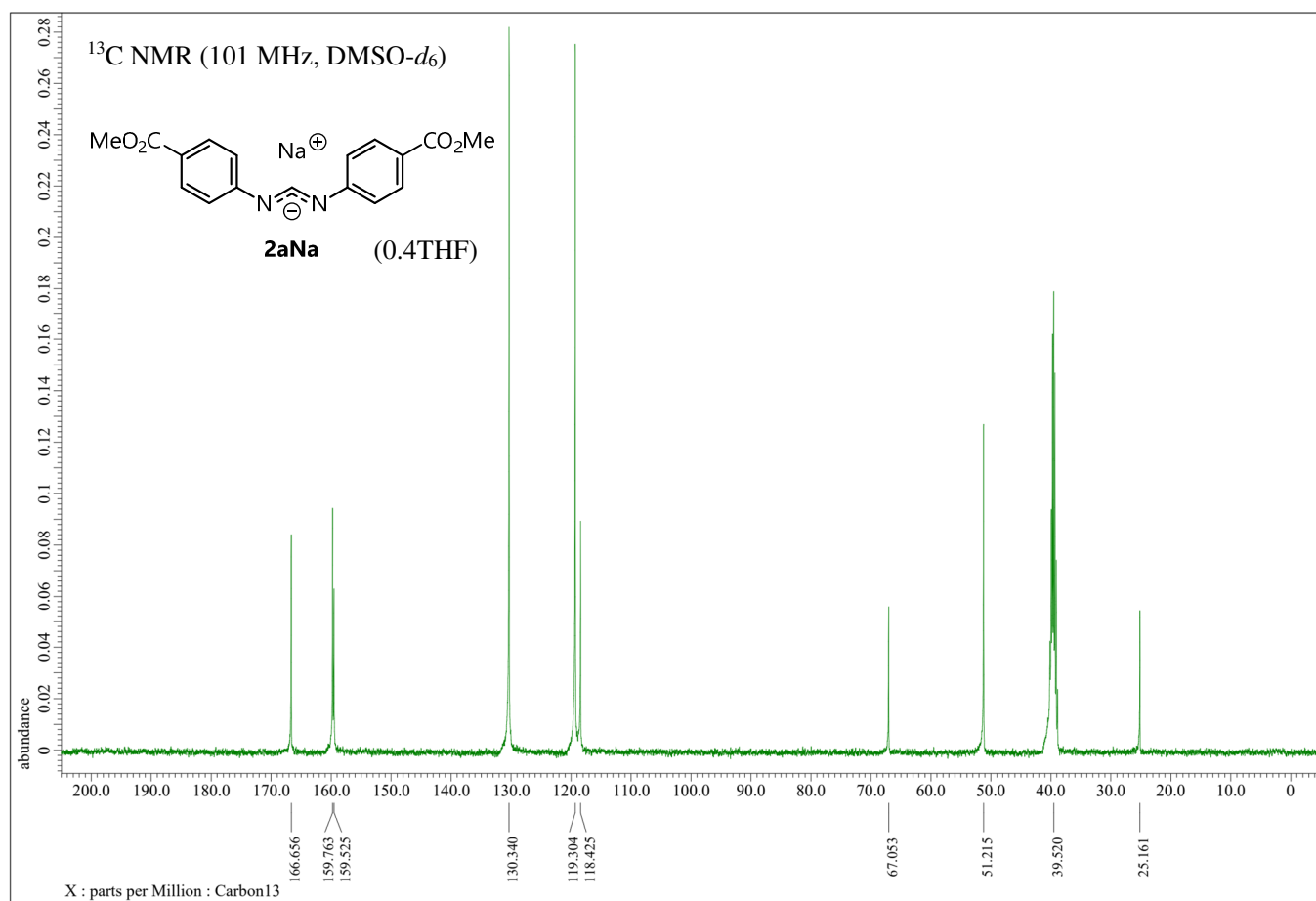
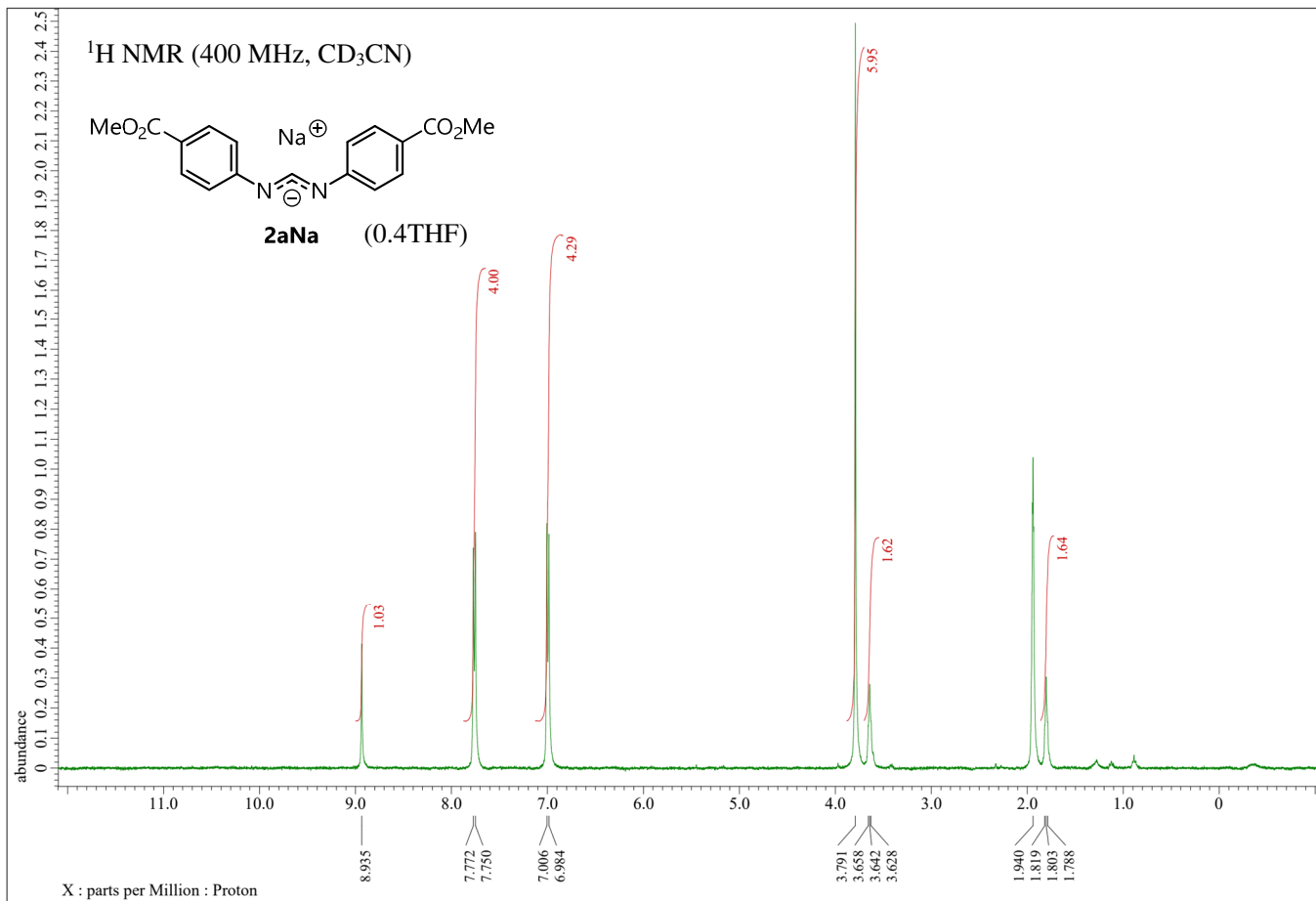


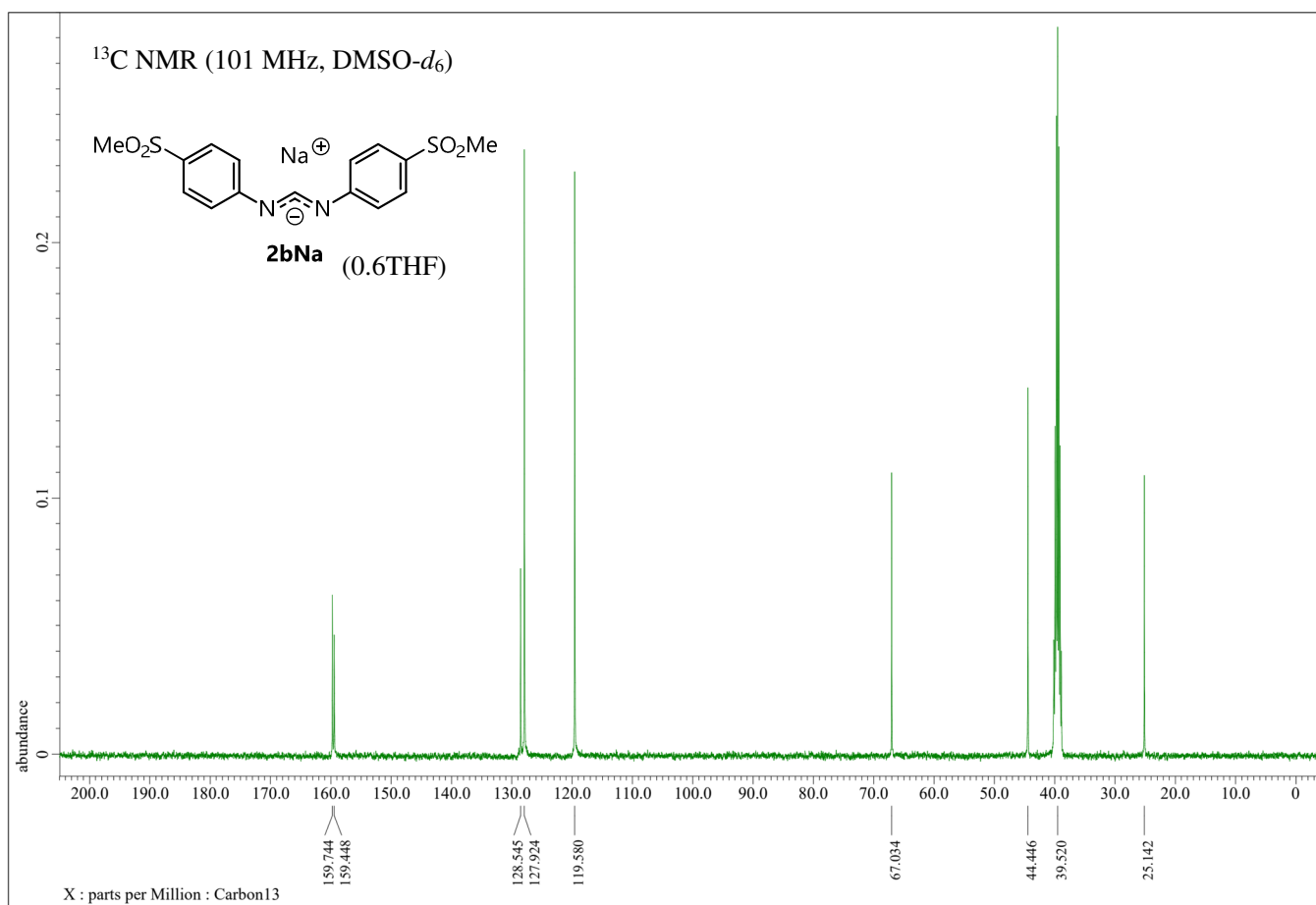
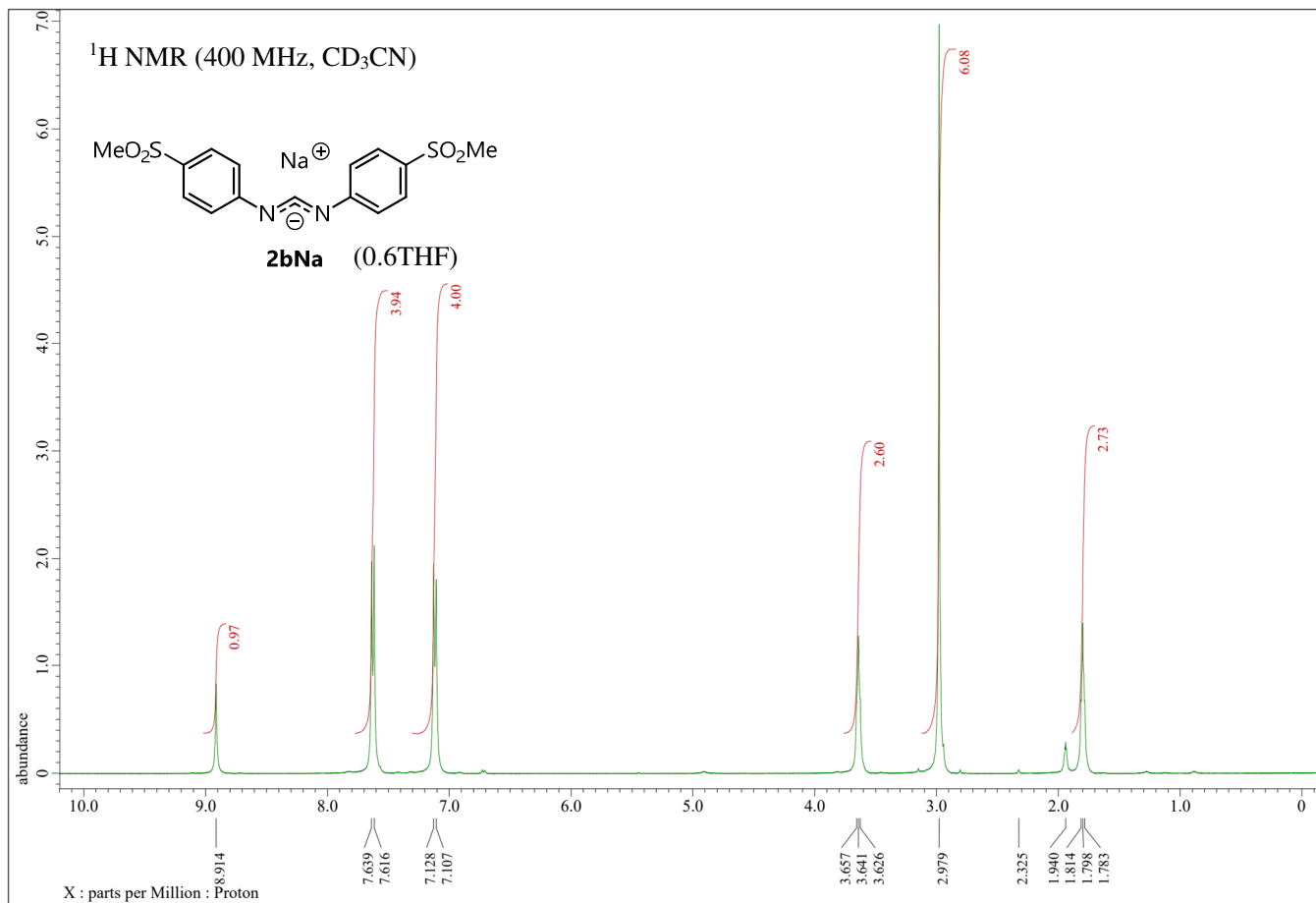


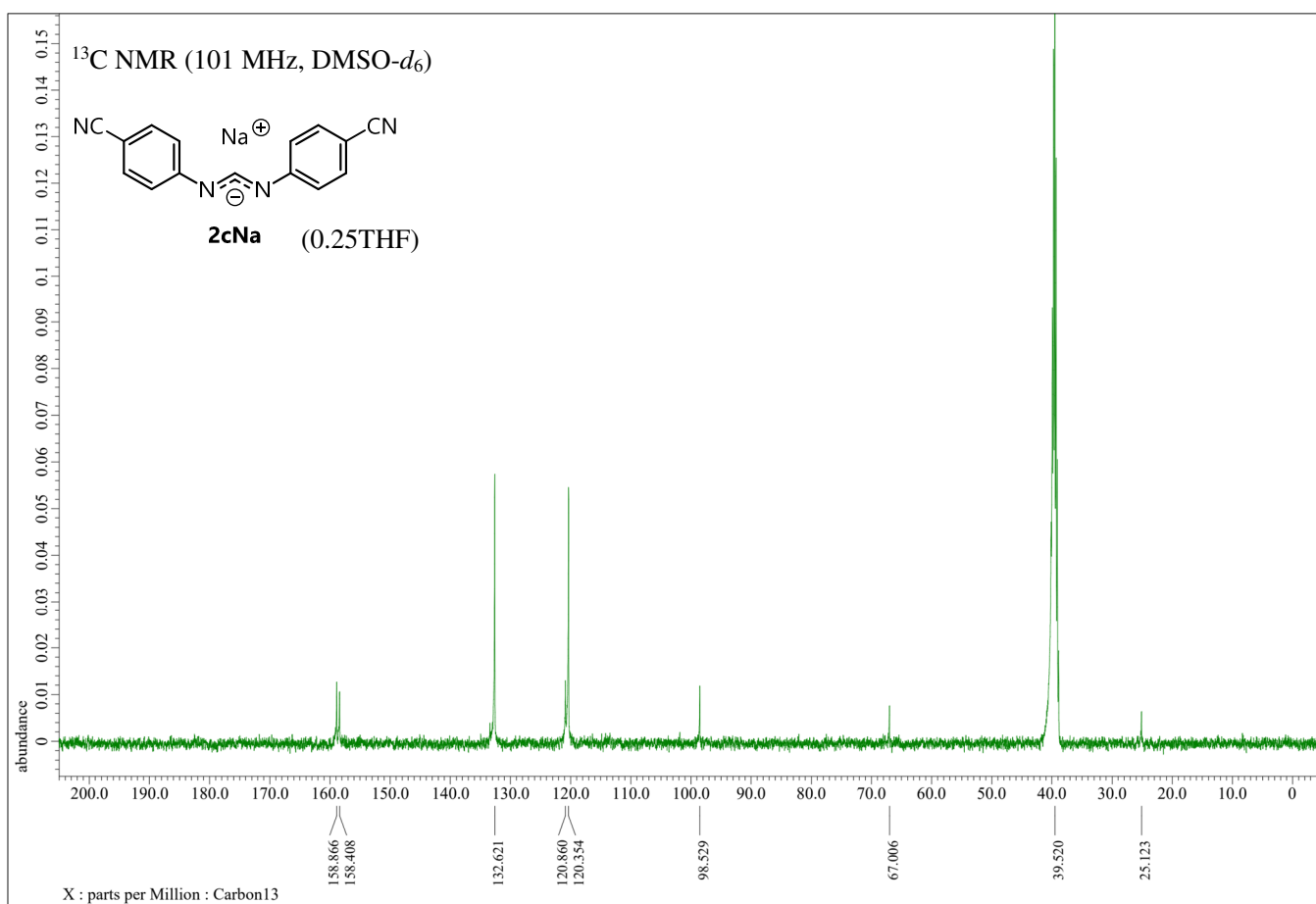
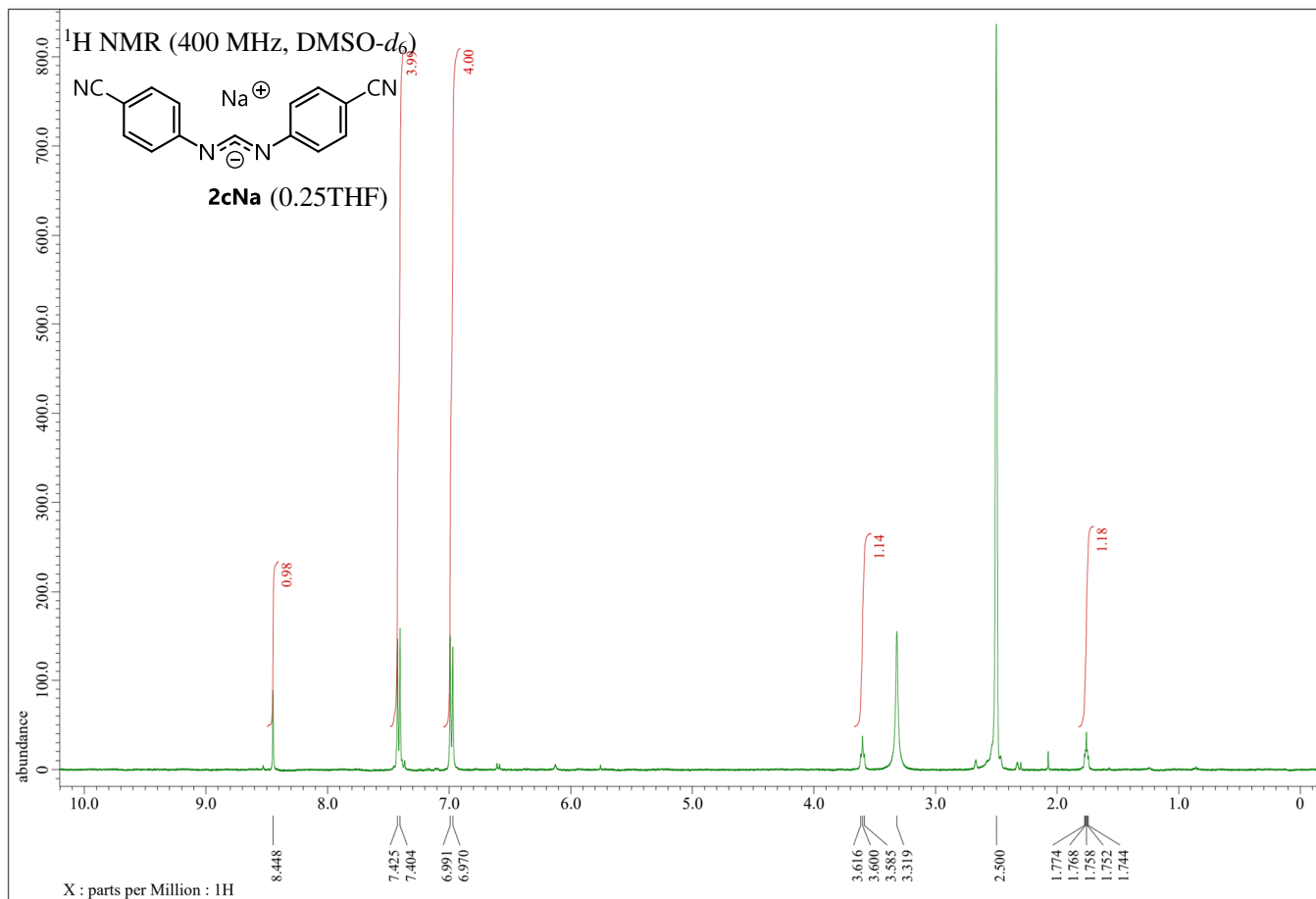


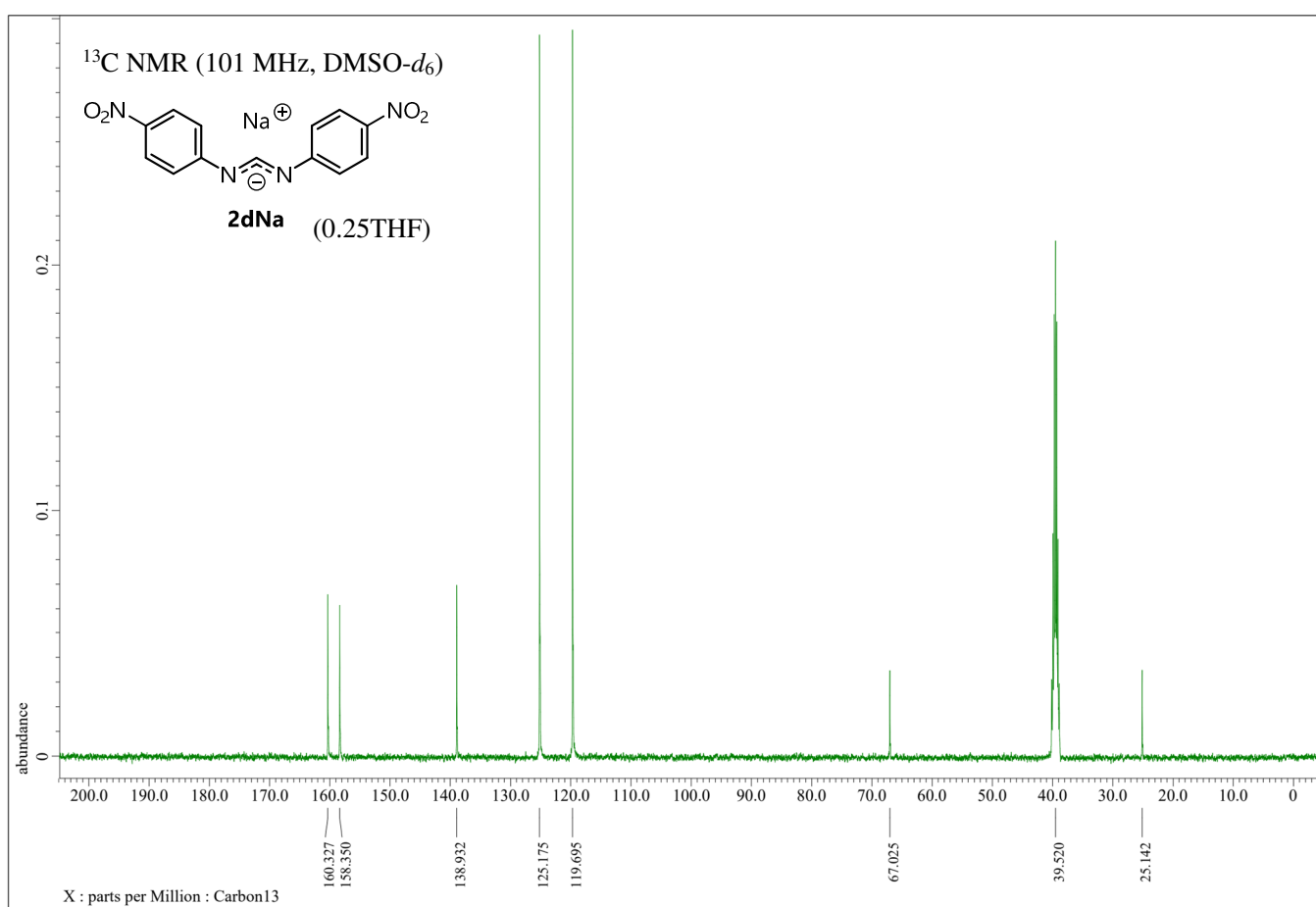
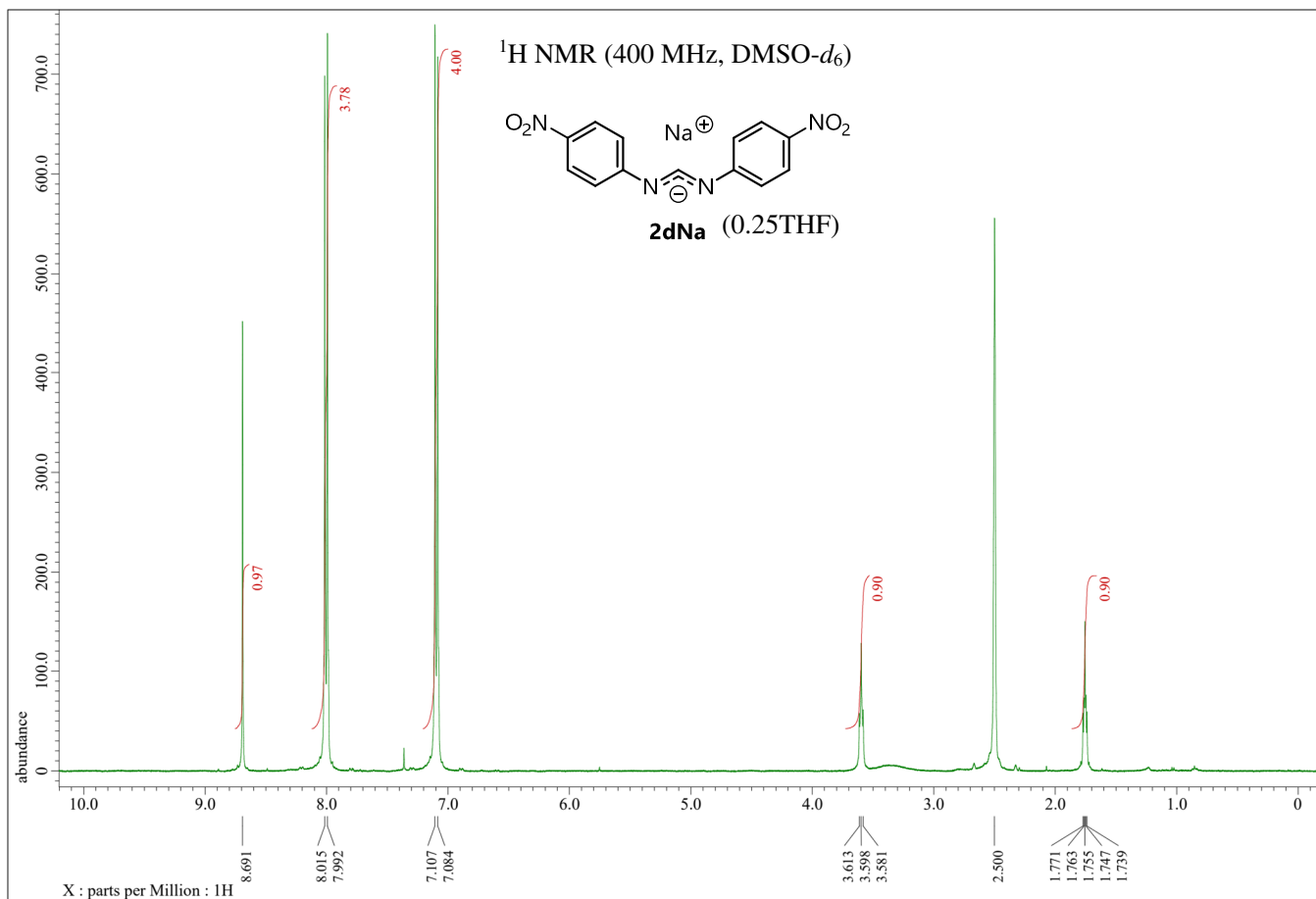


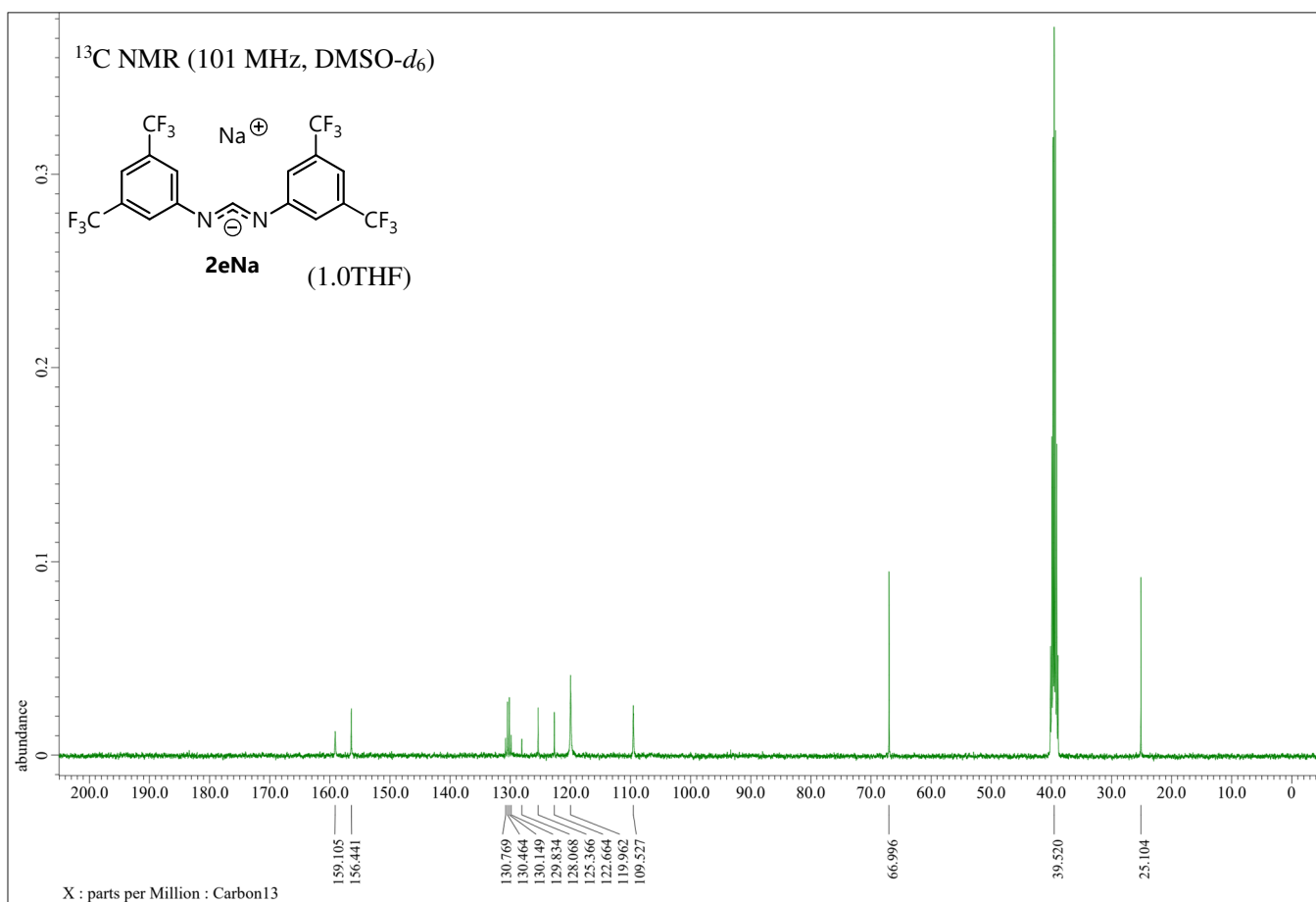
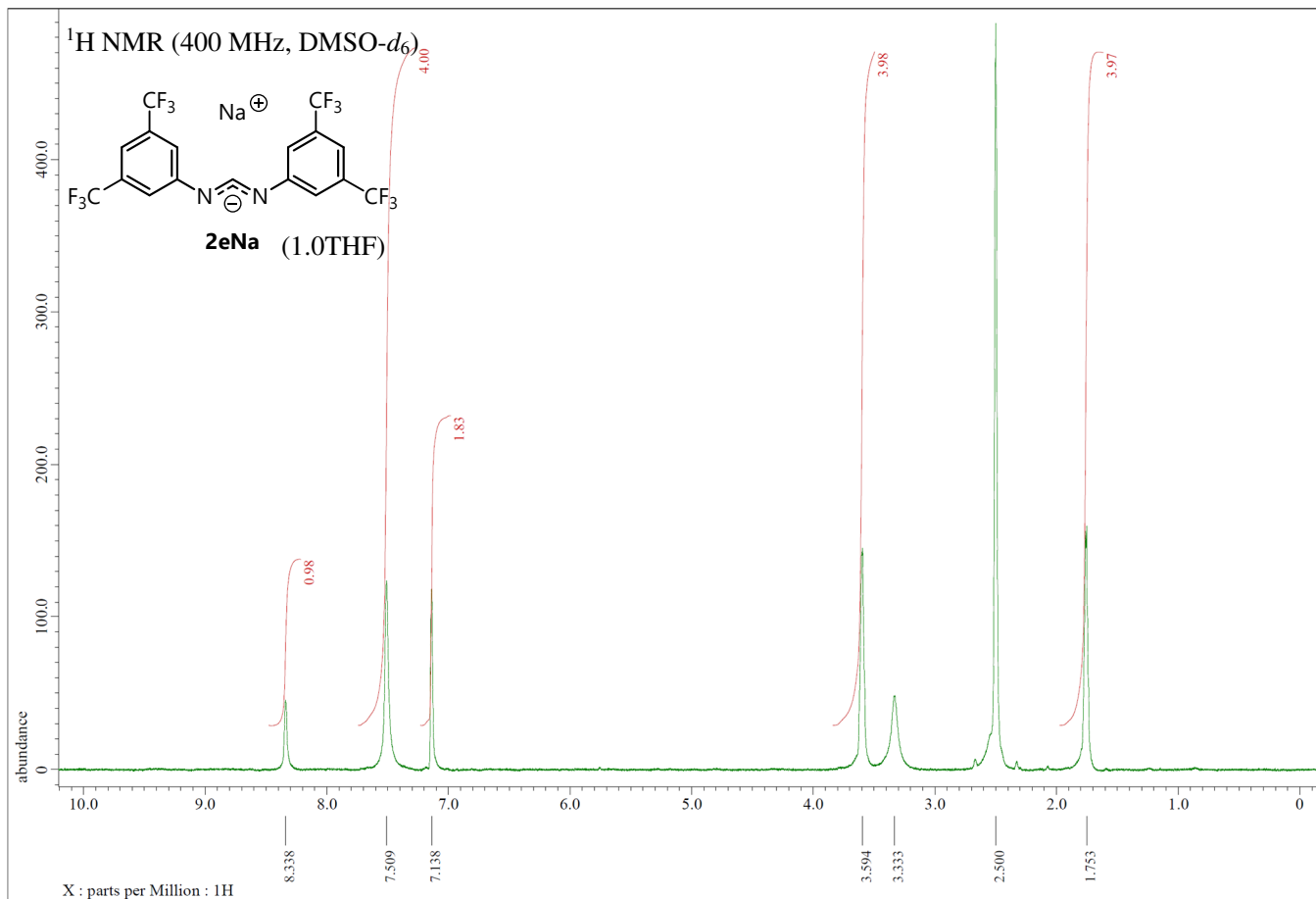


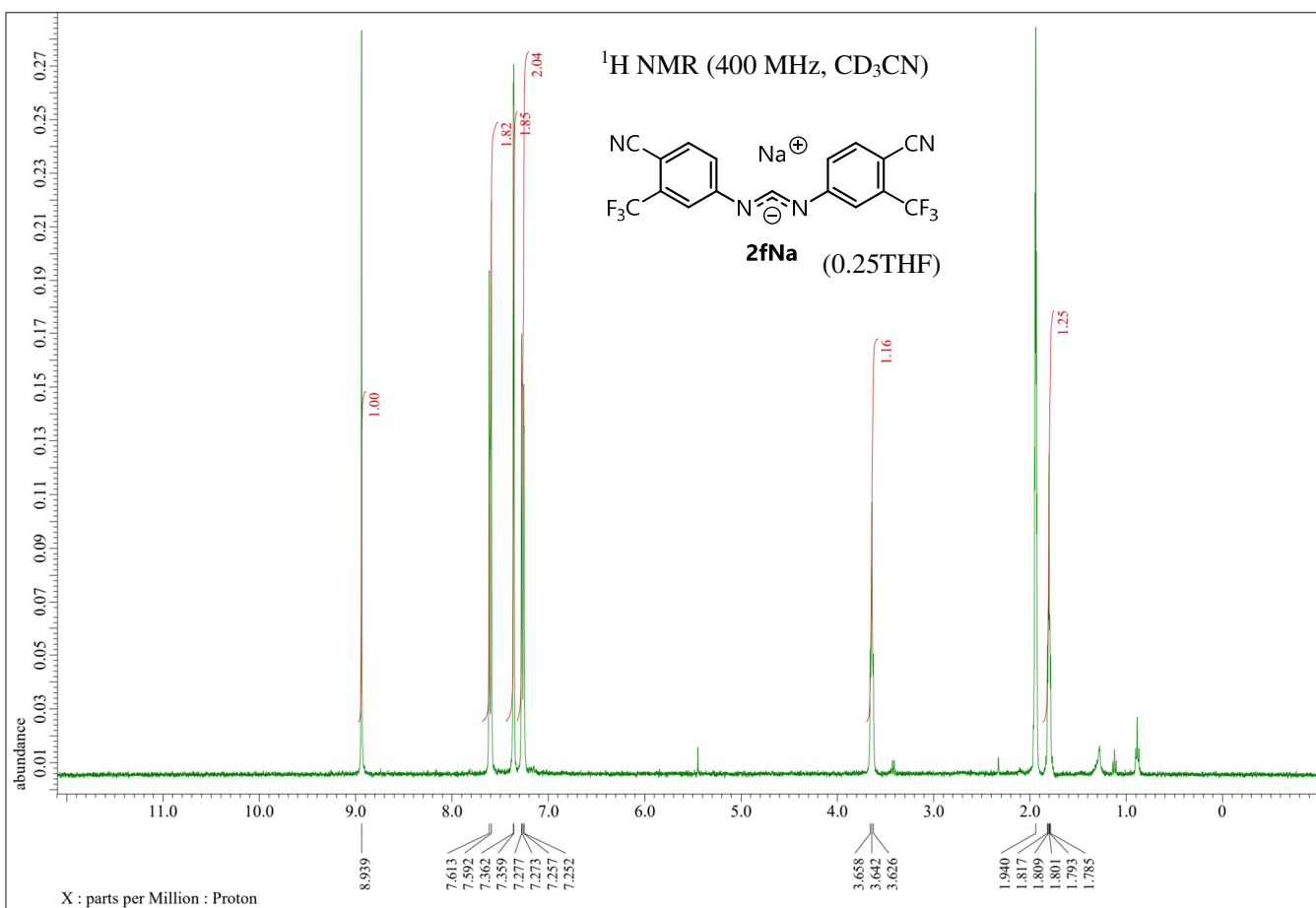
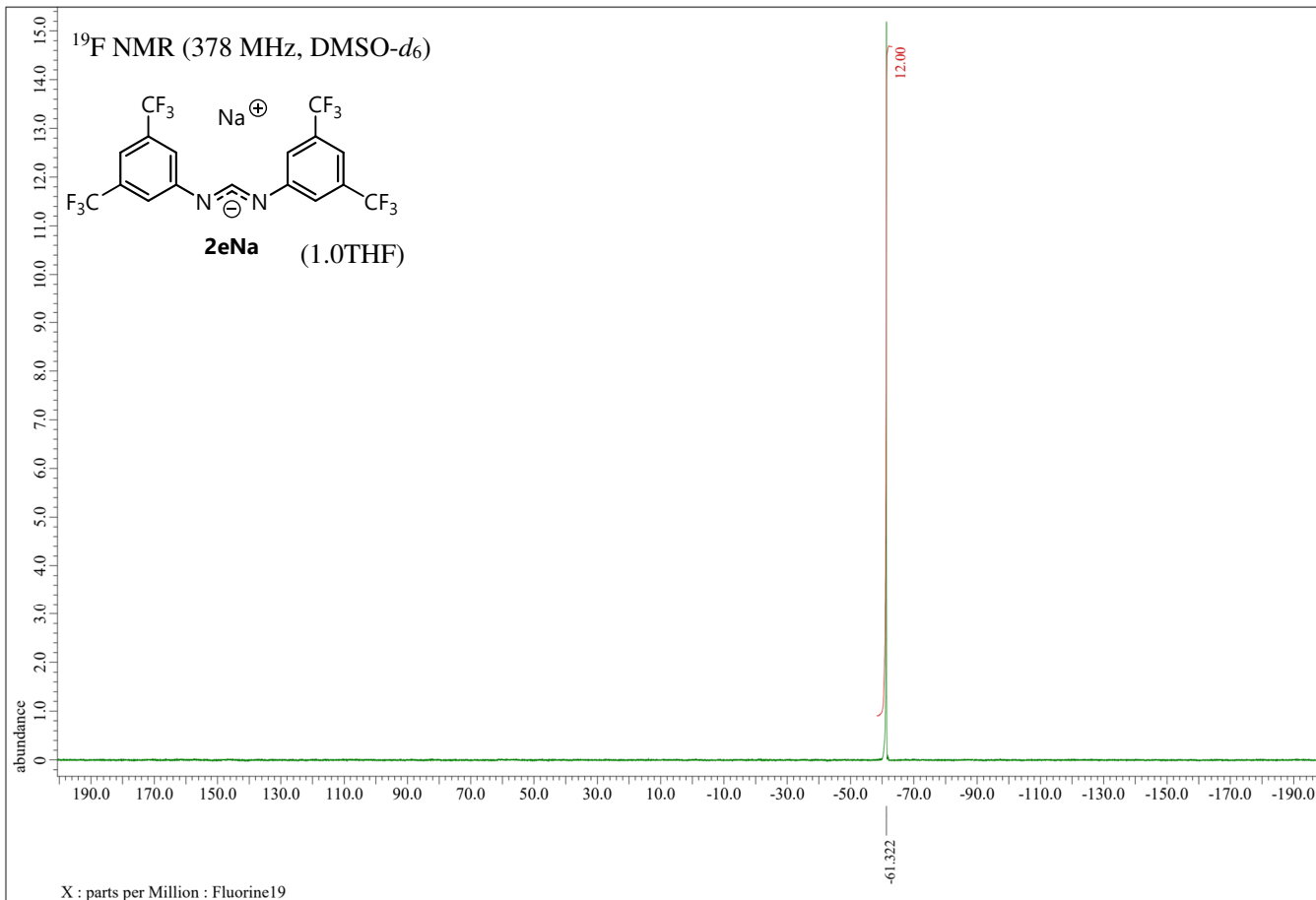


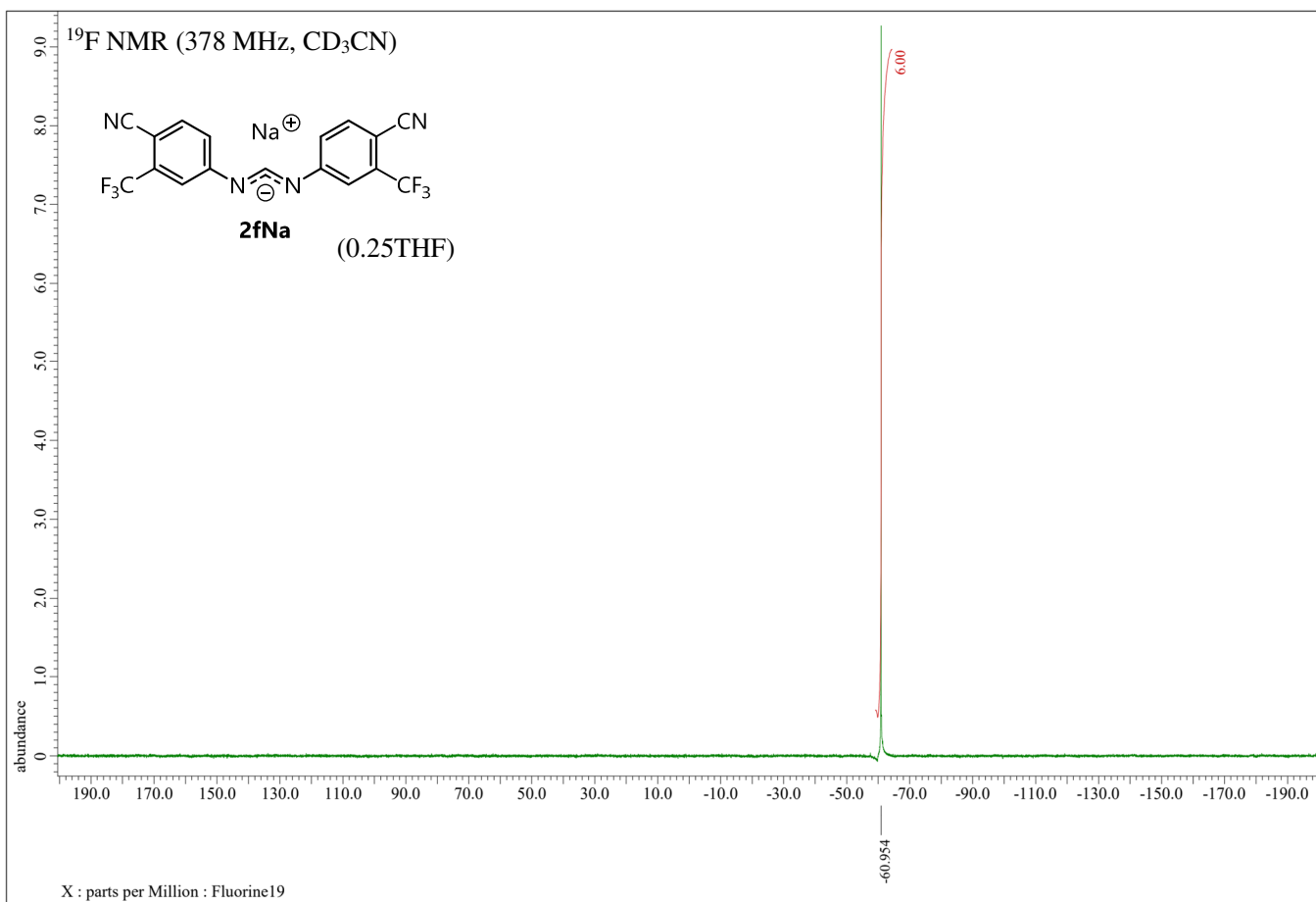
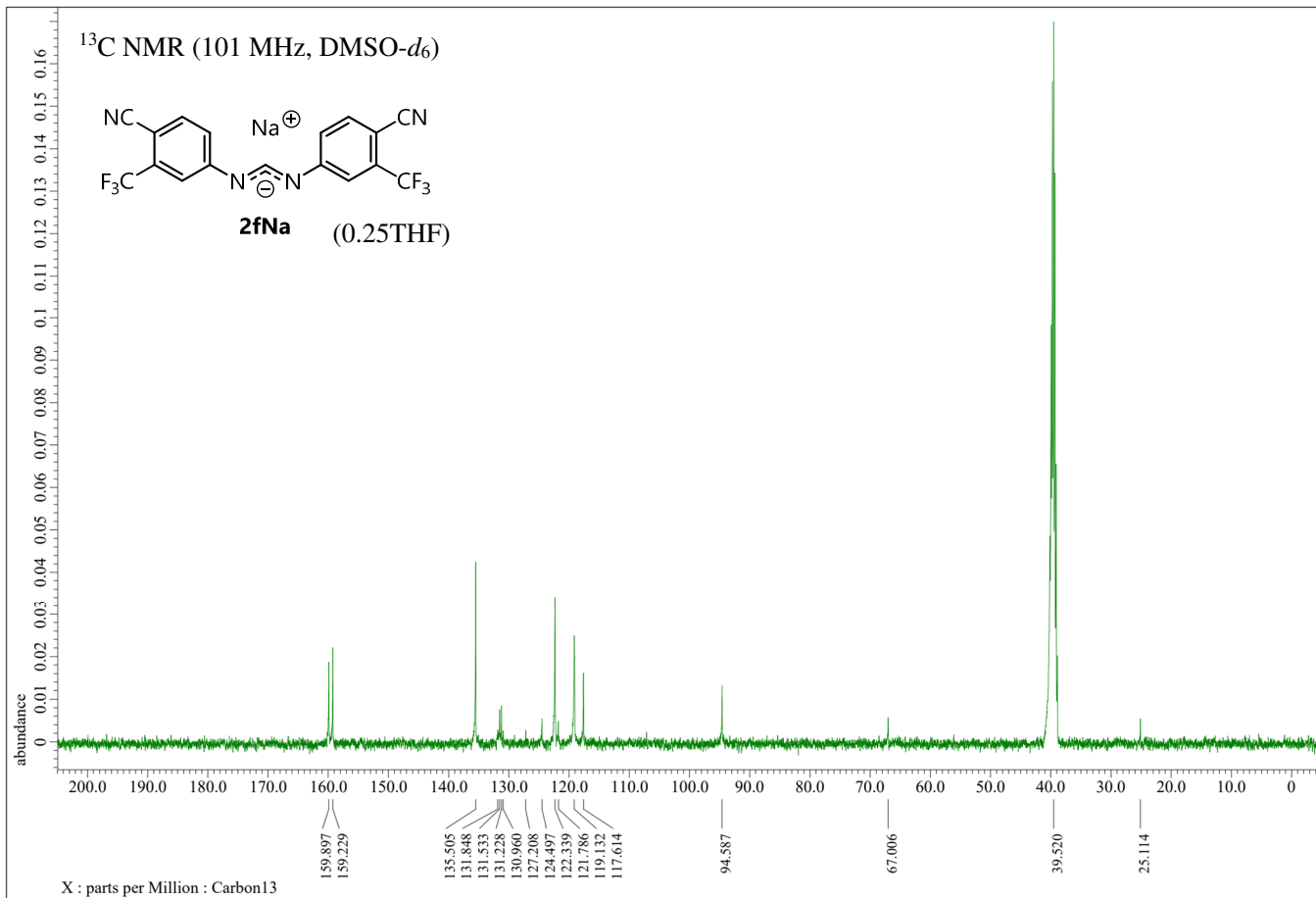


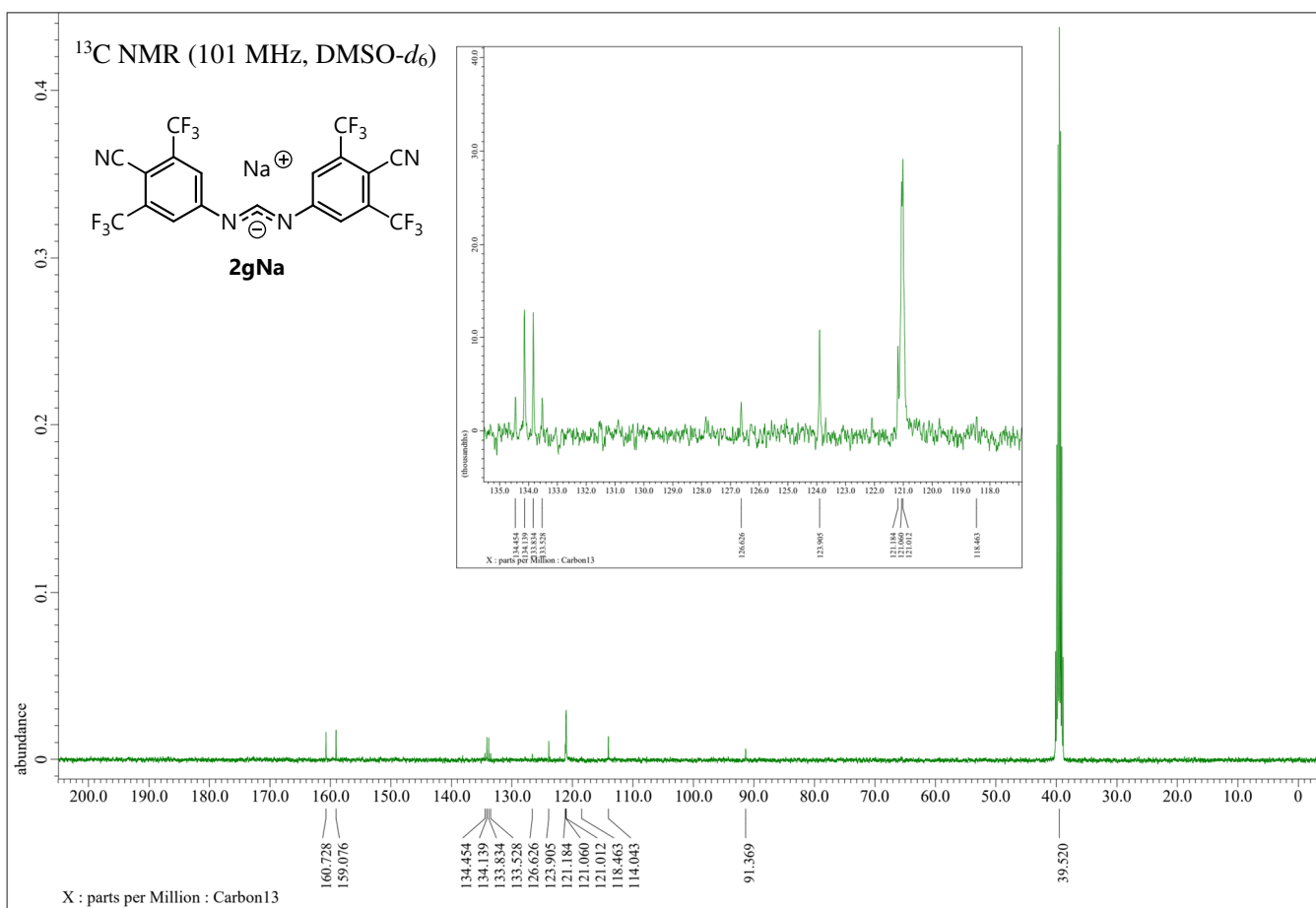
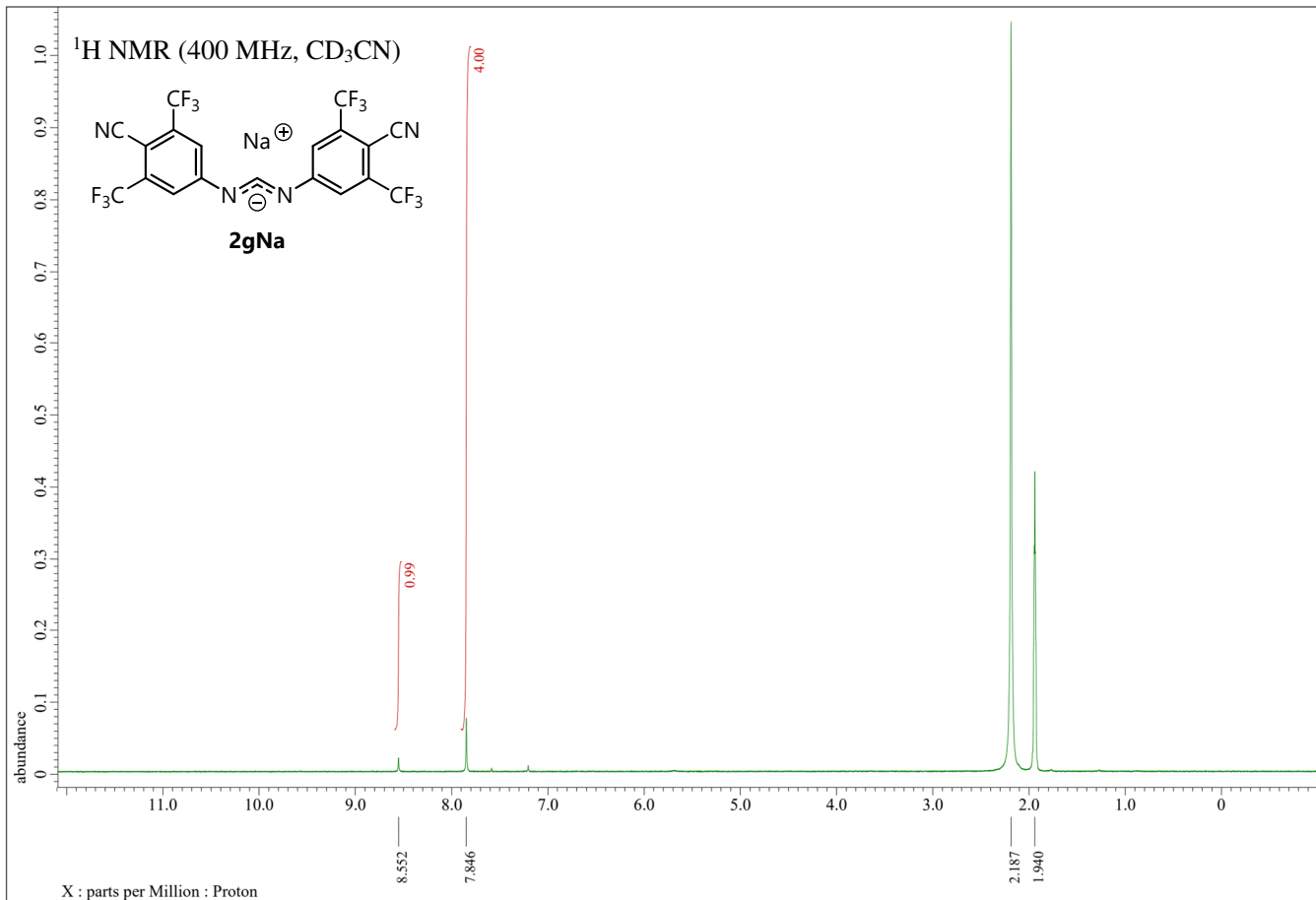


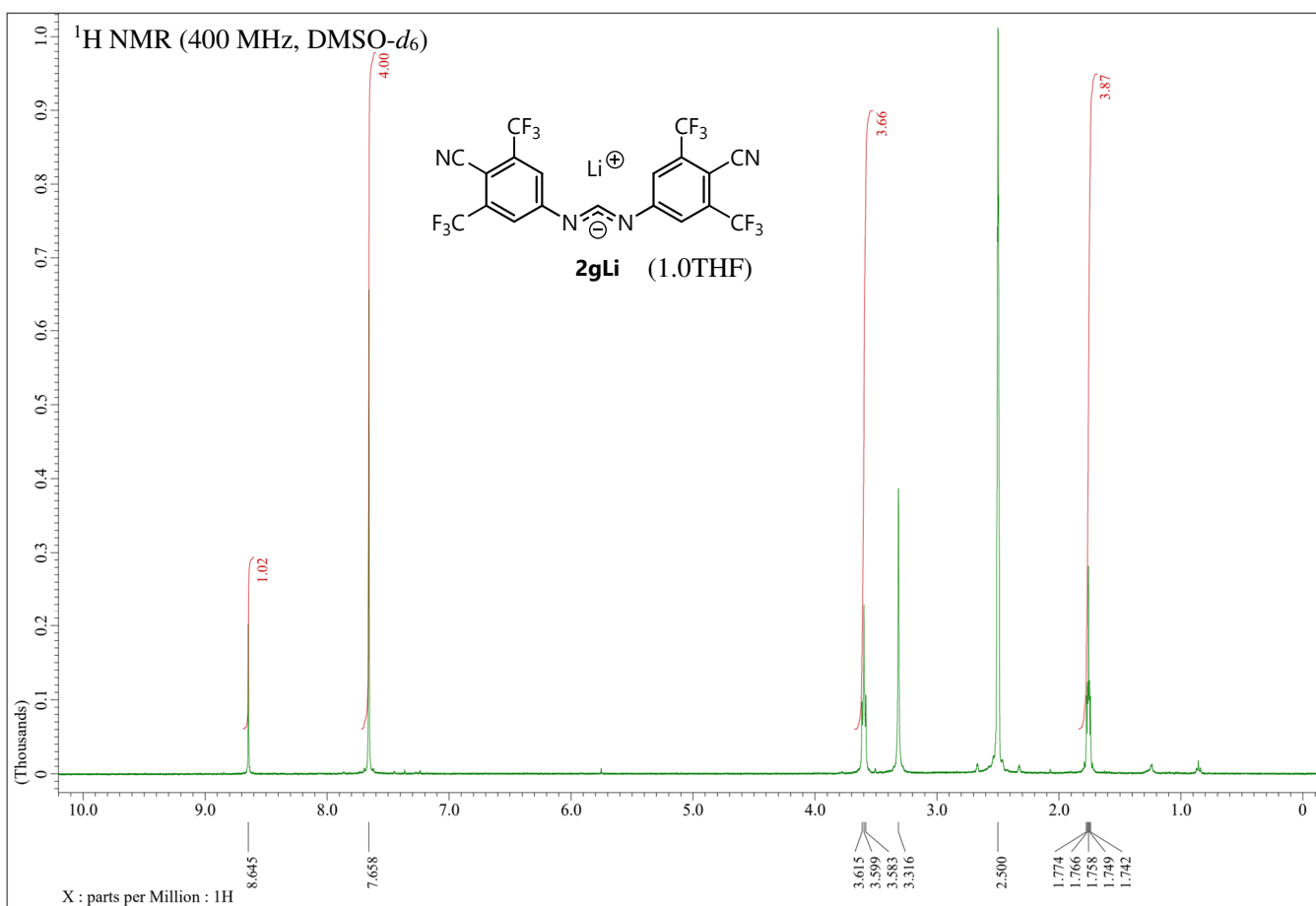
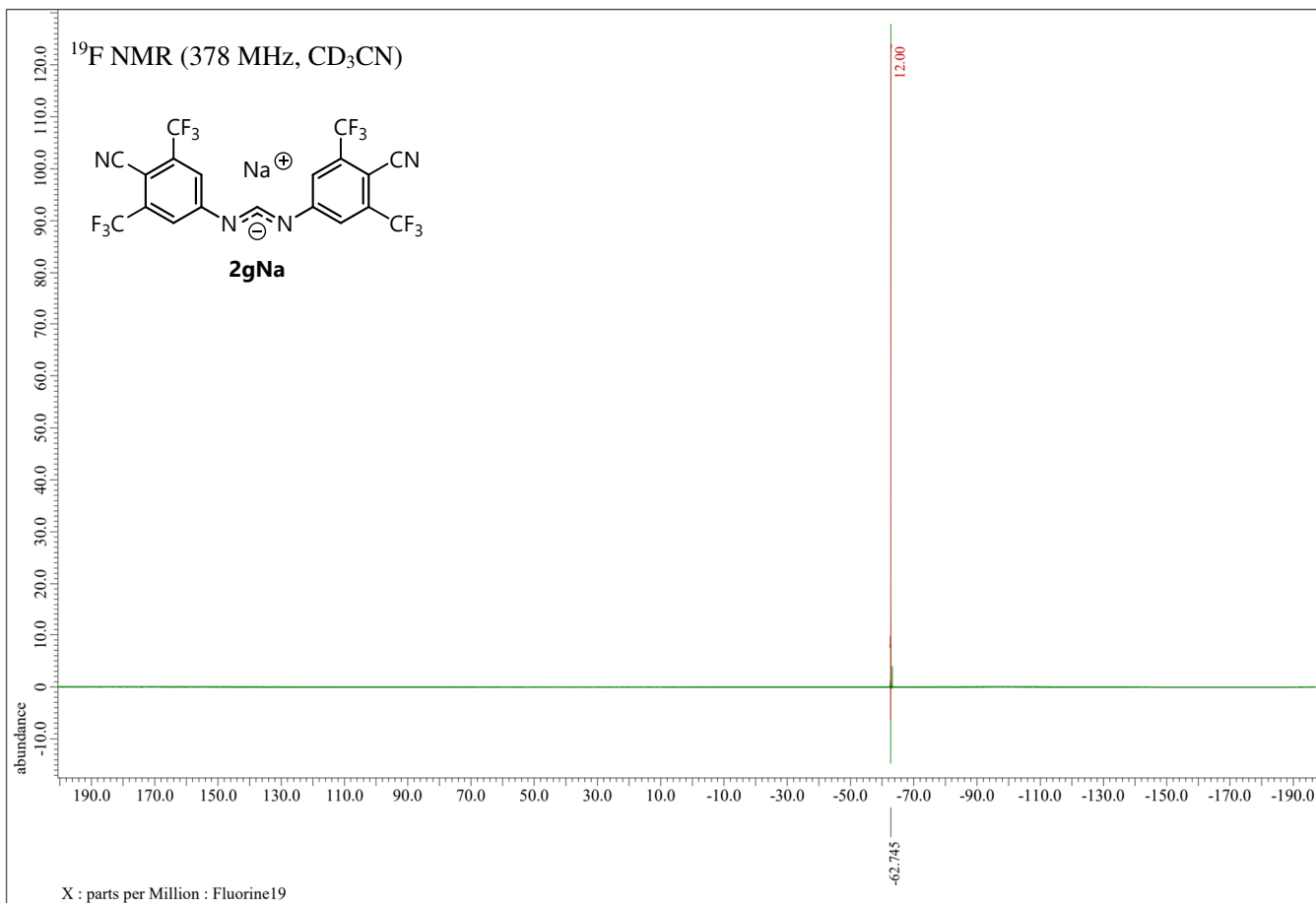


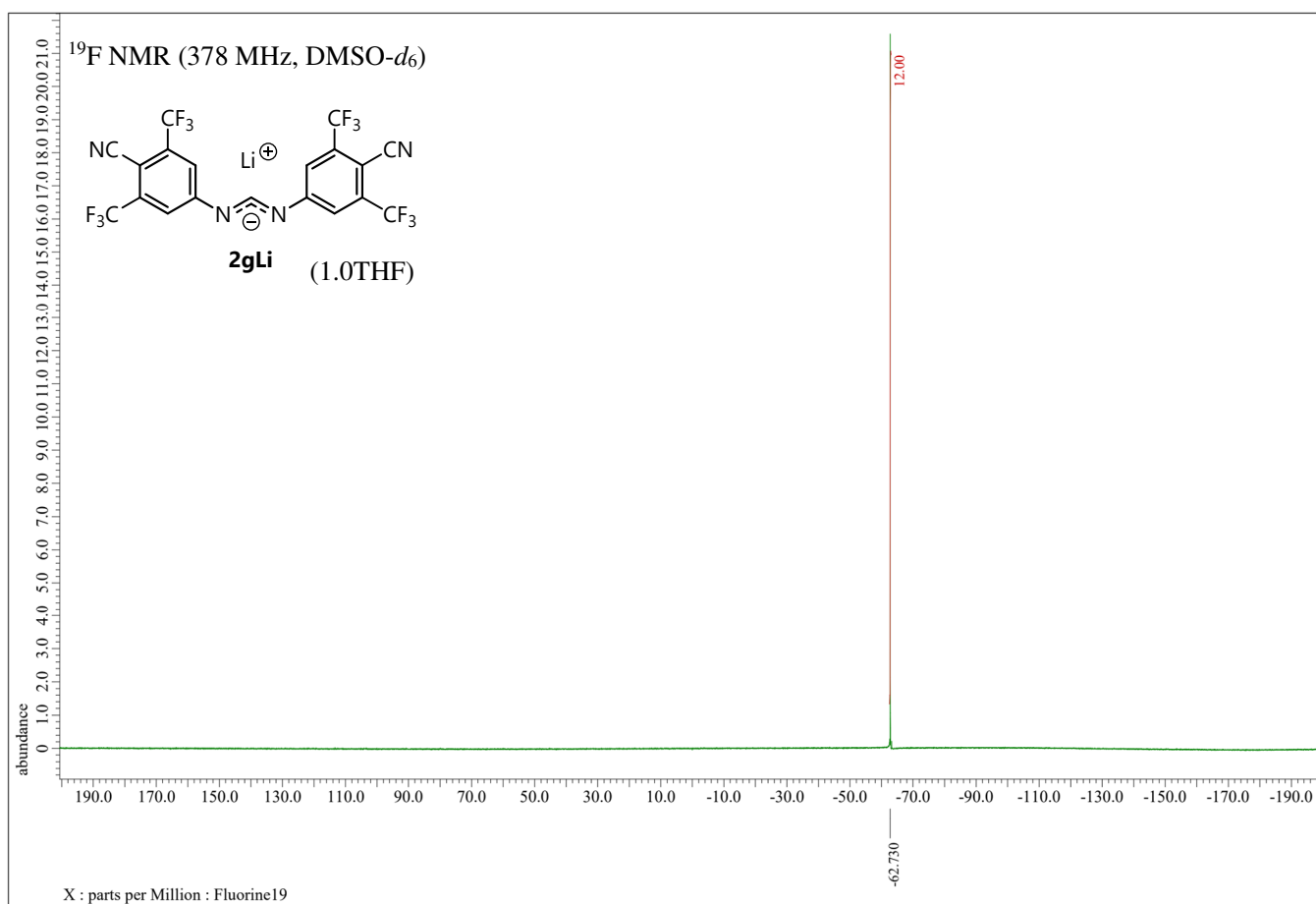
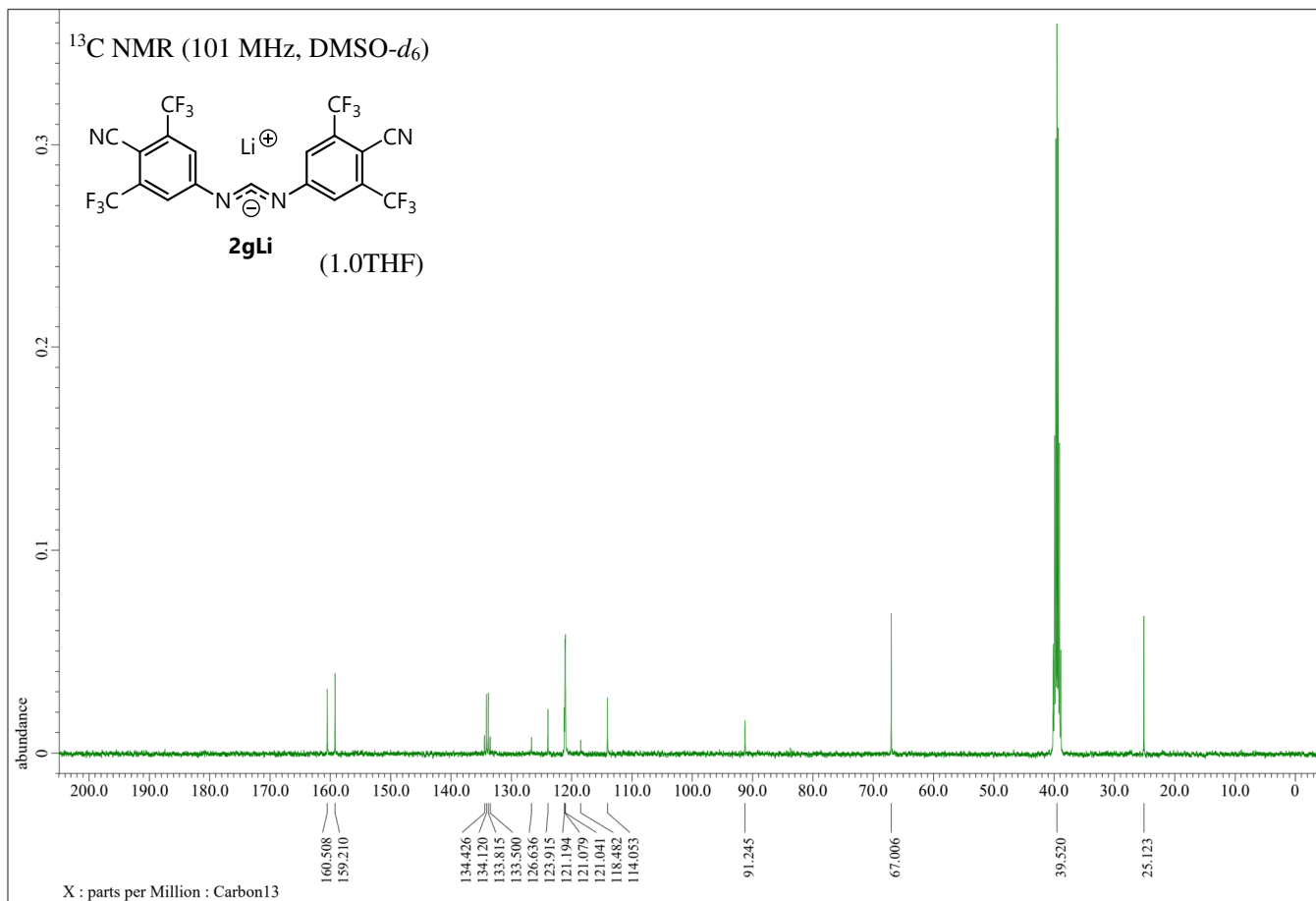


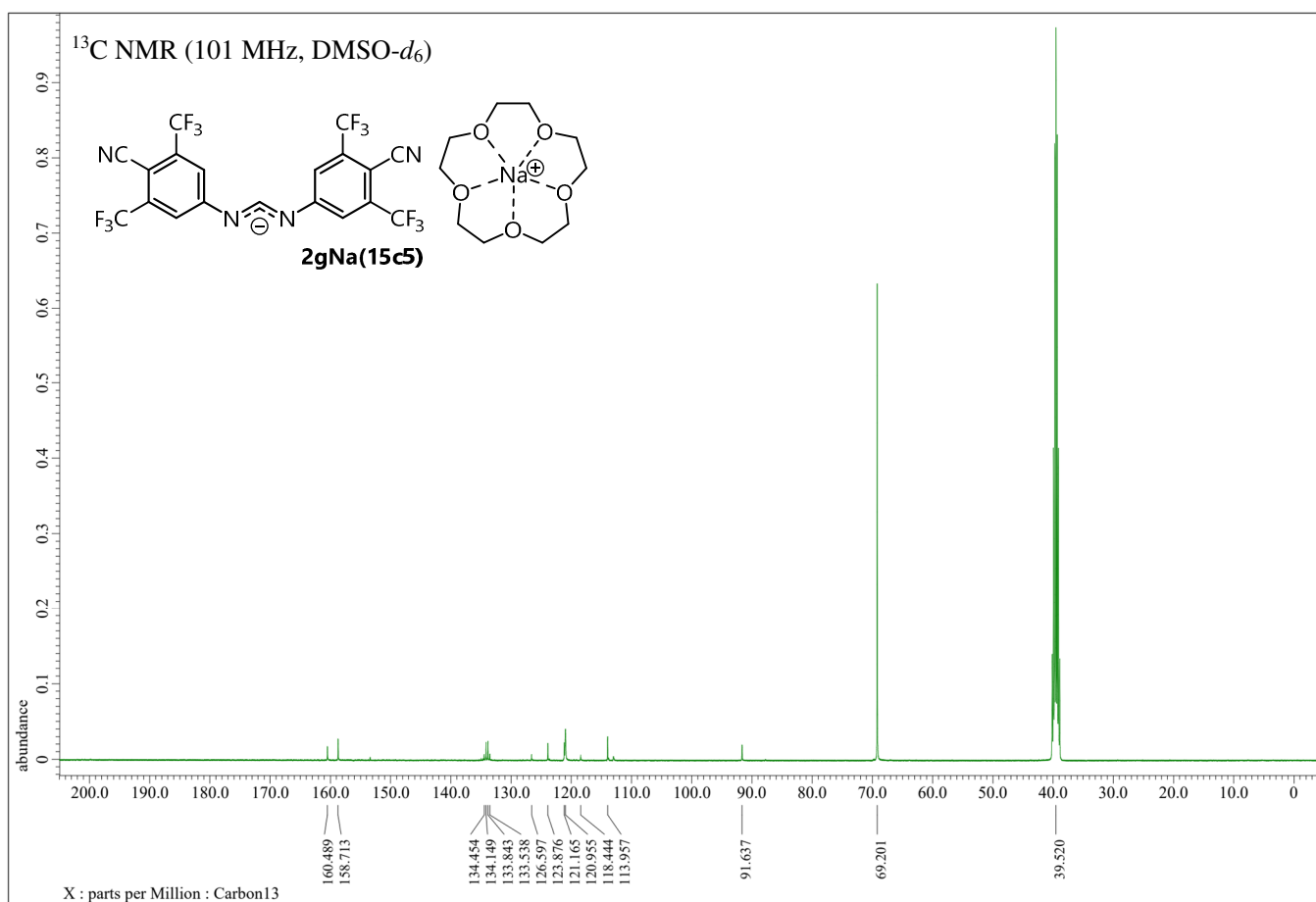
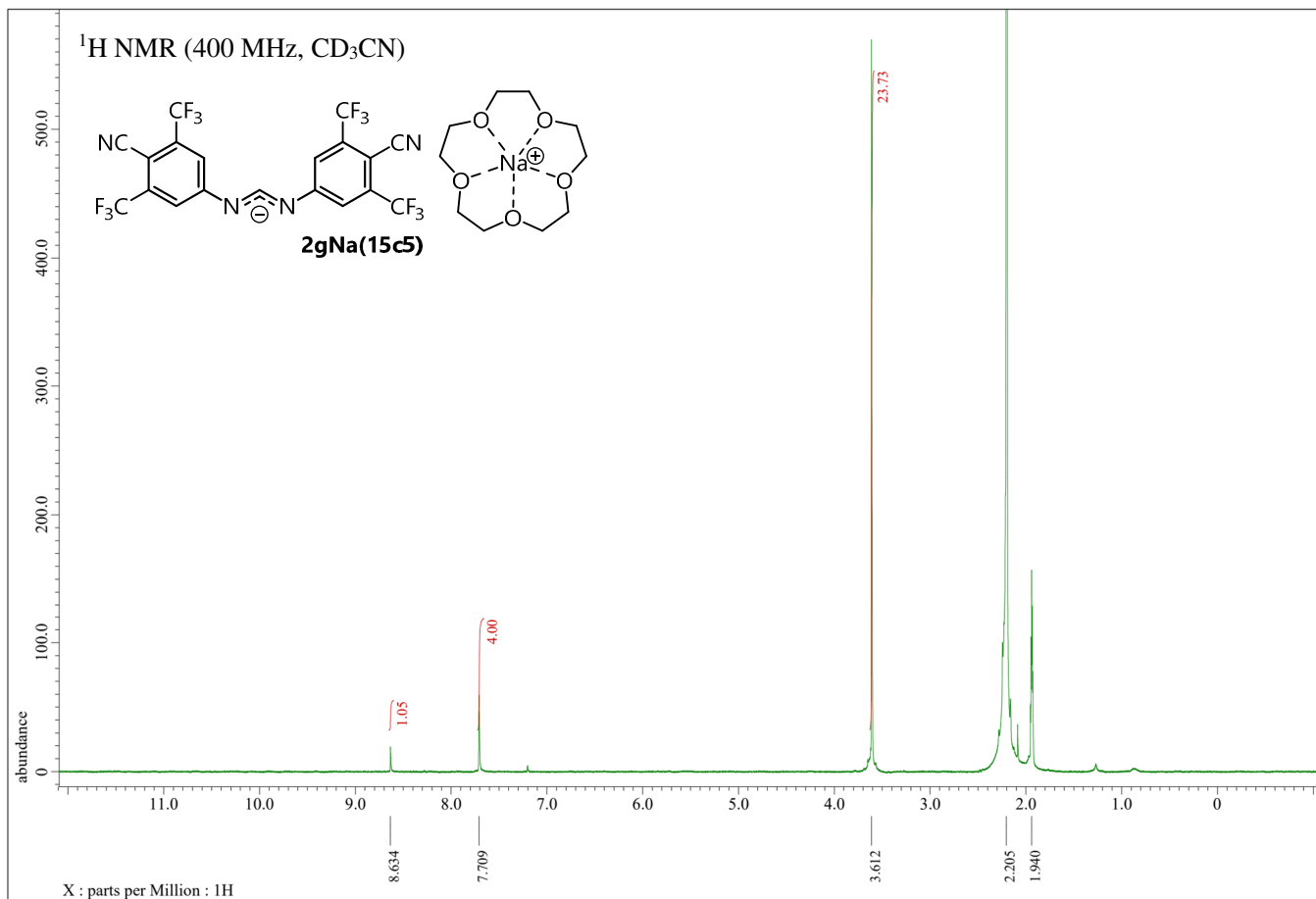


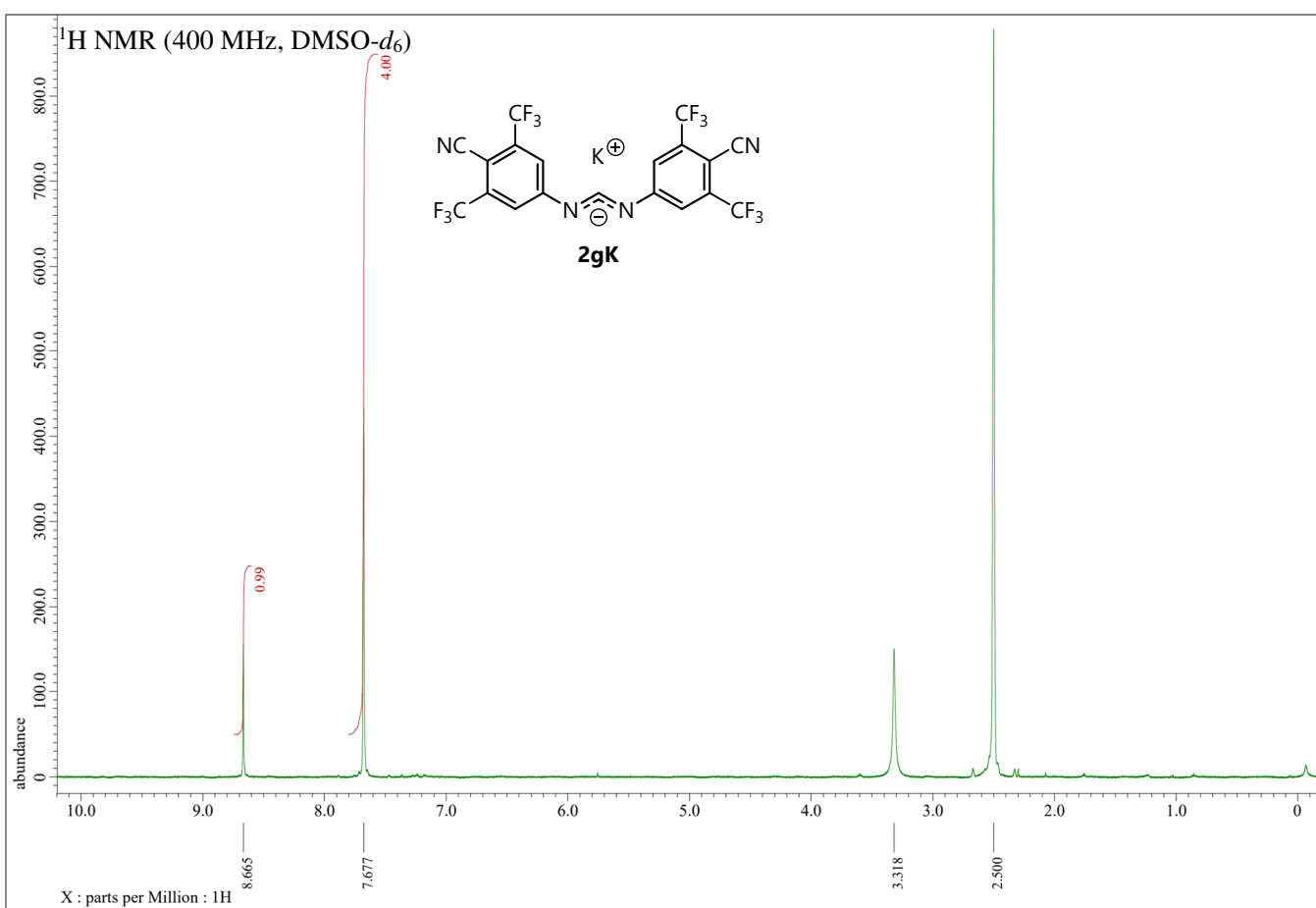
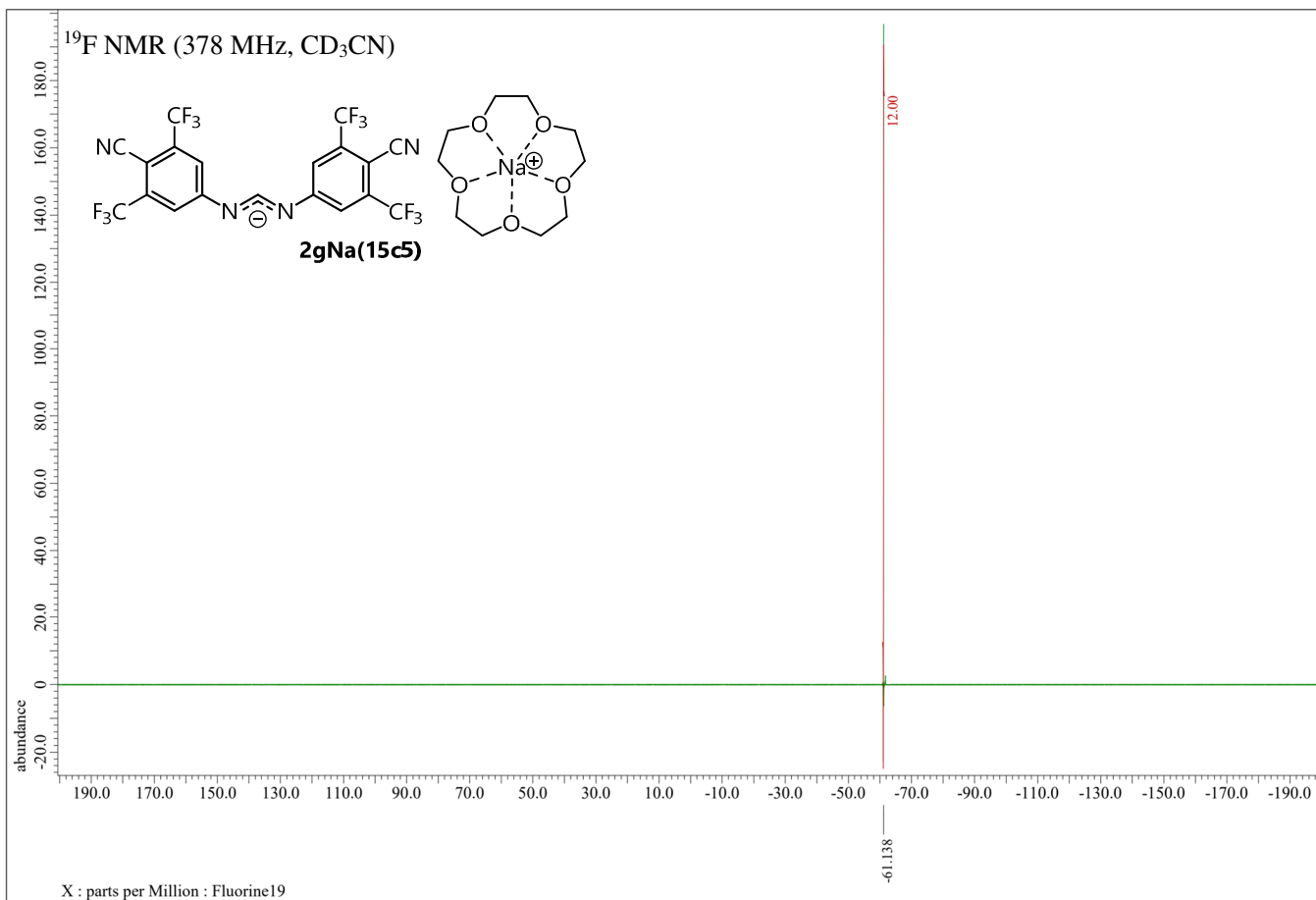


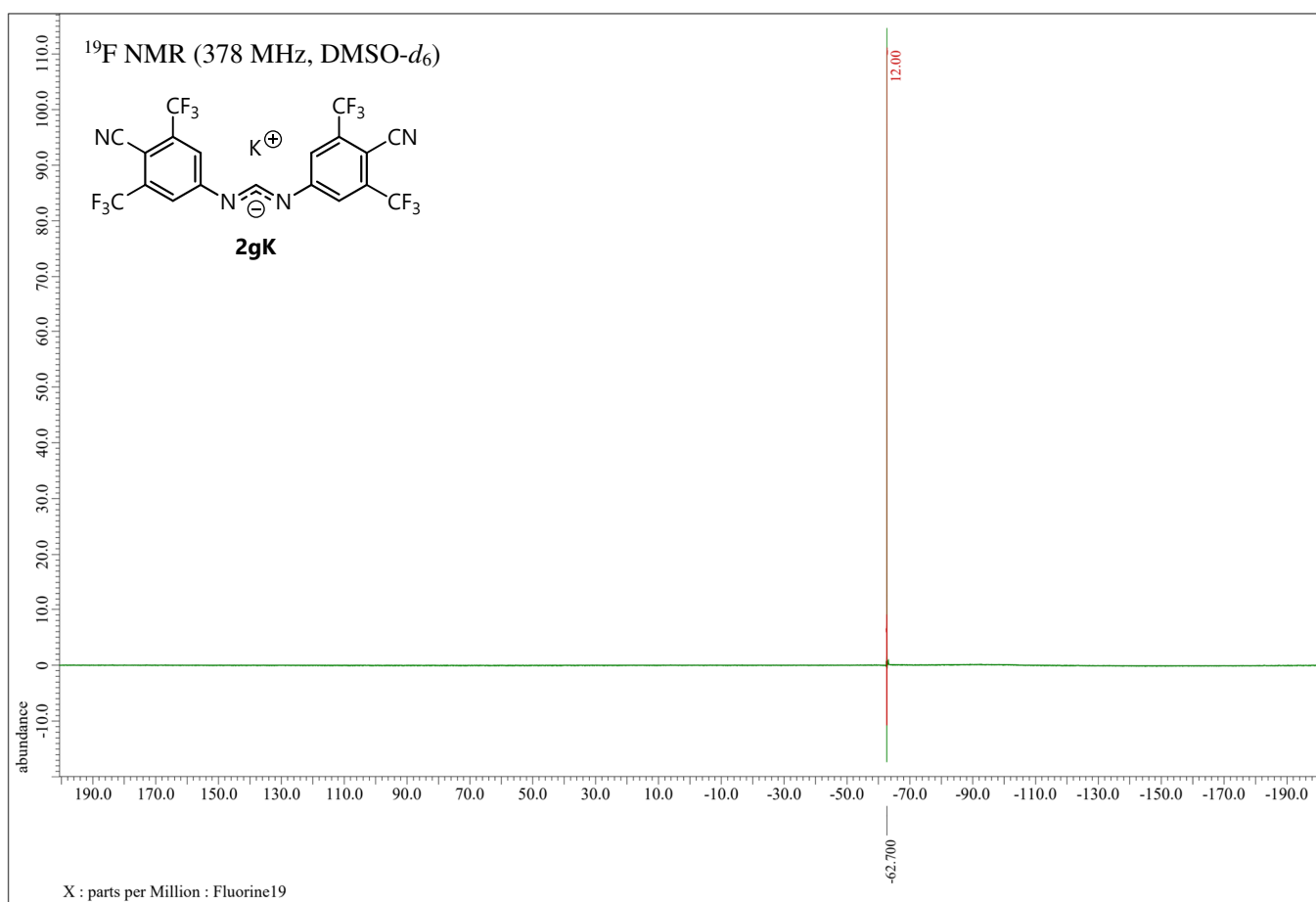
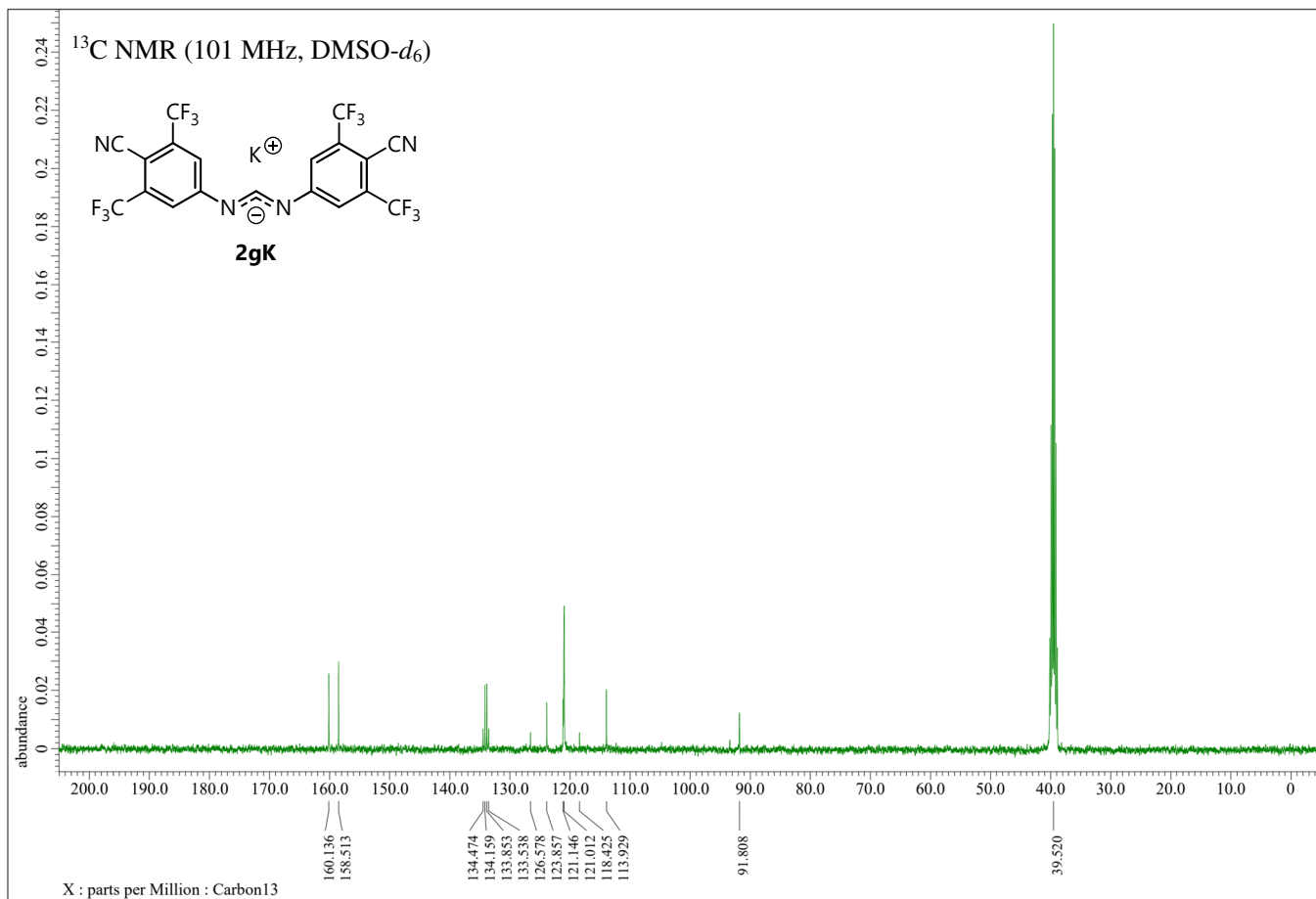


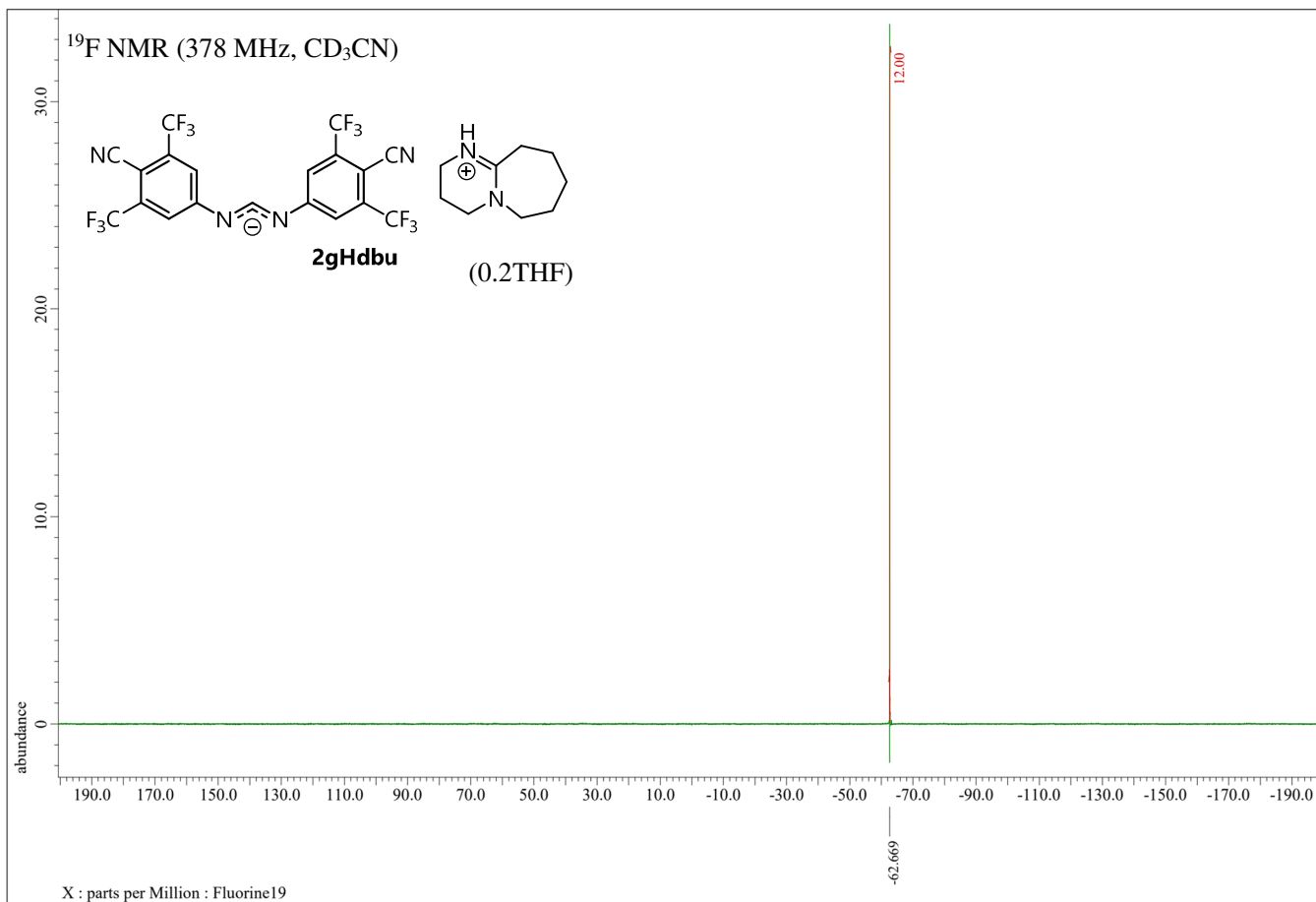












(L) References

- S1) C. Zhao, C. A. Sojda, W. Myint and D. Seidel, *J. Am. Chem. Soc.*, 2017, **139**, 10224.
- S2) P. Brulatti, R. J. Gildea, J. A. K. Howard, V. Fattori, M. Cocchi and J. A. G. Williams, *Inorg. Chem.*, 2012, **51**, 3813.
- S3) I.-Y. Lee, T. D. Gruber, A. Samuels, M. Yun, B. Nam, M. Kang, K. Crowley, B. Winterroth, H. I. Boshoff and C. E. Barry III, *Bioorg. Med. Chem.*, 2013, **21**, 114.
- S4) S. Bulut and W. L. Queen, *J. Org. Chem.*, 2018, **83**, 3806.
- S5) W. Bradley and I. Wright, *J. Chem. Soc.*, 1956, 640.
- S6) E. Crundwell, *J. Chem. Soc.*, 1956, 368.
- S7) I. A. Z. Squire, C. A. Goult, B. C. Thompson, E. Alexopoulos, A. C. Whitwood, T. F. N. Tanner and L. A. Wilkinson, *Inorg. Chem.*, 2022, **61**, 19144.
- S8) L. Onsager, *J. Am. Chem. Soc.*, 1936, **58**, 1486.
- S9) M. J. Frisch, G. W. Trucks, H. B. Schlegel, G. E. Scuseria, M. A. Robb, J. R. Cheeseman, G. Scalmani, V. Barone, B. Mennucci, G. A. Petersson, H. Nakatsuji, M. Caricato, X. Li, H. P. Hratchian, A. F. Izmaylov, J. Bloino, G. Zheng, J. L. Sonnenberg, M. Hada, M. Ehara, K. Toyota, R. Fukuda, J. Hasegawa, M. Ishida, T. Nakajima, Y. Honda, O. Kitao, H. Nakai, T. Vreven, J. A., Montgomery, Jr., J. E. Peralta, F. Ogliaro, M. Bearpark, J. J. Heyd, E. Brothers, K. N. Kudin, V. N. Staroverov, R. Kobayashi, J. Normand, K. Raghavachari, A. Rendell, J. C. Burant, S. S. Iyengar, J. Tomasi, M. Cossi, N. Rega, J. M. Millam, M. Klene, J. E. Knox, J. B. Cross, V. Bakken, C. Adamo, J. Jaramillo, R. Gomperts, R. E. Stratmann, O. Yazyev, A. J. Austin, R. Cammi, C. Pomelli, J. W. Ochterski, R. L. Martin, K. Morokuma, V. G. Zakrzewski, G. A. Voth, P. Salvador, J. J. Dannenberg, S. Dapprich, A. D. Daniels, Ö. Farkas, J. B. Foresman, J. V. Ortiz, J. Cioslowski, D. J. Fox, *Gaussian 09*, Revision C.01; Gaussian, Inc.: Wallingford, CT, 2009.
- S10) (a) A. D. Becke, *J. Chem. Phys.*, 1993, **98**, 5648. (b) C. Lee, W. Yang and R.G. Parr, *Phys. Rev. B*, 1988, **37**, 785. (c) P. J. Stephens, F. J. Devlin, C. F. Chabalowski and M. J. Frisch, *J. Phys. Chem.*, 1994, **98**, 11623.
- S11) (a) S. Grimme, J. Anthony, S. Ehrlich and S. Kreig, *J. Chem. Phys.*, 2010, **132**, 154104. (b) S. Grimme, S. Ehrlich and L. Goerigk, *J. Comput. Chem.*, 2011, **32**, 1456.
- S12) A. V. Marenich, C. J. Cramer and D. G. Truhlar, *J. Phys. Chem. B*, 2009, **113**, 6378.
- S13) (a) B. Mennucci, E. Cancès and J. Tomasi, *J. Phys. Chem. B*, 1997, **101**, 10506. (b) E. Cancès, B. Mennucci and J. Tomasi, *J. Chem. Phys.*, 1997, **107**, 3032. See also a review: J. Tomasi, B. Mennucci and R. Cammi, *Chem. Rev.*, 2005, **105**, 2999.